Effects of thermal hydrolysis process (THP) on struvite crystallisation from reject water of anaerobically digested sludge

Master Thesis

Widya Prihesti Iswarani

This page intentionally left blank

Effects of thermal hydrolysis process (THP) on struvite crystallisation from reject water of anaerobically digested sludge

By

Widya Prihesti Iswarani

in partial fulfilment of the requirements for the degree of

Master of Science

in Civil Engineering

at the Delft University of Technology,

to be defended publicly on Tuesday, 14 July 2020 at 14:00

Thesis committee:	Prof. Dr. Ir. Merle de Kreuk	Chair, TU Delft, Sanitary engineering
	Prof. Dr. Ir. Jules van Lier	TU Delft, Sanitary engineering
	Prof. Dr. Antoine van der Heijden	TU Delft, Process and energy
	Javier Pavez Jara, MSc.	TU Delft, Sanitary engineering

This thesis is confidential and cannot be made public until 14 July 2021.

An electronic version of this thesis is available at http://repository.tudelft.nl/.

TUDelft

iii

This page intentionally left blank

By complaining that something we have to do is too hard, we add another layer of difficulty. Take a deep breath, and then just do it.

– Haemin Sunim

For indeed, with hardship [will be] ease. Indeed, with hardship [will be] ease.

– Quran 94:5–6

This page intentionally left blank

Acknowledgements

It is still unbelievable that I can make it up to this point. Studying in The Netherlands has been my dream since I started writing my bachelor thesis. I was conducting an experiment about struvite recovery from fertiliser industry wastewater, but it only ended up on paper. I was wondering if it would be possible to see struvite reactor in the real-life and perform research related to struvite based on a real problem in a real wastewater treatment plant. I am lucky that life has brought TU Delft to me, and I am finally able to turn my dream into reality.

This thesis marks the end of my two years journey as a master student in civil engineering with track environmental engineering. A journey that not only broadened my knowledge in the field of environmental engineering but also thought me many life lessons. Eight months of research finally resulted in this thesis. Even though struvite is not a new thing for me, I learned many new things about sludge (pre)treatment, reject water treatment, and crystallisation by conducting this research. This thesis has brought me through ups and downs; therefore, I would like to thank people who have helped me during this period.

I would like to thank the chair of my thesis committee, Merle de Kreuk, who introduced me to this project. I really appreciate her valuable guidance to improve my thesis. Jules van Lier, who always shared his knowledge and noticed even the smallest details where I can make my thesis even better. Antoine van der Heijden, who gave insights about crystallisation and ideas to analyse my data. Javier Pavez Jara as my daily supervisor, thank you for always helping me with every problem that I encountered during my thesis. Javier has always been very positive, supportive, and helpful, and I could not ask for a better daily supervisor than him. Thanks to Fred Penha who helped me with crystals analysis.

I would also thank my beloved friends. Sasha, for helping me to stay strong and answering silly questions about THP. Ayu, for being so supportive since my first day in TU Delft. Dennis, Sander, and Bor, for helping me with coding, listening to my stories, and showering me with positive vibes. Ron, for his cheesy jokes, efforts to cheer me up, and reminding me that "alles komt goed". Azza, for being my online karaoke mate during COVID-19 quarantine period. Lastly, I would thank my family for encouraging me to pursue my study in TU Delft and always praying for my success.

<div align="right">

Widya Prihesti Iswarani

Delft, The Netherlands
July 2020

</div>

This page intentionally left blank

Abstract

Various technologies have been implemented in wastewater treatment plants (WWTPs) to generate clean effluent with minimised impacts on the environment. Thermal hydrolysis process (THP) and struvite crystallisation reactors are two examples of these technologies. THP generates humic-like substances, known as melanoidins, that are presumed to disrupt struvite crystallisation. THP also solubilises trace elements that are prone to complex with melanoidins. The fate of the trace elements is still a matter of doubt. On the one hand, they might stay bound to the melanoidins in the supernatant or on the other hand, might be present in struvite as impurities. As both THP and struvite crystallisation are promising technologies, the objective of this study was to understand the effects of THP on struvite crystallisation.

Lab-scale batch-test struvite crystallisation using synthetic wastewater was done to determine the effects of THP on struvite crystallisation from reject water of anaerobically digested sludge. pH values and melanoidins concentrations were varied to understand how each factor affected struvite crystallisation. In addition to that, PHREEQC modelling was used to predict the complexation between humic substances (HS) and various metals, as well as co-precipitation of trace elements and heavy metals during struvite crystallisation. Finally, the Response Surface Methodology (RSM) was used to predict the optimum conditions for struvite crystallisation.

Results showed that melanoidins generated by THP affected P removal in struvite crystallisation at pH 6.5 and 7.25, but not at pH 8. In contrary to melanoidins, humic acids (HA) were found to reduce P removal efficiency at pH 8 drastically. Melanoidins resulted in slightly higher $N-NH_4$ concentration in the supernatant in all pH values. Melanoidins affected the amount of produced struvite at pH 6.5 and 7.25, but not at pH 8. Melanoidins and HA also changed crystal colour from white into brown and black, respectively. Furthermore, melanoidins and HA changed the morphology of struvite crystals from X-shaped and long rod-like crystals into square-shaped crystals and at the same time reduced the diameter of struvite crystal. Regardless of the effects on struvite crystal, melanoidins did not change the $Mg:N-NH_4:P-PO_4$ molar ratio. Melanoidins did not significantly influence induction time, except at pH 7.25 and 2 g TOC/L melanoidins. In addition to this, melanoidins were found to form complexes with magnesium which subsequently decreased the supersaturation and affected struvite crystallisation.

Different elements had different fate on struvite crystallisation. Melanoidins formed complexes with Mn and Ni, resulting in a higher concentration in the supernatant compared to the condition without melanoidins. Based on PHREEQC modelling, HS formed complexes with Ca, Cu, and Fe. Certain trace elements (Ca, Co, Cu, Fe, and Mn) and heavy metals (Al and Cr) were found to co-precipitate with struvite in all experimental conditions; meanwhile, Se minerals only co-precipitated at pH 8. All minerals showed decreasing SI with increasing HS concentrations. The decrease of SI implied that there would be less co-precipitation of Al, Ca, Co, Cr, Cu, Fe, Mn, and Se in struvite crystals. Nevertheless, their presence in the supernatant would not guarantee the bioavailability of the trace elements for bacteria in partial nitritation/anammox (PN/A) processes due to the chance of complexation with HS.

This study has given the relevant fundamental understanding of the effects of THP on struvite crystallisation. Eventually, it could be concluded that THP affected struvite crystallisation and RSM confirmed that the optimum conditions for struvite crystallisation with maximised N and P contents and big diameter were pH of 7.9 and 0 g TOC/L melanoidins. Nonetheless, melanoidins prevented co-precipitation of trace elements in struvite crystals. Further research is still required to ensure the production of good quality struvite crystals in WWTPs with THP installation, such as granulation properties and settleability of struvite crystals, P and N complexations with melanoidins, as well as minimising melanoidins concentration.

This page intentionally left blank

x

Contents

List of figures

List of tables

List of tables

This page intentionally left blank

List of abbreviations

AAO	Anaerobic ammonium oxidisers
AD	Anaerobic digester
AOB	Ammonia oxidising bacteria
Anammox	Anaerobic ammonium oxidation
ANOVA	Analysis of variance
EDTA	Ethylenediaminetetraacetic acid
COD	Chemical oxygen demand
FA	Fulvic acids
FTIR	Fourier-transform infrared spectroscopy
HA	Humic acids
HMW	High molecular weight
HS	Humic substances
IAP	Ion activity product
Ksp	K-value of solubility product (Solubility product constant)
LMW	Low molecular weight
NMR	Nuclear magnetic resonance
NOM	Natural organic matter
RSM	Response surface methodology
PN/A	Partial nitritation/anammox
sCOD	Soluble chemical oxygen demand
SEM-EDX	Scanning electron microscopy and energy-dispersive X-ray spectroscopy
tCOD	Total chemical oxygen demand
TAN	Total ammonia nitrogen
THP	Thermal hydrolysis process
TOC	Total organic carbon
TS	Total solids
TSS	Total suspended solids
WAS	Waste activated sludge
WWTP	Wastewater treatment plant
XRD	X-ray powder diffraction

This page intentionally left blank

1.   Introduction

1.1.   Background information

Phosphorus (P) is a vital element that plays a role in the growth of living organisms (Cusick & Logan, 2012; Ebbers et al., 2015; Roy, 2017; Shepherd et al., 2016; Zohar et al., 2017). Phosphorus acts as the key element of nucleic acids (DNA and RNA), contributes in crucial metabolism processes as ATP and complementary coenzymes which transfer chemical energy, and holds up cellular anatomy as phospholipids (Pasek, 2019). Furthermore, together with nitrogen and potassium, phosphorus is an important nutrient for crops growth (Cordell & Neset, 2014). A steady supply of phosphorus-based fertilisers which can be incorporated into the soils is required to support crops growth and global food production (Shepherd et al., 2016). However, phosphorus is a finite resource which is available in limited amount in earth's crust (Cusick & Logan, 2012; Zohar et al., 2017). At the moment, the non-renewable phosphate rock remains as the primary source of phosphorus-based fertilisers, and it is approximated to last within 30 and 300 years (Cordell & Neset, 2014; Reijnders, 2014). On the other hand, extensive application of nutrient-rich fertiliser may lead to the discharge of phosphorus and nitrogen into water bodies which subsequently results in eutrophication, especially in rivers and lakes (Dodds et al., 2009).

As global phosphorus deposits decline, renewable methods for phosphorus production have been gaining more attention (Ebbers et al., 2015; Roy, 2017; Shepherd et al., 2016). Municipal wastewater and sewage sludge have high chance to be used as the secondary source of phosphorus and other nutrients (Ebbers et al., 2015). Numerous studies have investigated the possibility of phosphorus recovery from P-enriched wastewater streams (Egle et al., 2016). Some of the technologies used to recover phosphorus from wastewater streams include phosphorus extraction from incinerated sludge ash, phosphorus recovery as calcium phosphate, and phosphorus recovery as struvite (Donatello & Cheeseman, 2013; Li, Boiarkina, et al., 2019; Vasenko & Qu, 2019). Phosphorus recovery as struvite is favoured because it acts as phosphorus fertiliser which contains a significant quantity of nitrogen and magnesium (Md Mukhlesur Rahman et al., 2014).

Struvite is a mineral with an equal molar concentration of magnesium (Mg^{2+}), ammonium (NH_4^+), and phosphate (PO_4^{3-}) combined with six water molecules, with a chemical formula of $MgNH_4PO_4.6H_2O$ (Md M. Rahman et al., 2011). Struvite crystallisation occurs when the concentrations of Mg^{2+}, NH_4^+, and PO_4^{3-} exceed the solubility product constant for struvite formation (Cusick & Logan, 2012). Struvite precipitation may happen spontaneously in wastewater treatment plants (WWTPs), resulting in scaling and encrustation, which then lead to higher maintenance costs (de Boer et al., 2018). Controlled struvite precipitation has been utilised in some WWTPs in order to lower both nitrogen and phosphorus concentrations in wastewater, and at the same time produce phosphorus-based fertiliser (Li, Huang, et al., 2019; Shepherd et al., 2016). More WWTPs in north-western Europe are beginning to install struvite reactors in order to save maintenance costs (de Vries et al., 2017). Struvite reactors have been implemented in full-scale in WWTPs in The Netherlands to treat reject water of anaerobically digested sludge (Abma et al., 2010; de Vries et al., 2017; Driessen et al., 2020). However, the fundamental objective for the application of struvite reactor in The Netherlands is only to reduce the P and N contents (STOWA, 2010). This effort is in line with the EU Water Framework Directive which regulates that the allowed P concentration in wastewater discharge is reduced to 0.1 mg P/L in the near future (Shepherd et al., 2016). Even though there has been an increase in the number of struvite reactors, there is hardly any market for struvite produced in the country (de Vries et al., 2017). The market price of struvite based on its Mg, N, and P contents is only 5.50€ per 100 kg when sold as struvite granules or as raw material for fertiliser production (STOWA, 2016). The use of recovered struvite in The Netherlands is still limited by some constraints, including product quality, legislation issue, and social acceptance (STOWA, 2016; Verhults, 2017). Product quality of struvite is still doubted, mainly for the application of struvite as fertiliser, due to the presence of impurities in it (Li, Boiarkina, et al., 2019; STOWA, 2016).

Some WWTPs in The Netherlands employ thermal hydrolysis process (THP) as sludge pre-treatment to enhance the processes in an anaerobic digester (AD), mainly to increase the solids loading rate to the AD

and improve sludge dewaterability (Oosterhuis et al., 2014). By applying THP, it is expected that operational costs for sludge treatment can be minimised and biogas production is maximised (Driessen et al., 2020). Earlier studies reported that the application of THP resulted in higher soluble chemical oxygen demand (sCOD), increase in nutrients release, and production of refractory organic compounds (Barber, 2016). THP generates brown-coloured refractory organic compounds, termed as melanoidins, that behave similarly as humic substances (HS) (P. Huang et al., 2005; Dandan Zhang et al., 2019). HS are presumed to disrupt struvite crystallisation by complexing with struvite reactants, thus affecting P and N removal efficiencies and the characteristics of struvite crystal (Li, Huang, et al., 2019; Wei et al., 2019; Zhou et al., 2015). However, no studies have investigated the influence of melanoidins on struvite crystallisation.

THP also escalates the solubilisation of inorganic matters, including the trace elements which normally adsorbed to organic compounds (Appels et al., 2010). These solubilised trace elements are prone to complex with melanoidins (Lipczynska-Kochany & Kochany, 2008), which consequently affect the overall downstream processes in WWTPs, including struvite crystallisation. The complexation of trace elements with melanoidins has the possibility to decrease the bioavailability of vital trace elements required by the later treatment unit after struvite crystallisation, e.g. partial nitritation/anammox (PN/A) (Driessen et al., 2020; Van De Graaf et al., 1996). The fate of the trace elements in reject water is still a matter of doubt, on the one hand, they might stay bound to the humic-like substances or on the other hand, might be present in struvite as impurities. There is a lack of knowledge about the relationship between melanoidins generated in THP, trace elements released from THP, and struvite formation. Therefore, the overall effects of THP in struvite crystallisation needs to be scrutinised.

1.2. Knowledge gaps and problem statement

1.2.1. Knowledge gaps

Based on the background information elucidated in Section 1.1, there are some knowledge gaps to be explored and further elaborated:

1. The effect of melanoidins on struvite formation has not been reported yet, especially on a full-scale WWTP. Even though some studies declared similarities between melanoidins and HS, to what extent melanoidins affect struvite crystallisation remains unclear. There are questions whether melanoidins change P and N removal efficiencies, amount of produced struvite, or crystal morphology. As melanoidins behave similarly to HS, its solubility is also influenced by pH. pH is one of the most influential parameters on struvite crystallisation as it affects the thermodynamics of struvite reaction and phosphorus removal efficiency. Thus, the understanding of the relationship between pH, melanoidins, and struvite crystallisation is required.

2. There is uncertainty on the mechanism of how melanoidins affect struvite crystallisation. Melanoidins are predicted to form complexes with other constituents (including magnesium, ammonium, and phosphate used to form struvite and trace elements) in wastewater. As a result, melanoidins may hinder the nucleation and growth of struvite crystals or alter crystal morphology. How the complexes are formed and affect struvite crystallisation need to be investigated.

3. No study explains the fate of trace elements released from THP. Some studies reported an interaction between trace elements and struvite, in which the trace elements co-precipitate on the crystal surface and affect the morphology. Despite that, the interaction between struvite, melanoidins, and trace elements required for the following PN/A processes is rarely investigated.

1.2.2. Problem statement

Stringent regulation to achieve lower phosphorus in the effluent of WWTP is going to be applied in EU according to Water Framework Directive. At the same time, sustainable methods to obtain phosphorus-based fertilisers from waste streams are needed to satisfy worldwide demand. Therefore, suitable treatment unit must be applied to meet these requirements (Shepherd et al., 2016). Struvite reactors have been implemented in full-scale in WWTPs in The Netherlands to decrease the phosphorus and nitrogen concentrations; however, struvite product quality is still disputable (STOWA, 2010; Verhulst, 2017). The

reason behind this is because struvite may contain impurities, including heavy metals (Li, Boiarkina, et al., 2019; STOWA, 2016). Concerning the uncertainties mentioned in Section 1.2.1, it is crucial to understand the overall effect of THP on struvite crystallisation. The brown-coloured melanoidins may affect the colour of produced struvite and hence affecting market acceptance. Animal manure, compost, and other fertilisers which also contain Mg, N, and P may have a prominent position in the market compared to struvite (STOWA, 2016). Optimal conditions for struvite crystallisation in WWTPs that utilise THP should be understood to produce high purity struvite with maximised Mg, N, and P contents, and low impurities (such as heavy metals) content. Research is needed to ensure if THP changes the quality of produced struvite and how it can be improved.

1.3. Research objectives, questions, and approaches

1.3.1. Research objectives
To investigate the relationship between substances generated in THP and struvite crystallisation, the objective of this research was:

"Understanding the effects of the thermal hydrolysis process (THP) on P removal using struvite crystallisation from reject water of anaerobically digested sludge."

1.3.2. Research questions
The main research question of this thesis was:

"What are the effects of the thermal hydrolysis process (THP) on struvite crystallisation from reject water of anaerobically digested sludge?"

In order to answer the main research question, the following three sub-research questions were formulated:

1. What are the effects of humic-like substances (melanoidins and humic acids) on P removal, N removal, and struvite characteristics in struvite crystallisation?
2. How do melanoidins affect struvite crystallisation?
3. What is the fate of trace elements released from THP in struvite crystallisation?

1.3.3. Research hypotheses
It was hypothesised that melanoidins form complexes with the reactants of struvite and trace elements. The formation of complexes between melanoidins and reactants of struvite would decrease the P and N removal efficiencies and reduce the amount of produced struvite. In addition to that, it was presumed that melanoidins would alter crystal morphology and prolong nucleation and growth of struvite crystals. The formation of complexes between melanoidins and trace elements might result in some trace elements being end up in struvite or water (supernatant of struvite reactor). It was predicted that there would be more trace elements ending up in supernatant with the presence of melanoidins. By answering the research question and sub-research questions, the formulated hypotheses can be accepted or rejected.

1.3.4. Research approaches
In order to answer the research questions, this research was conducted by two approaches. The first approach was literature review and the second approach was a lab-scale experiment followed by PHREEQC modelling.

Literature review
Literature review was done to understand the theories related to this research, including the processes in thermal hydrolysis process (THP), fundamentals of crystallisation and precipitation, and struvite crystallisation. The results of literature review are written in Chapter 2.

Lab-scale experiment

Synthetic wastewater was used in this study. Synthetic wastewater which represented the quality of reject water of anaerobically digested sludge was used to understand the effect of synthetic melanoidins and humic acids on struvite crystallisation with different final pH values. The lab-scale experiment was also complemented with PHREEQC modelling. The detailed experimental design and procedure are described in Chapter 3.

1.4.   Thesis outline

This thesis report is divided into six chapters, as follows:

Chapter 1 – Introduction gives the background information, knowledge gaps and problem statement that will be solved by this thesis, and research objectives, questions, and approaches.

Chapter 2 – Literature review provides relevant theoretical information about THP and struvite.

Chapter 3 – Materials and methods present the experimental configurations and analytical techniques used in this study.

Chapter 4 – Results and discussions elucidate the obtained results from this study enriched with comparison to earlier studies and relevant literature.

Chapter 5 – Research limitations and recommendations describe the limitations of the present study and recommendation for future research.

Chapter 6 – Conclusions summarise the overall results of this study.

2. Literature Review

2.1. Thermal hydrolysis process

2.1.1. Process and technology descriptions

THP is one of sludge pre-treatment technologies that can be used to enhance the performance of AD (Appels et al., 2010). As a sludge pre-treatment technology, THP is generally introduced prior to AD. THP applies high temperature ranging from 60–275°C into the sludge in a specific time between 10–180 minutes (Barber, 2016). High temperature and high pressure in THP will cause cell wall lysis, which converts macromolecular organics into dissolved and degradable molecules afterwards (Dandan Zhang et al., 2019). The motivations for the utilisation of THP involve the raise of loading rates of AD, improvement of sludge dewaterability, higher production of renewable energy in the form of biogas, and disinfection of sludge (Barber, 2016). During the processes in THP, sugars and proteins may react to generate brown-coloured refractory heterogeneous polymers, termed as melanoidins, as by-products (Barber, 2016). Figure 2.1 shows the reactions that occur during the THP of waste activated sludge (WAS).
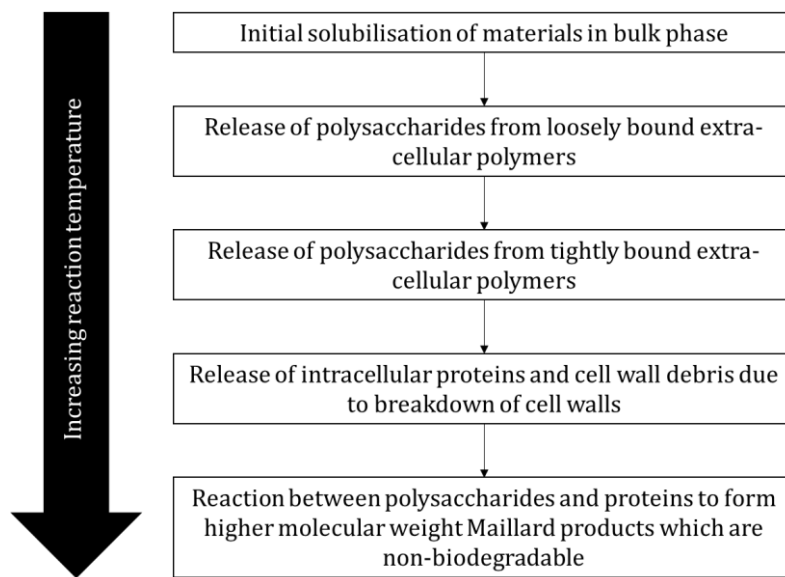
Figure 2.1 Reactions during THP of WAS (Barber, 2016)

2.1.2. Commercial THP system configurations

As THP has been commercially available for more than 20 years (Ødeby et al., 1996), various THP technologies are available in the market. Three technologies that correspond with the WWTPs in The Netherlands are described in this section. The three technologies are Cambi™, Sustec TurboTec®, and Lysotherm® systems.

Cambi™

Cambi™ THP process has been developed from 12 m³ reactor (referred as Mark I), into multiple reactor arrangements with different sizes (Mark II). Typically, Cambi™ process is comprised of four steps as follows: 1) Heat recovery, thermal buffering, and sludge heating occur in the pulper tanks, 2) Thermal hydrolysis takes place in the reactor tanks, 3) Pressure setback and steam flash happen in the flash tank, and 4) Cooling of the hydrolysed sludge prior to AD. The typical Mark II arrangement of Cambi™ THP process is depicted in a schematic diagram in Figure 2.2 (Williams & Burrowes, 2016).
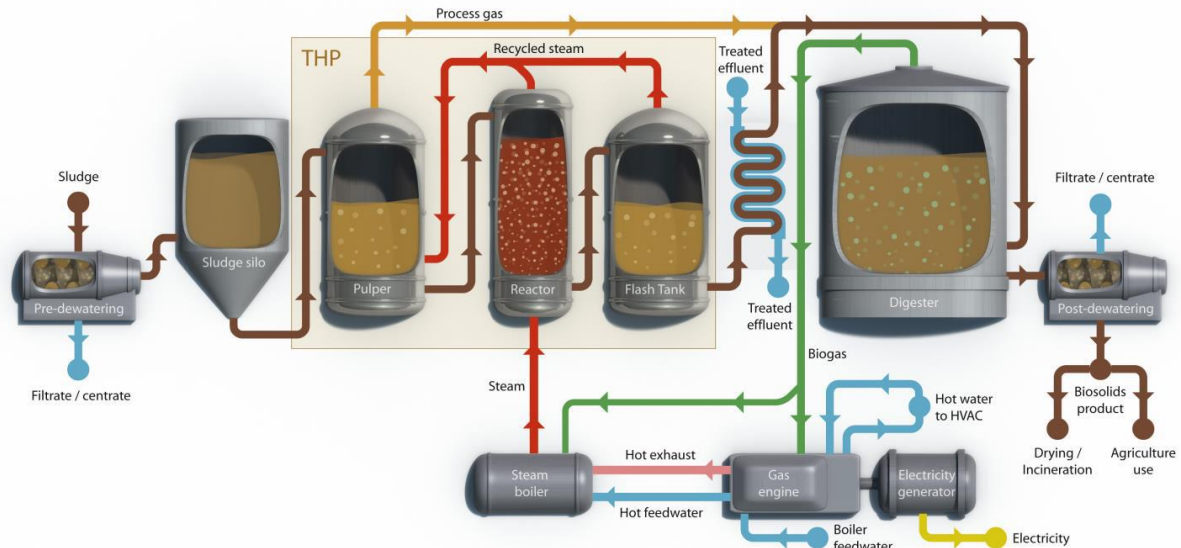
Figure 2.2 Cambi™ THP process schematic diagram (Typical Mark II arrangement) (Williams & Burrowes, 2016)

In Cambi™ system, pre-dewatered sludge with 15–17% solids concentration is loaded to the pulper tank. The pulper tank is heated by harnessing the recycled steam from the flash tank. The sludge is detained in the pulper tank until the reactor is all set for batch processing. The sludge is pumped to the reactor where the reaction takes place for 20–30 minutes at 155–175°C and 6 bar pressure. Depending on the temperature, steam is injected to attain this temperature and pressure. Finally, the sludge flows to the flash tank where a sudden pressure drop causes the bacterial cells to break down, and the processed solids have substantially lower viscosity. The temperature of the solids is also reduced by flashing, but sometimes additional cooling is also needed to meet the required temperature for the feed to AD of 37°C (99°F). Addition of condensed water from the steam and dilution water results in 6–10% solids concentration fed to AD (Williams & Burrowes, 2016; Dandan Zhang et al., 2019). Dilution is also done to dilute the concentration of total ammonia nitrogen (TAN) in order to reduce its toxicity in AD (Barber, 2016). The time required for Cambi™ process is approximately 64–74 minutes, being 29 minutes for loading the sludge and injecting steam into the reactor; 20–30 minutes retention time in the reactor; and 15 minutes of blowdown to the flash tank. Multiple sequencing Cambi™ reactors can be operated to accomplish a semi-continuous flow between pre-dewatering and AD (Williams & Burrowes, 2016; Dandan Zhang et al., 2019). In The Netherlands, Cambi™ system is used in Tilburg and Hengelo WWTPs (Lou, 2019).

Sustec TurboTec®
In TurboTec® system, raw sludge with a temperature of about 20°C is combined with partly cooled hydrolysed sludge with a temperature of 105°C. The mixture reaches a temperature of approximately 65°C. TurboTec® uses its patented Mobius separator to isolate the thinner hydrolysed sludge and thicker un-hydrolysed sludge. The thinner sludge is fed into the digester, whereas the thicker sludge is fed into a heat exchanger and then into the hydrolysis reactor (Williams & Burrowes, 2016). The schematic diagram of TurboTec® is shown in Figure 2.3. Sustec declares that by applying this process, a minimum amount of steam is required to heat the already pre-heated sludge to the reactor temperature of 140–180°C for 30–60 minutes (Pereboom et al., 2014). Sustec also proclaims that the amount of COD that goes through the post digestion dewatering filtrate is less due to operation at the lower reactor temperature than other THP systems (Williams & Burrowes, 2016). As the vendor states on their website, Sustec TurboTec® THP system has 60% lower operating costs in comparison to conventional batch THP processes (Sustec, 2014). TurboTec® is employed in WWTPs in Apeldoorn and Venlo (Lou, 2019; Pereboom et al., 2014).
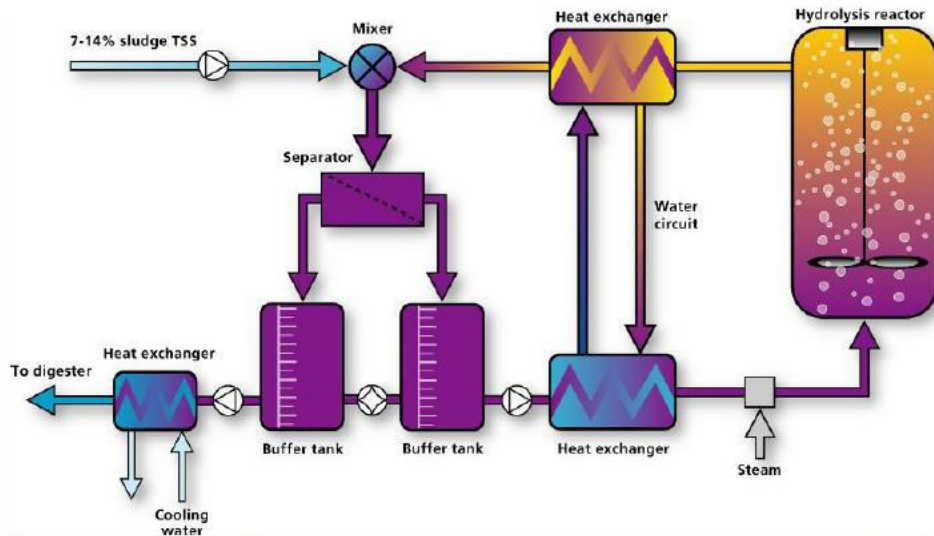
Figure 2.3 SusTec TurboTec® process schematic diagram (Williams & Burrowes, 2016)

Lysotherm®

The Lysotherm® process supports the continuous operation and is built upon the indirect heating of sludge with two heating circuits, namely thermal oil circuit and regenerative circuit (Geraats et al., 2014). No steam is used as a heat transfer medium in this system (Williams & Burrowes, 2016). As an alternative, the thermal oil circuit is used to transport the heat. In this system, the heat generated by the Combined Heat and Power (CHP) engines (cooling water and exhaust gas heat) is employed to warm up the digesters and to steer the sludge hydrolysis process (Eliquo Water & Energy, 2015). In the first stage, the sludge is pre-heated using recovered heat from the cooling phase. The thermal oil circuit provides the tubular hydrolysis reactor with the required process heat. The heat is obtained using a heat exchanger from the flue gas of the associated CHP engines. In the next stage, hydrolysis occurs at 140–170°C in the reactor for 15–30 minutes. After hydrolysis, sludge temperature is lower down in the heat exchanger to the suitable temperature for feeding to AD. The regenerative circuit uses water as the heat transfer medium (Williams & Burrowes, 2016). The regenerative circuit recovers the heat from the hydrolysed sludge cooling system; therefore, it can be reused for pre-heating the first stage (Geraats et al., 2014). Figure 2.4 illustrates the process flow of the Lysotherm® thermal hydrolysis system.
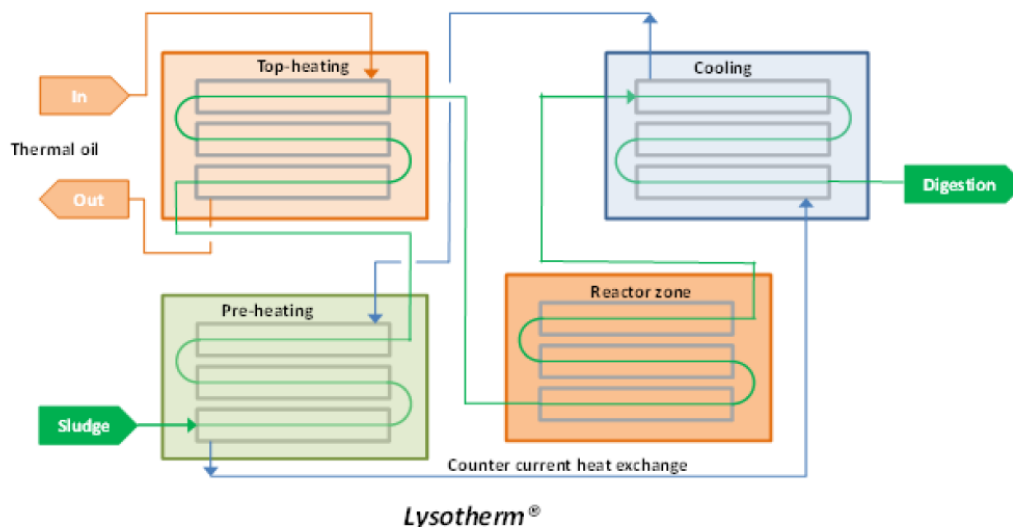
Figure 2.4 Lysotherm® process schematic diagram (Geraats et al., 2014)

Comparison between Cambi™, Sustec TurboTec®, and Lysotherm®

The summary of the comparison between the three THP systems described in the preceding paragraphs is given in Table 2.1.

Table 2.1 Comparison between Cambi™, Sustec TurboTec®, and Lysotherm®

Difference	Cambi™	Sustec TurboTec®	Lysotherm®
Flow	Batch or semi-continuous	Continuous	Continuous
Heat transfer medium	Steam	Steam	Oil
Hydrolysis temperature	155–175°C	140–180°C	140–170°C
Hydrolysis reaction time	20–30 minutes	30–60 minutes	15–30 minutes
Pre-heating technique	Using recycled steam from the flash tank	Mixing the feed with partly-cooled hydrolysed sludge	Using recovered heat from the cooling phase

2.1.3. Benefits and drawbacks of THP

The previous sections have elucidated the different THP system configurations. Despite the benefits of THP, thermal processing of sludge also results in some drawbacks. Table 2.2 and Table 2.3 summarise the benefits and drawbacks of THP.

Table 2.2 Benefits of THP

Benefits	References
Increases the biodegradability of waste activated sludge	Liao et al., 2016; Xue et al., 2015
Increases the biodegradability of primary sludge in terms of COD, proteins, and polysaccharides	Wilson & Novak, 2009
Allows significantly higher loading rates of an anaerobic digester, resulting in smaller reactor	Xue et al., 2015
Increases rate of biogas production	Barber, 2016
Decreases sludge viscosity	Bougrier et al., 2006; Liao et al., 2016; Liu et al., 2012; Xue et al., 2015
Improves sludge dewaterability on all dewatering technologies	Oosterhuis et al., 2014; Phothilangka et al., 2008
Biosolids leaving the THP reactor is sterile	Barber, 2016
Removes scum and foaming	Alfaro et al., 2014

Table 2.3 Drawbacks of THP

Drawbacks	References
High energy demand (dependent on system configurations)	Barber, 2016
Increases of ammonia concentration in anaerobic digester effluent compared to without THP	Wilson & Novak, 2009
Production of refractory materials from the Maillard reaction (melanoidins)	Dwyer et al., 2008; Liu et al., 2012; Wilson & Novak, 2009
More difficult operation and maintenance than anaerobic digester without THP	Barber, 2016
Requires cooling down of the sludge before digestion	Barber, 2016
Releases more nutrients hence increases the potential of uncontrolled salt crystallisation	Barber, 2016
Drives the dissolution of complex particulate matter including heavy metals	Barber, 2016

2.1.4. Increase of soluble organic matter and nutrients

As explained in Section 2.1.3, one of the advantages of THP is an increase in the biodegradability of waste activated sludge (WAS). This happens because some parts of complex organic matter in sludge is converted

into the degradable organic matter during THP. When the microbial cells in WAS break down due to high temperature and high pressure, macromolecule organics are dissolved into degradable molecules (Dandan Zhang et al., 2019). Dissolution primarily occurs to proteins and carbohydrates, the two major organic compounds in WAS (Xue et al., 2015). The release of soluble organic matter during THP is indicated by the increase of sCOD/tCOD and a decrease of TSS/TS concentrations (Liao et al., 2016; Dandan Zhang et al., 2019). Alongside with the increase of soluble organic matter, sludge viscosity also decreases due to the decomposition of extracellular polymeric substances (EPS) (Liao et al., 2016).

The increased solubility and decreased viscosity of thermally hydrolysed sludge will accelerate the hydrolysis process in AD which eventually increase biogas production for more than 10% and reduce digestion duration (Liao et al., 2016). However, the higher biogas production does not directly correspond to energy benefit, because the additional biogas produced during AD is partially used to compensate the energy required to provide high temperature in THP (Barber, 2016). The main energy benefit from THP comes from the fact that THP also improves the dewaterability of digested sludge, which evidently reduces the costs of downstream sludge transport and drying (Barber, 2016).

In addition to organic matter dissolution, THP also releases more nutrients (Barber, 2016). An increase in the concentration of TAN in water is discovered after THP due to degradation of proteins in THP (Barber, 2016; Dandan Zhang et al., 2019). Phosphorus that is bound to WAS is also released as phosphate ions during THP (Laurent et al., 2011). The application of THP will predominantly result in the production of reject water of anaerobically digested sludge with a high concentration of nutrients, especially ammonia nitrogen and phosphorus (Driessen et al., 2018). Therefore, the side-stream or reject water treatment after AD should also be evaluated in the presence of THP.

2.1.5. Formation of refractory compounds

One of the significant disadvantages of THP is the formation of refractory humic-like substances (Dwyer et al., 2008; X. Liu et al., 2012; Wilson & Novak, 2009). The notable ones are the production of Malliard and Amadori products, e.g. melanoidins. Melanoidins are brown-coloured heterogeneous polymers (Dwyer et al., 2008; X. Liu et al., 2012; Xue et al., 2015). Melanoidins are produced by non-enzymatic chemical reactions between reducing sugars and the amino groups of amino acids, peptides, or proteins (Martins et al., 2008; H. Y. Wang et al., 2011). Melanoidins are distinguished from the brown-coloured compound melanins, which are produced by enzymatic browning reactions (Nursten, 2005). The Malliard reaction is a complex reaction, which can be divided into three stages in seven different reactions. In addition to those three stages and seven reactions, there is also the eighth reaction, reaction H, which represents Maillard reaction intermediates (Nursten, 2005). The scheme of the Maillard reaction is presented in Figure 2.5.

The different stages and reactions of the Maillard reaction are as follows:

I. **Initial stage**: production of colourless compounds without ultraviolet (UV) absorption
   Reaction A: Sugar-amine condensation
   Reaction B: Amadori rearrangement
II. **Intermediate stage**: production of colourless or yellow-coloured compounds with strong UV absorption
   Reaction C: Sugar dehydration
   Reaction D: Sugar fragmentation
   Reaction E: Amino acid degradation
III. **Final stage**: production of highly coloured compounds
   Reaction F: Aldol condensation
   Reaction G: Aldehyde-amine condensation and formation of heterocyclic nitrogen compounds
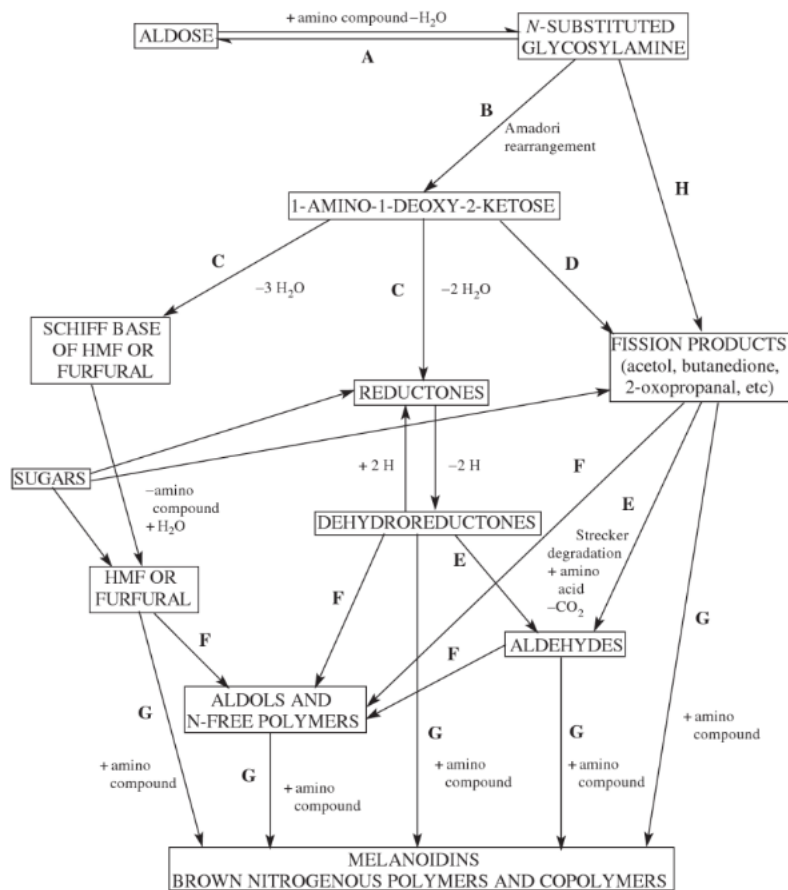
Figure 2.5 Maillard reaction and melanoidins formation (Nursten, 2005)

As heterogenous polymers, melanoidins can be classified as high molecular weight (HMW, more than 10 kDa) and low molecular weight (LMW, less than 3.5 kDa) fractions (Ćosović et al., 2010; H. Y. Wang et al., 2011). The production of either HMW or LMW melanoidins is dependent on the reaction time and heating intensity. HMW melanoidins are generated at longer reaction time; meanwhile, LMW melanoidins are generated at the initial stages of Maillard reaction. It is considered that LMW melanoidins go through polymerisation reactions or form cross-linkages with other products of Maillard reaction to produce HMW melanoidins in the later stages of the reaction (H. Y. Wang et al., 2011). Furthermore, the fraction of hydrophobic groups in the melanoidins is reported to increase along with the reaction duration (Ćosović et al., 2010). A lower heating temperature and time, for example at 95–100 °C for 2–5 hours, will mainly produce LMW melanoidins while HMW melanoidins are generally obtained under a higher temperature or a longer time, for example at 121 °C for 30 min or 100 °C for more than 48 hours (Dian Zhang et al., 2020). For the average operating temperature of THP, e.g. 140–165 °C for 30 min, the increase in colour and release of melanoidins have been primarily associated to HMW melanoidins (Dwyer et al., 2008). The temperature has an essential role in determining the Maillard reaction rate constant for each step mentioned in Figure 2.5, and it also controls the dominant reaction pathways and the degree of polymerisation and crosslinking (Dian Zhang et al., 2020). In addition to reaction time and temperature, pH acts as a key factor that influences the formation of melanoidins and its reactivity (H. Y. Wang et al., 2011; Dian Zhang et al., 2020). More alkaline environment leads to the formation of unprotonated amine, which is regarded as the reactive amino group and eventually increases the melanoidins formation rate. pH also determines which reaction pathway will take place, either to form furfural (pH < 7), fission products (pH = 7), or reductones (pH > 7) (Dian Zhang et al., 2020).

Despite efforts made by previous studies, the overall structure of melanoidins is not fully understood because of their heterogenicity. In spite of its heterogenicity, it has been reported that melanoidins are

negatively charged (H. Y. Wang et al., 2011). The melanoidins from model systems, bread crust, coffee, and the ones generated after thermal degradation, were shown to be mainly composed of furans accompanied by carbonyl compounds, pyrroles, pyrazines, and pyridines (H. Y. Wang et al., 2011). The structures of melanoidins-like compounds are shown in Figure 2.6. Melanoidins have been reported to have similar chemical characteristics with HS (Ćosović et al., 2010; P. Huang et al., 2005). HS themselves can be classified into three different compounds: humin which is insoluble at all pH range, humic acids (HA) which is soluble at pH above 2, and fulvic acid (FA) which is soluble at all pH range (Adusei-Gyamfi et al., 2019).
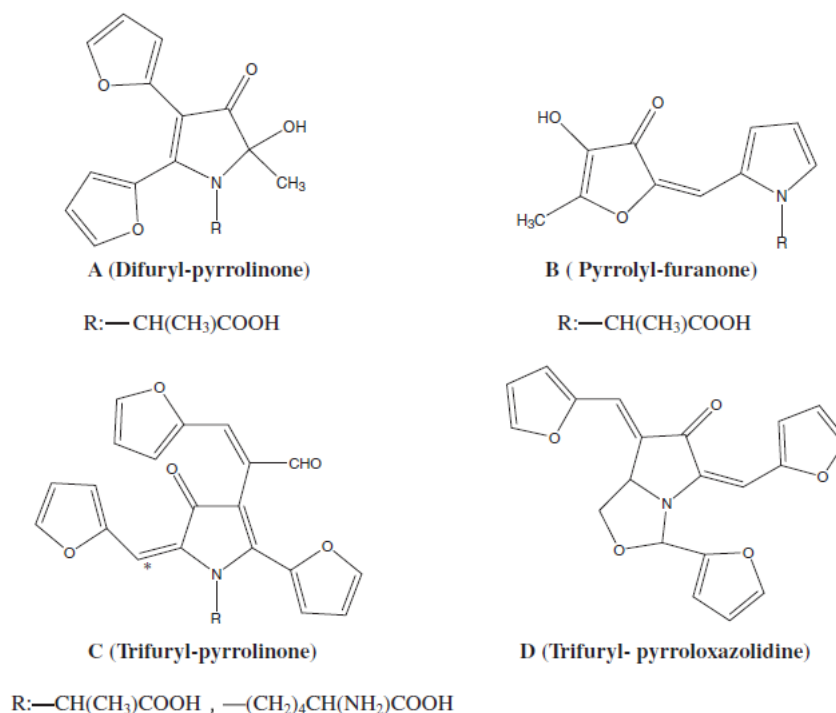
Figure 2.6 Some LMW compounds with similar structures as melanoidins

The presence of melanoidins reduces the biodegradability of thermally hydrolysed sludge, as it reduces the fraction of biodegradable organic matter (Dandan Zhang et al., 2019). The increase in the reaction temperature affects the production of these compounds (Bougrier et al., 2006; X. Liu et al., 2012). It is evident by the fact that the amount of sCOD produced during THP pre-treatment becomes less biodegradable at higher temperatures (Dwyer et al., 2008). Because the production of melanoidins is dependent on the reaction temperature, operation of THP at a lower temperature is suggested to relieve the issues related to melanoidins and colour formation (Barber, 2016; Dwyer et al., 2008). Lowering the reaction temperature of THP below 160°C may lessen the production of brown coloured polymers caramelans (Villamiel et al., 2007) with insignificant influence on digestion performance (Dwyer et al., 2008). The production of melanoidins does not only reduce the biodegradability of thermally hydrolysed sludge but also obstructs UV disinfection of the digestate because the colour absorbs the UV beams (Adusei-Gyamfi et al., 2019). In addition to that, nitrogen-containing refractory compounds can also be produced during Maillard reaction. Melanoidins are known to contain refractory nitrogen (Dian Zhang et al., 2020). The refractory nitrogen in melanoidins will undoubtedly increase the concentration of nitrogen in the effluent as well (Dwyer et al., 2008). The intensive generation of refractory compounds hence affects the fulfilment of stringent nutrient regulations in certain countries, including in EU and USA (Shepherd et al., 2016; Dian Zhang et al., 2020). Release of the refractory nitrogen is predicted to be three times higher compared to conditions without THP (Barber, 2016).

2.1.6. Release of heavy metals and trace elements
Another major disadvantage of THP is the solubilisation of heavy metals. Typically, the higher operating temperature and longer reaction time favour the release of both organic and inorganic matters, including

heavy metals and trace elements (Appels et al., 2010). Heavy metals are metals that are usually toxic at low concentrations and not essential for the growth of living organisms (such as Ag, As, Cd, Cr, Hg), whereas trace elements are not toxic and essential for the growth of living organisms at low concentrations (for instance B, Co, Mo, Se, Zn) (Marcovecchio et al., 2007; Van De Graaf et al., 1996; Zoroddu et al., 2019). The higher the energy that is applied to the sludge, the more of these elements are dissolved into the liquid phase (Appels et al., 2010).

THP increases the chance of heavy metals release, but as THP changes the physicochemical characteristics of the sludge, the sludge may also adsorb heavy metal ions that are initially already present in the liquid phase. Depending on their chemical characteristics, certain elements will end up in the solid phase (sludge) or liquid phase (supernatant) after the application of THP (Laurent et al., 2011). This thesis will go deeper into the elements that remain in the liquid phase because these are more relevant to reject water treatment of anaerobically digested sludge. It has been reported that the concentrations of Cr, Cu, Zn, and Ni in liquid phase were highly multiplied after the application of THP at various temperature and reaction time (Appels et al., 2010). The fate of heavy metals released during the application of THP should be taken into consideration, as they will end up either in the sludge or leak through the treated wastewater (Laurent et al., 2011).

The release of heavy metals by THP happens due to the destruction of the sludge. Heavy metals, which are embodied in the sludge, is being diffused from the sludge to the aqueous phase at elevated temperature because the diffusivity of ions is enhanced at high temperatures (Veeken & Hamelers, 1999). The changes in physicochemical properties such as pH and ionic strength will further promote the mobility and solubilisation of metal ions (Appels et al., 2010; Dewil et al., 2007). Additionally, heavy metals are also bound to the extracellular polymeric substances (EPS), which present much potential anionic and cationic binding sites including carboxylates, amines, thiols and phosphates (Appels et al., 2010; Dewil et al., 2007). The degradation of these structures drives to the dissolution of the bounded heavy metals (Dewil et al., 2007).

The solubilised carbohydrates, proteins, and humic-like substances provide free active sites for heavy metals complexation in the liquid phase (Laurent et al., 2011). Humic-like substances generated during THP are prone to bind with metal ions and expected to control their bioavailability (Driessen et al., 2020). Although HS have diverse functional groups, the most important ones for metal binding are the carboxyl and the phenolic groups, which have strong affinities for metals, depending on the pH. Once the complexation occurs, the newly formed substance will be different from the individual components, resulting in new physical properties. In the complexation between HS and metals, the metals act as the central atom and HS act as ligands (Adusei-Gyamfi et al., 2019). The metals may form different configurations with the ligands. The ligand can provide either a single or multiple donor atoms. If only one donor atom is coordinated, it is designated as a monodentate ligand, and if multiple donor atoms are associated, it is termed as polydentate ligands. Bidentate ligands then mean two ligands that are coordinated with two metal ions. For polydentate ligands, the next lone pair of electrons after the first coordination is oriented in a way that impedes them to coordinate with the same central metal atom. In a specific condition where the existing covalent bond is distorted, two lone electron pairs from a ligand can be linked to the same central atom, resulting in a cyclic compound known as a chelate (Figure 2.7) (Lawrance, 2010). There are different types of complexation between HS and metal, where HS can bind to the metal directly (inner-sphere complexation) or bridged by water molecules (outer-sphere complexation) (Adusei-Gyamfi et al., 2019). The properties of both HS and the metals will affect the complexation mechanism. Table 2.4 summarises the preferential binding sites for HS-metal complexation.
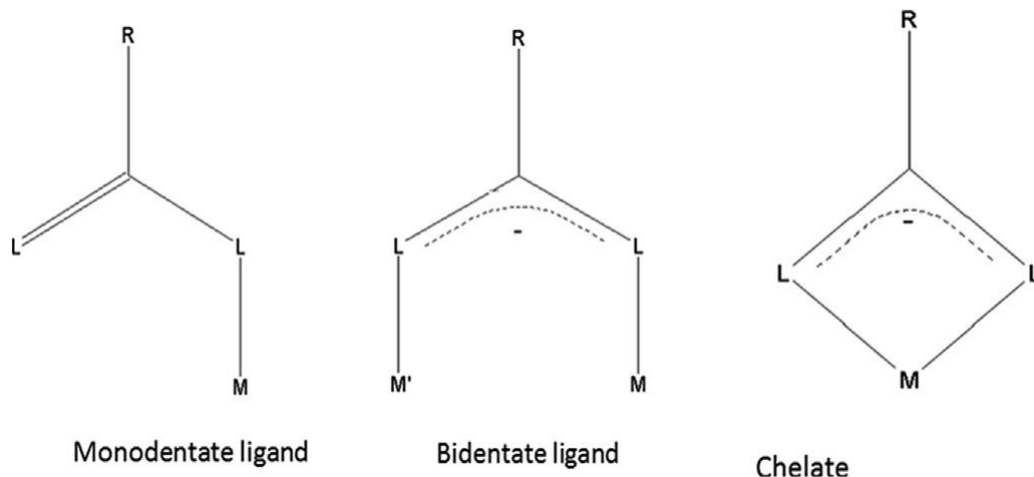
Figure 2.7 Possible configuration of metal (M) and ligand (L) (Lawrance, 2010)

Table 2.4 Preferential binding sites for HS-metal complexation

Metal	Preferred binding sites	References
Ca	Both carboxylic and phenolic groups	Adusei-Gyamfi et al. (2019)
Cu	Phenolic groups at pH 4–8, but complexes formed with carboxyl groups and HMW fractions are stronger	Manceau & Matynia (2010)
Ni	Amine groups at LMW fractions	Cabaniss (2011)
Zn	Amine groups	Cabaniss (2011)
Fe	Both carboxylic and phenolic groups	Marsac et al. (2013)
Al	Phenolic groups	Adusei-Gyamfi et al. (2019)

General scheme of natural organic matter (NOM, general terminology for complex organic compounds that have HS as its fraction) complexation with metals and metal hydroxide is shown in Figure 2.8. The fact that humic-like substances generated by the THP process are known to bind with these metals is essential to be understood because it results in the decrease in the bioavailability of essential trace elements that are required for the subsequent side-stream treatment units like PN/A reactors (Driessen et al., 2020).
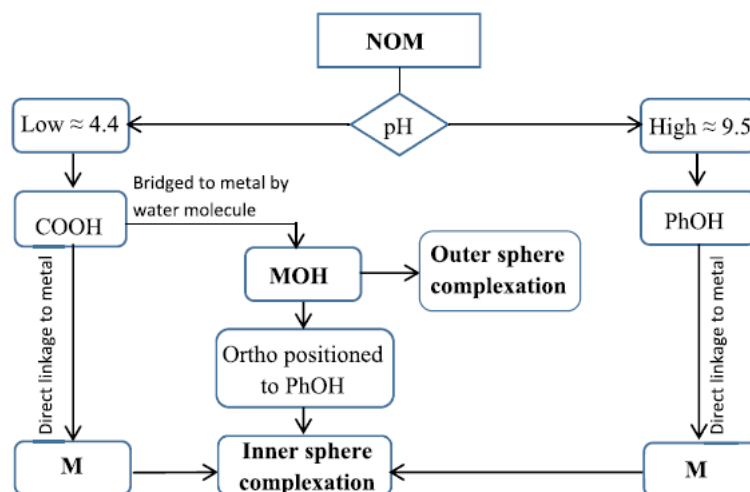
Figure 2.8. A scheme of the carboxyl (COOH) and phenolic (PhOH) groups complexation with metals (M) and metal hydroxide (MOH) (Adusei-Gyamfi et al., 2019)

2.2.1. Struvite formation and influencing factors

Struvite is formed when magnesium, ammonium, and phosphate with the same molar ratio react with six water molecules, resulting in a compound with a chemical formula of $MgNH_4PO_4.6H_2O$ (de Buck, 2012). The formation of struvite is shown in Equation 1 (Shih & Yan, 2016). Struvite is formed when solutions containing phosphate ions react with magnesium and ammonium ions in alkaline conditions (7 < pH < 11) (Hutnik et al., 2013). Increase in pH (6–10) results in a decrease in the maximum solubility of struvite, thereby increasing the potential for deposition of struvite (Mehta & Batstone, 2013). Struvite has low solubility in water with pKsp values varying between 13.22±0.02 at 20°C (Wei et al., 2019) and 13.15 at 25°C (Warmadewanthi & Liu, 2009). Based on its composition, per mass unit struvite contains 13% phosphorus which can be used as fertiliser. Struvite is also a useful source for nitrogen and magnesium, as it consists of as much as 6% and 10%, respectively (Li, Boiarkina, et al., 2019). However, due to the low magnesium concentration in almost all wastewater streams, the addition of magnesium is always needed for struvite crystallisation (Muhmood et al., 2018). The magnesium source most often used for this reaction is magnesium salts which dissolve easily in water, such as $MgCl_2$ and $MgSO_4$ (H. Huang et al., 2016).

$$Mg^{2+} + NH_4^+ + H_nPO_4^{n-3} + 6H_2O \rightarrow MgNH_4PO_4.6H_2O + nH^+ \qquad (1)$$
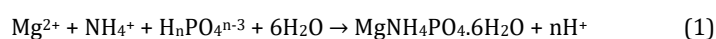
One of the advantages of struvite compared to other commercial P-based fertilisers is its slow-release characteristic, which implies its capability to release nutrients slowly during the growing season (Md Mukhlesur Rahman et al., 2014). The slow-release characteristic of struvite comes from the low solubility of struvite in water compared to regular P-based fertilisers. It is therefore considered that the availability of P from struvite at the short time is lower than that of common P-based fertilisers (de Vries et al., 2017). Furthermore, the N leaching rate of struvite is three times lower than common N-based fertilisers (Md M. Rahman et al., 2011). The slow nutrient leaching feature of struvite prevents plant roots from deterioration (H. Huang et al., 2019). Phosphorus recovery as struvite fertiliser also has a positive impact on environmental preservation because it can utilise the available material in wastewater, reduce P and N discharge, decrease the need of rock phosphate, and minimise greenhouse gases emissions from excessive N fertilisation (Md Mukhlesur Rahman et al., 2014).

Several conditions and factors affect struvite crystallisation. These include molar ratio, pH, and the method used for the crystallisation process (Tang et al., 2019). Temperature, mixing speed, presence of impurities, and seeding also influence the formation of struvite (Decrey et al., 2011). All of these factors will be further discussed in the following paragraphs.

Molar ratio of reactants
The molar ratio is a factor that greatly influences the conditions of supersaturation in solution (Li, Huang, et al., 2019). The concentration of each struvite-forming element strongly influences the condition of supersaturation. When ion activity product (IAP) is exceeding the solubility product constant (Ksp), the solution is supersaturated; hence struvite will nucleate and grow until the system reaches equilibrium again (Md Mukhlesur Rahman et al., 2014).

Various studies have investigated the effective Mg:P-PO_4 molar ratio for struvite crystallisation, ranging from 1:0.8 until 1:1.2 (Hutnik et al., 2013; Y. H. Liu et al., 2011; Md M. Rahman et al., 2011). As seen in Equation 1, the coefficients of the reactants are 1:1:1, which imply that phosphate should be the limiting reagent so that phosphate could be removed efficiently. This explains why a slightly higher Mg:P-PO_4 is preferred for struvite crystallisation (Li, Huang, et al., 2019). However, a further increase of Mg:P-PO_4 molar ratio will not increase phosphorus removal efficiency substantially, as it will increase the chemical dosage cost (Desmidt et al., 2013). The addition of excess magnesium may escalate the removal efficiency of the process by increasing the supersaturation; however, it will also decrease the purity of the obtained struvite due to the precipitation of undesirable precipitates such as newberyte ($MgHPO_4.3H_2O$), bobierrite ($Mg_3(PO_4)_2.8H_2O$), and brucite ($Mg_3(PO_4)_2.22H_2O$) (Li, Huang, et al., 2019; Warmadewanthi & Liu, 2009). Overall, the optimum Mg:P-PO_4 ratio varies depending on wastewater composition, and it cannot be

generalised for all types of wastewater. Phosphorus removal efficiency, product purity, and chemical dosage costs should be considered to determine the optimum Mg:P-PO$_4$ ratio.

Excess ammonium would be beneficial in the formation of struvite because it increases the saturation index (SI) of struvite and enhances the chance to obtain struvite with high purity (Warmadewanthi & Liu, 2009). Besides, the removal efficiency of phosphorus increases along with increasing molar ratio N-NH$_4$:P-PO$_4$ (Nelson et al., 2003; Warmadewanthi & Liu, 2009). Struvite crystallisation is also more favourable when the N-NH$_4$:P-PO$_4$ molar ratio of the solution is above one (Capdevielle et al., 2014). In general, the molar concentration of N in domestic wastewater is higher than P (Decrey et al., 2011; Driessen et al., 2018; Oosterhuis et al., 2014; Ronteltap et al., 2010). Besides, with the presence of THP, the concentration of ammonium in reject water of anaerobically digested sludge can increase three times higher (Oosterhuis et al., 2014), resulting in even higher N-NH$_4$:P-PO$_4$ molar ratio available for struvite crystallisation.

pH

The pH plays a vital role in struvite crystallisation because it influences the solubility and supersaturation of struvite (Li, Huang, et al., 2019; Md Mukhlesur Rahman et al., 2014). The solubility of struvite decreases with the increase in pH (Md Mukhlesur Rahman et al., 2014). Bases such as MgO, Mg(OH)$_2$, NaOH, KOH, and K$_2$CO$_3$ are typically added to increase the pH for struvite crystallisation (Li, Huang, et al., 2019). Addition of bases is necessary because, in principle, struvite forming reaction releases protons (Equation 1) (Shih & Yan, 2016). Struvite can be precipitated at a broad range of pH, ranging from 7–11.5, but the efficient pH for optimum P and N removal ranges between 7.5 to 9 (Md Mukhlesur Rahman et al., 2014). Generally, a higher pH will result in a higher P removal efficiency (Li, Huang, et al., 2019); however, this is limited to some extent because high pH will also transform soluble ammonium into volatile ammonia gas (Md Mukhlesur Rahman et al., 2014). pH also influences the development of other Mg and P-containing precipitates, such as newberyite, bobierrite, and brucite (Li, Huang, et al., 2019). Newberyite is formed when the pH is lower than 7; meanwhile, bobierrite and brucite start forming at pH higher than 9 (Chimenos et al., 2006; Md Mukhlesur Rahman et al., 2014). In addition to that, the presence of calcium ions in wastewater may also compete with Mg to form undesirable hydroxyapatite in higher pH value (Md M. Rahman et al., 2011). Some studies, therefore, concluded that the neutral pH promotes the production of pure struvite with struvite content higher than 90% (X. Hao et al., 2013; X. D. Hao et al., 2008; Md Mukhlesur Rahman et al., 2014; C. C. Wang et al., 2010). On top of that, pH also influences the crystal size of struvite. Several studies revealed that higher pH would decrease the crystal size of struvite (Li, Huang, et al., 2019; Md Mukhlesur Rahman et al., 2014). Increase in pH promotes the formation of more nuclei, hence causing the production of smaller crystals. Higher pH in the struvite reactor will also lead to a bigger variation in particle size (Md Mukhlesur Rahman et al., 2014).

Temperature

In addition to pH, the temperature is another factor that is related to the solubility of struvite. Increase in temperature will also increase the solubility of struvite (Li, Huang, et al., 2019). In open systems, high temperatures lead to the volatilisation of free ammonia, and hence the solubility of struvite increases to restore the ammonium equilibrium (Capdevielle et al., 2014). This means that at high temperatures, struvite dissolution is more favourable than struvite precipitation (Crutchik & Garrido, 2016). Several studies also confirmed that pKsp value of struvite decreases with increasing temperature from 15 until 30°C (Bhuiyan et al., 2007; Crutchik & Garrido, 2016; Hanhoun et al., 2011). It has also been reported that high temperature promotes the crystallisation of other amorphous struvite-like minerals, and thus decreases struvite purity (Capdevielle et al., 2014). However, different reaction mechanisms occur in wastewater with varying composition; therefore the effect of temperature on struvite crystallisation of different wastewater needs to be fully understood (Li, Huang, et al., 2019).

Mixing

A sufficient mixing for struvite crystallisation is consistently required (Li, Huang, et al., 2019). Mixing intensifies the mass transfer from solute to crystal during the crystallisation reaction, and subsequently improves the development of crystal nuclei and growth (Kim et al., 2009; Li, Huang, et al., 2019). The

formation of crystal nuclei is affected by mixing intensity or gradient; meanwhile, the growth is influenced by mixing duration (Jones, 2002). The increase in the mixing intensity, nonetheless, does not always increase the development of crystals because excessive mixing can reduce the tendency of crystals to nucleate (Mullin, 2001). Two most common mixing techniques for struvite crystallisation include mechanical stirring and fluidised bed (Li, Boiarkina, et al., 2019). Different mixing techniques will result in different crystal size (Ronteltap et al., 2010), but in general, mixing will enhance the removal efficiencies of N and P (Kim et al., 2009). Li, Huang, et al. (2019) reported that the phosphorus removal without mixing would only reach up to approximately 73%; meanwhile, it goes up to 97% under the mixing rate of 160 rpm. Mixing rate higher than 240 rpm will not enhance phosphorus removal efficiency any further. Lower stirring rate favours nucleation over crystal growth because it increases the local supersaturation (Ronteltap et al., 2010). For these reasons, the control in the mixing should be taken into account for struvite crystallisation process optimisation (Li, Huang, et al., 2019).

Impurities

The presence of impurities or foreign ions other than Mg^{2+}, NH_4^+, and PO_4^{3-} is known to either influence the reaction rate, N and P removal efficiencies, morphology, or the purity of recovered struvite (Li, Huang, et al., 2019). These foreign ions are prone to co-precipitate in the form of slightly soluble hydroxides or phosphates in alkaline solution, which will change the chemical composition of struvite (Md Mukhlesur Rahman et al., 2014). In addition to foreign ions, organic matter also contributes to the disturbance of struvite crystallisation (Li, Huang, et al., 2019). This thesis will further discuss the effect of impurities in the form of melanoidins and trace elements on struvite crystallisation in Section 2.2.3 and 2.2.4.

Seeding

Seed materials act as a body on which further aggregation of the crystals happens (Tarragó et al., 2016). In struvite formation, seeding enhances struvite crystallisation by providing a surface for the reaction and subsequently reduces induction time for crystal establishment (Ali & Schneider, 2005). Seeding with struvite crystals or inert material can be used to improve nucleation in struvite crystallisation and increase the efficiency of phosphorus recovery (Tarragó et al., 2016). Seeding can also increase the final product quality because struvite crystallisation is accelerated on the surface of seeding materials (Li, Boiarkina, et al., 2019). The excellent characteristics of seed material are large surface area to aid nucleation, unreactive to the crystallising solution, and isomorphism (similarity of crystal form) with the crystallising crystal (Ali & Schneider, 2005; Whittaker, 1981). Effective seeding does not mean that the seed crystals must be the same as the material being crystallised, as isomorphous solids are often promising to induce crystallisation (Mullin, 2001).

2.2.2. Nucleation and growth

There are two different phases during struvite crystallisation, namely the nucleation phase and the growth phase. Nucleation is defined by the establishment of an initial crystal foundation, formed by ion particles that are clustered together (Ohlinger et al., 1999). The time interval between the supersaturation condition and the formation of the crystal nuclei is termed as the induction time (Mullin, 2001). Induction time is remarkably influenced by several factors, including the degree of supersaturation, mixing, presence of impurities, viscosity, temperature, etc. (Mullin, 2001). The growth phase is the phase when the nuclei grow into crystals with detectable size (Kataki et al., 2016).

Nucleation

Nucleation is divided into two different categories: primary nucleation and secondary nucleation. Primary nucleation is further categorised into homogenous and heterogeneous nucleation. Primary nucleation is a nucleation case that happens in a system with no crystalline matter; meanwhile, secondary nucleation is the nucleation that is promoted by crystals that are already present in the system (Mullin, 2001). In primary nucleation, homogenous nucleation occurs spontaneously and heterogenous nucleation occurs by the induction of foreign particles. It is certainly recognised that pure homogeneous nucleation is not a prevalent occasion. It is nearly impossible to have a solution without any foreign bodies; thus, primary heterogeneous nucleation is more common (Mullin, 2001). Nucleation that happens with the existence of

microscopic impurities of size smaller than 0.45 µm in the solution is referred to heterogeneous nucleation (Mehta & Batstone, 2013). Primary heterogeneous nucleation occurs, for example, with the presence of dust particles in the solution (Md Mukhlesur Rahman et al., 2014). The secondary nucleation is a terminology used to define the formation of nuclei in a supersaturated solution when crystals of the solute are already present or intentionally added to the system (Mehta & Batstone, 2013; Mullin, 2001). Supersaturated solution nucleates much faster when the crystals already exist, therefore the addition of the seed crystals can induce crystallisation, and thus the nucleation goes faster (Mullin, 2001). The secondary nucleation plays an essential part in determining the final particle size distribution. The secondary nucleation rate is controlled by various parameters such as temperature, mixing speed, amount of seed materials, and supersaturation (Mehta & Batstone, 2013). The basic scheme of classification of nucleation is shown in Figure 2.9.

Several studies proposed ways to measure nucleation and induction time in struvite crystallisation. These studies mainly rely on pH as an indication of nucleation and induction time. The time elapsed between pH adjustment and pH change which could be detected in the solution, e.g. pH drop by 0.001 – 0.05 is considered as induction time (Borcan, 2019; Mehta & Batstone, 2013; Tarragó et al., 2016; Wei et al., 2019). However, pH is a sensitive parameter, and the accuracy of the pH measuring system will determine the sensitivity of this method.
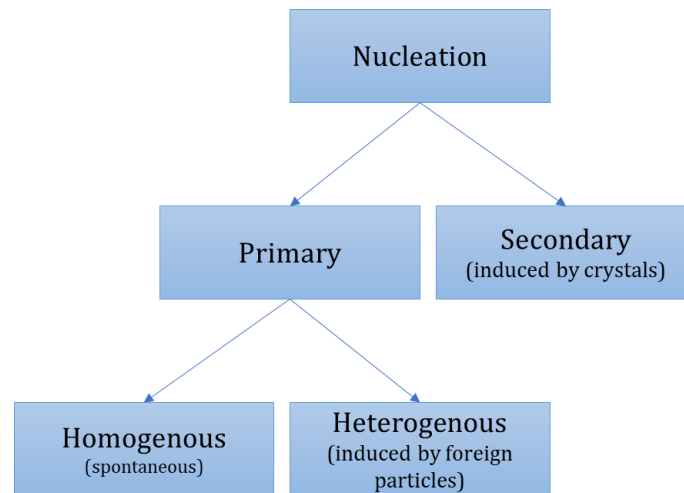
Figure 2.9 Classification of nucleation (Mullin, 2001)

Growth

The growth phase is a phase when a stable formed nucleus starts to grow into a crystal with distinguishable size (Mullin, 2001). Growth will continue until the system reaches equilibrium (Ohlinger et al., 1999). Crystal growth is a complex process which is influenced by many parameters including pH, temperature, supersaturation, mixing intensity, and presence of impurities (Mehta & Batstone, 2013; Mullin, 2001). The crystal growth process comprises of two consecutive mechanisms, e.g. mass transfer (by diffusion or convection) of solute molecules from the bulk solution and the integration of solute molecules into crystal surface (Mehta & Batstone, 2013). As mentioned in Section 2.2.1, the presence of seed materials holds substantial importance in providing a surface for the growth of crystals; therefore, crystal growth is also enhanced by seeding.

Crystal growth rates can be determined by measuring the average size of the crystals as they grow or by measuring the decrease of reactant concentration as the result of the growth of crystals. However, the first method is challenging to be done in unfiltered wastewaters because suspended solids may obstruct the measurement of the crystal size (Mehta & Batstone, 2013). In addition to that, if the reaction happens very fast, the second method is also difficult to be done. Generally, the crystal growth rate is expressed as linear

growth rate, which shows the amount of mass deposited per unit of time per unit area of crystal surface (Hutnik et al., 2013; Mullin, 2001).

2.2.3. Effect of organics and melanoidins on struvite crystallisation

Wastewater contains various constituents, including biodegradable and refractory organics (Metcalf & Eddy, 2014). Studies have been done to understand the effects of various biodegradable and refractory organics on struvite crystallisation (Li, Huang, et al., 2019). Biodegradable organics such as acetic acid, citric acid, and succinic acid have been found to alter the morphology of struvite crystals and decrease phosphorus removal efficiency by complexing with magnesium and ammonium ions (Song et al., 2014). Refractory organics such as HS and Ethylenediaminetetraacetic acid (EDTA) also have similar negative influences on struvite crystals (Prywer & Olszynski, 2013; Zhou et al., 2015). The attachment of organics onto struvite crystals might cause negative impacts on struvite crystallisation (Li, Huang, et al., 2019). Organics can disrupt the reaction kinetics, but it can also increase the size of struvite crystals if the colloidal parts are attached to struvite surface (Capdevielle et al., 2016).

As mentioned in Section 2.1.5, melanoidins are considered similar to HS. Wei et al. (2019) have shown that humic acid (HA) has unfavourable impacts on struvite crystallisation because it prolonged the induction time, decreased the growth rate of struvite crystals, and changed the morphology of the crystals. The reason behind this is the fact that HA is susceptible to form complexes with the reactants of struvite, and it also tends to get adsorbed on the surface of struvite crystals (Wei et al., 2019). Magnesium interacts with HS and produces soluble and solid complexes, which is dependent on pH and the ability of Mg ions to bind to carboxylic and phenolic groups of HS (Yan et al., 2015). This phenomenon will inactivate the growing nuclei (Mullin, 2001). As a result, the presence of HA altered the shape of struvite crystals (Wei et al., 2019). HS containing more than 90% FA can also co-precipitate with struvite, hence change the crystal morphology, decrease its purity, and reduce the P removal efficiency (Zhou et al., 2015). The shape of struvite crystals with and without the presence of HS are depicted in Figure 2.10 and Figure 2.11. From the figures, it is clear that crystal shape changes from long rod-like into triangle or square.
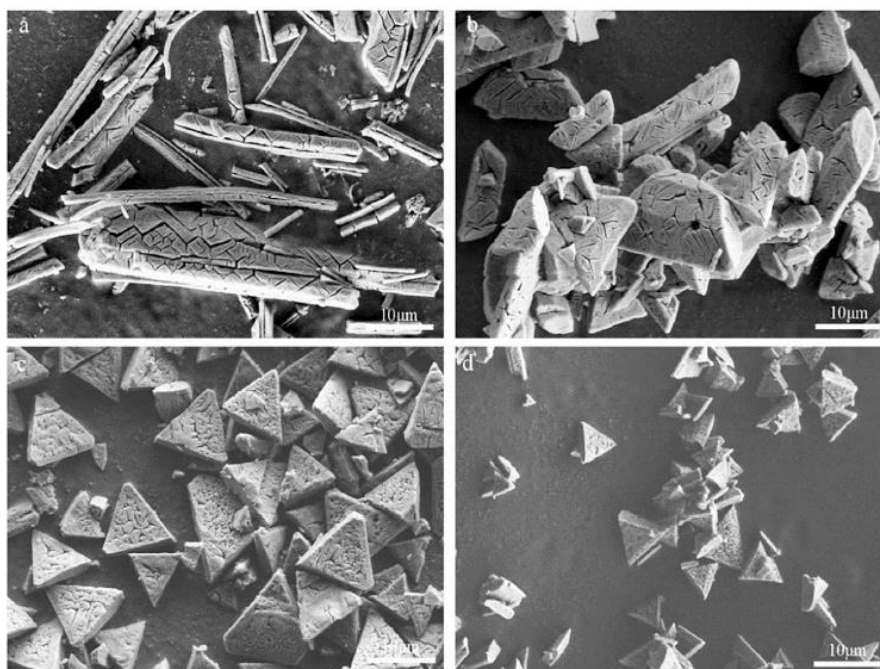
Figure 2.10 SEM pictures of struvite crystals (a) Control without HA, (b) 40 mg/L HA, (c) 80 mg/L and (d) 100 mg/L HA (Wei et al., 2019).
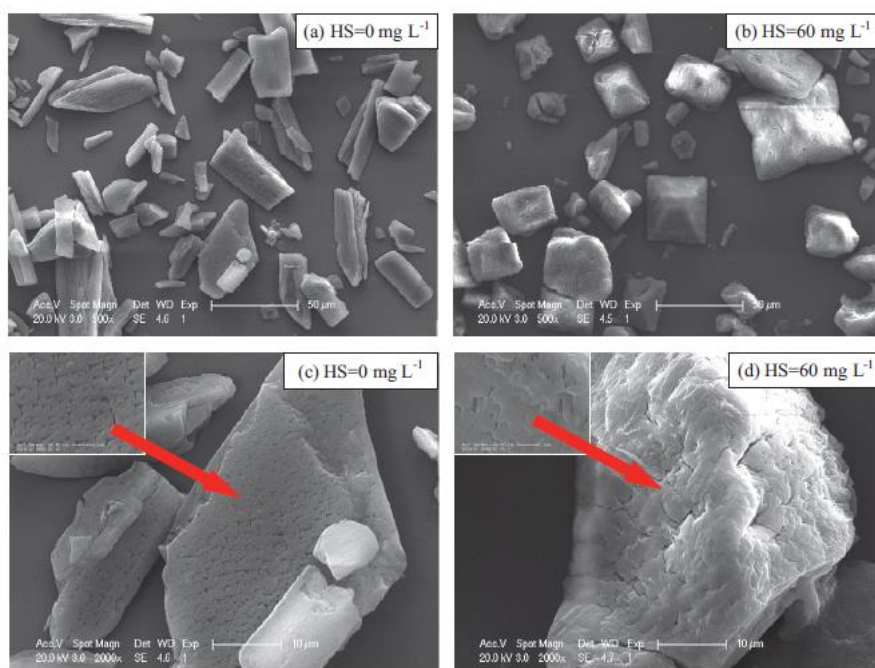
Figure 2.11 SEM pictures of the struvite crystals with and without the presence of HS (Zhou et al., 2015)

2.2.4. Effect of heavy metals and trace elements on struvite crystallisation

Foreign cations in a crystallisation system can influence the crystallisation process, including on nucleation and growth rates of the crystal. They play a role by breaking the structure of the crystals. Cations with higher charge tend to have stronger inhibiting effect, for example $Cr^{3+} > Fe^{3+} > Al^{3+} > Ni^{2+} > Na^+$. Other than breaking crystals structure, foreign cations also act by changing the equilibrium of the solution, by adsorption or chemisorption on nuclei, and also by reacting with the available reactants and forming complexes in the solution (Mullin, 2001).

In the case of struvite crystallisation, heavy metals ions can react with phosphate ions to form precipitates, for example, copper (II) phosphate, $Cu_3(PO_4)_2$ (Laurent et al., 2011). The presence of struvite crystals also promotes the heavy metal precipitation under a wide pH range. Various heavy metal hydroxides are found to be precipitated on the surface of struvite, including Cu, Ni, Pb, Zn, Mn, and Cr(III) (Tang et al., 2019). This phenomenon is likely to happen because the thermodynamic activation energy barrier on the metal hydroxide formation can be significantly diminished via heterogeneous nucleation on struvite surfaces (Tang et al., 2019). pH has an essential influence on heavy metals co-precipitation with struvite because an increase in pH can reduce Cu, Zn, and Cr contents in the recovered struvite crystals (H. Huang et al., 2019). Higher $N-NH_4:P-PO_4$ molar ratio is also beneficial to prevent the precipitation of heavy metals on struvite because an increase of ammonium concentration will significantly promote struvite crystallisation, in which ammonium will compete with heavy metals ions for phosphate ions. It should be highlighted that heavy metal content in the crystals tends to increase following the initial concentrations in the solution (H. Huang et al., 2019). However, as explained in Section 2.1.6, heavy metals and trace elements are prone to complex with humic-like substances, and it is not clear yet if these metals will end up in struvite or remain in treated effluent after struvite crystallisation.

Co-precipitation of trace elements in struvite crystallisation will lead to the inadequacy of trace elements required by the subsequent treatment units, such as PN/A reactors. Additionally, if heavy metals are incorporated into struvite crystals, they will increase the ecological risk of the application of struvite as fertilisers (H. Huang et al., 2019). The presence of heavy metals in fertiliser has a dangerous effect on animal and human health, due to their transport and accumulation through the food chain or by direct exposure. In general, it is presumed that heavy metal contents in the recovered struvite are lower than commercial fertilisers (Li, Boiarkina, et al., 2019). Heavy metals quality of struvite produced from WWTP in Apeldoorn,

The Netherlands is shown in Table 2.5 (de Vries et al., 2017). Compared to the regulatory framework (Uitvoeringsbesluit Meststoffenwet BWBR0019031), the quality of the heavy metals of struvite produced in Apeldoorn is below the limit, which is a good indicator of struvite as a potential P-based fertiliser.

Table 2.5. Heavy metals quality of struvite produced from WWTP in Apeldoorn, The Netherlands (de Vries et al., 2017) compared to the regulatory framework

Parameter	Value (mg/kg dry mass)	Maximum allowed values (mg/kg dry mass)
Copper (Cu)	3.0	75
Zink (Zn)	8.0	300
Arsenic (As)	0.15	15
Lead (Pb)	<1.0	100
Cadmium (Cd)	<0.10	1.25
Chromium (Cr)	10.0	75
Nickel (Ni)	4.0	30
Mercury (Hg)	0.01	0.75

2.2.5. The current state of struvite in The Netherlands

Struvite crystalliser reactors have been operated in full-scale in WWTPs in The Netherlands to treat reject water of anaerobically digested sludge, for example in WWTPs in Amersfoort, Apeldoorn, Olburgen, and Tilburg (Abma et al., 2010; de Vries et al., 2017; Driessen et al., 2018; Eliquo Water & Energy, 2015). Nowadays, it is also applied directly in the pre-dewatered anaerobically digested sludge in WWTP Amsterdam West and Echten (de Buck, 2012; Verdonk, 2017). Struvite from WWTP is recovered in the form of either sandy struvite or granulated struvite. Total sandy struvite production in WWTP Apeldoorn was 700 tonnes in 2017 (de Vries et al., 2017) and 900 tonnes granulated struvite in WWTP Amersfoort per year (Eliquo Water & Energy, 2015).

The primary objective for the application of struvite reactor in The Netherlands is mainly to cope with stringent P and N regulation (STOWA, 2010). Controlled struvite precipitation also helps to avoid clogging in pipelines, and hence minimising the maintenance costs (de Vries et al., 2017). The use of recovered struvite as fertiliser in The Netherlands is still limited by some constraints, including product quality, legislation issue, and social acceptance (Verhults, 2017). Furthermore, there is hardly any market for struvite in The Netherlands due to the surplus of P from livestock manure (de Vries et al., 2017). Animal manure, compost, and other fertilisers which also contain Mg, N, and P may have a stronger position in the market compared to struvite (STOWA, 2016). Farmers prefer livestock manure or commercial fertiliser with higher N content than struvite (de Vries et al., 2017). Sandy struvite form is hardly used, but it can be used as a raw material for fertiliser production. Granulated struvite can be used significantly more widely; however, it also has limited sales due to its N:P ratio which usually does not correspond directly to the need for agricultural and horticultural crops (STOWA, 2016). Therefore, fertiliser industries are potential market for struvite produced from WWTPs in The Netherlands, as they can process sandy struvite into granulated form and also correct the N:P ratio without the need of mining phosphorus rock.

3. Materials and Methods

3.1. Materials

3.1.1. Synthetic wastewater

Synthetic reject water was used in this study to mimic the full-scale conditions of reject water of anaerobically digested sludge. The synthetic wastewater was made by diluting sodium dihydrogen phosphate (NaH$_2$PO$_4$.H$_2$O, CAS: 10049-21-5, Sigma-Aldrich, Germany) and ammonium chloride (NH$_4$Cl, CAS: 12125-02-9, Merck, Germany) in demineralised water. The chemicals were weighed in an analytical balance (Mettler Toledo, USA). The pH of the synthetic wastewater was adjusted to 8 by the addition of sodium hydroxide (NaOH, CAS: 1310-73-2, Merck, Germany). The N and P concentrations in the stock solution were 2 g N-NH$_4$/L and 1 g P-PO$_4$/L, respectively. As there is no sufficient Mg in the synthetic wastewater, 1 M magnesium chloride (MgCl$_2$, CAS: 7786-30-3, Sigma-Aldrich, Germany) solution was added as the source of Mg for struvite crystallisation. The molar ratio of Mg:P-PO$_4$ was kept constant as 1:1. The addition of MgCl$_2$ was done just right before the experiment started because Mg reacts instantaneously with the available N and P in wastewater to form struvite. Table 3.1 shows the concentration of stock solutions of synthetic reject water and the final concentration in the reactor.

Table 3.1. The concentration of synthetic reject water

No.	Solution	Concentration in the stock solution	Concentration in reactor	Concentration in reactor
1	MgCl$_2$	1 M Mg/L	15 mM Mg/L	360 mg Mg/L
2	Synthetic reject water	2 g N-NH$_4$/L	66.45 mM N-NH$_4$/L	930.3 mg N-NH$_4$/L
		1 g P-PO$_4$/L	15 mM P-PO$_4$/L	465 mg P-PO$_4$/L

3.1.2. Synthetic melanoidins and humic acids

A synthetic melanoidins stock solution was used in the experiment. It was prepared by mixing 0.25 M glucose (C$_6$H$_{12}$O$_6$.H$_2$O, CAS: 14431-43-7, Sigma-Aldrich, Germany) and 0.25 M glycine (C$_2$H$_5$NO$_2$, CAS: 56-40-6, Sigma-Aldrich, Germany) with the addition of 0.5 M sodium bicarbonate (NaHCO$_3$, CAS: 144-55-8, Merck, Germany) (Dwyer et al., 2008). The solution was dissolved in demineralised water, and the pH was adjusted to 8 with NaOH. The solution was then autoclaved for 3 hours at 121°C and stored at 4°C (Dwyer et al., 2008).

HA stock solution was prepared by dissolving 20 g humic acids sodium salt (CAS: 1415-93-6, Sigma-Aldrich, Germany) in 2 L demineralised water. The pH was then adjusted to 8 by addition of NaOH. Humic acids stock solution was kept refrigerated at 4°C. Table 3.2 shows the characteristics of melanoidins and humic acids stock solution.

Table 3.2 Characteristics of melanoidins and HA stock solution

Stock solution	UV$_{254}$ (A)	Colour$_{475}$ (A)	Colour (mg Pt-Co/L)	TOC (mg C/L)	COD (mg O$_2$/L)
Melanoidins	605 ± 33	59 ± 8	239422 ± 33216	23967 ± 1553	58137 ± 1086
Humic acids	297± 17	45 ± 3	182610 ± 10736	3697 ± 172	-

The synthetic melanoidins solution was further characterised to check the amount of humic and fulvic fractions. The solution was acidified using 2 M HCl (Titripur®, Merck, Germany) until pH < 2. Afterwards, the solution was centrifuged (14000, 20 min). The supernatant was separated as the fulvic fraction (Zahmatkesh et al., 2018). Both the uncentrifuged solution and the supernatant were analysed for TOC analysis. Afterwards, the TOC proportions were used to determine humic and fulvic fractions. The synthetic melanoidins used in this study contained 6.6% humic and 93.4% fulvic fractions.

3.1.3. Trace elements solutions

As explained in Section 2.1.6, THP releases trace elements that are prone to complex with melanoidins and affecting struvite crystallisation. Synthetic trace elements solutions were made to represent the required culture medium by anammox biomass. Four different solutions were made to avoid the formation of precipitate if they were all mixed. The concentrations of the trace elements solutions are shown in Table 3.3.

Table 3.3 Concentrations of trace elements in the stock solutions. The concentration shown here is the concentration for the whole molecule.

Stock solution number	Reagents	Concentration in stock solution (g compound/L)	Concentration in reactor (mg compound /L)	Reference
1	$CaCl_2.2H_2O$	18	180	van de Graaf et al., 1996
2	$FeSO_4$	5	5	van de Graaf et al., 1996
3	$ZnCl_2$	0.0199	0.199	van de Graaf et al., 1996
	$CoCl_2.6H_2O$	0.0247	0.247	
	$MnCl_2.4H_2O$	0.0994	0.994	
	$CuSO_4$	0.0164	0.164	
	$Na_2MoO_4.2H_2O$	0.0221	0.221	
	$NiCl_2.6H_2O$	0.0196	0.196	
	Na_2O_3Se	0.0105	0.105	
	H_3BO_3	0.0014	0.014	
4	$AlKO_8S_2.12H_2O$	0.1378	8	H. Huang et al., 2014
	$Cr(NO_3)_3.9H_2O$	0.1371	18	Tang et al., 2019

The stock solutions were made more concentrated than what was required in the culture medium of the reactor to reach a specific concentration in the final synthetic reject water. Stock solutions 1, 2, 3, and 4 were made 100, 1000, 100, and 20 times more concentrated, respectively. The concentrations of solutions 1, 2, and 3 are referring to an earlier study about the culture medium of anammox biomass (van de Graaf et al., 1996). Solution 4, which contained Aluminium (Al) and Chromium (Cr(III)) was made to investigate the fate of heavy metals that may present in wastewater in struvite crystallisation.

3.2. Methods

3.2.1. Batch-test struvite crystallisation

The reactor used in the experiment was a jar test apparatus (VELP Scientifica, Italy) operated in a batch system. 500 mL beaker glass with baffles (Louwers Hanique, The Netherlands) was used to perform the experiments. The detail of feed composition volumes is explained in Appendix 1. The reaction lasted for an hour with the mixing speed of 160 rpm (Li, Huang, et al., 2019). The solutions were then let to settle for 30 minutes. During the reaction, pH was adjusted using 5 M NaOH and 2 M HCl. The volume addition due to pH adjustment was negligible because it was less than 1% of the total volume. All of the experiments were done in triplicates. pH and EC were monitored continuously using multi-meters (WTW 3630 IDS, Germany) which were connected to a laptop. The reactor set up is shown in Figure 3.1. Once the experiment was done, supernatant and the solid precipitate sample were collected and analysed. Both supernatant and solid were analysed for N-NH$_4$, P-PO$_4$, and trace elements concentrations. In addition to that, TSS analysis was done for supernatant, and crystal analysis was done for the solids. Figure 3.2 shows the experimental procedure.
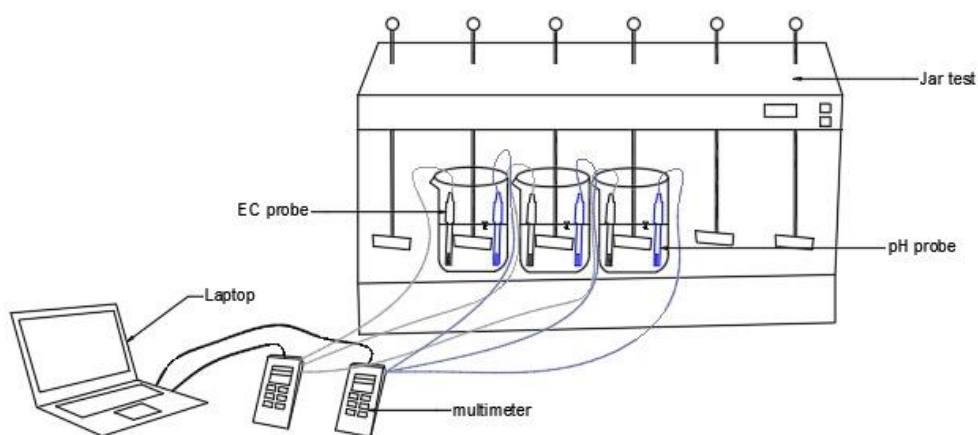
Figure 3.1. Reactor set-up
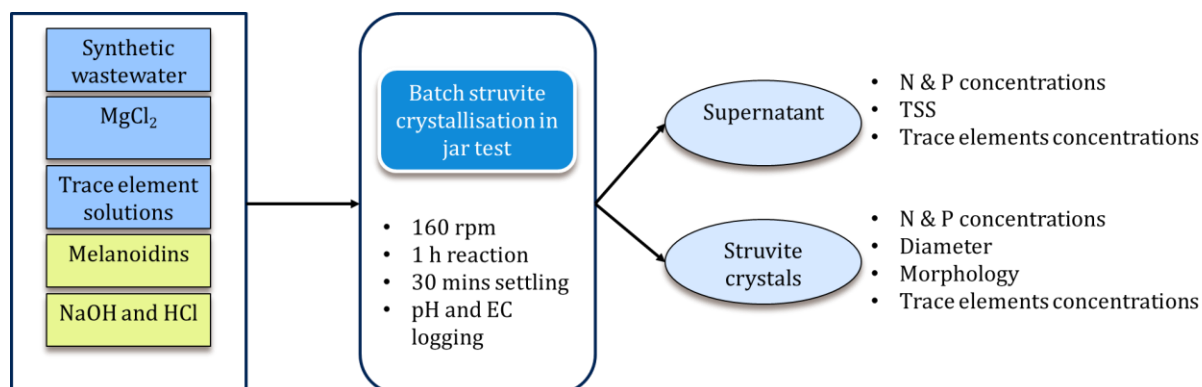
Figure 3.2 Experimental procedure

Preliminary research was done using synthetic wastewater, $MgCl_2$, and melanoidins or HA solutions without the addition of trace element solutions to investigate whether melanoidins and HA have similar effects on struvite crystallisation. The details about the volume of wastewater, $MgCl_2$ solution, melanoidins, and HA are explained in Appendix 1. The final reaction pH was set into 8 for the preliminary research. The concentrations of melanoidins and HA used for preliminary research are shown in Table 3.4.

Table 3.4 Concentrations of melanoidins and humic acids used for preliminary research

Run no.	Humic acid concentrations (g TOC/L)	Melanoidins concentration (g TOC/L)
1	0	0
2	0.5	0.5
3	1	1
4	1.5	1.5
5	-	2

It is important to highlight that different techniques for $MgCl_2$ dosing were used for preliminary research and primary research. For the preliminary research, $MgCl_2$ was added gradually, meanwhile for the primary research $MgCl_2$ was added all at once. However, this was not the variable of this research. It was decided to

do instant dosing of $MgCl_2$ in the primary research in order to simplify the data analysis of EC in the later stage of the experiment.

The concentrations of melanoidins in the reactor were varied into 0, 1, and 2 g TOC/L of melanoidins. These melanoidins concentrations were chosen based on the result of the preliminary research. The supernatant and struvite crystals obtained from the experiments were analysed to understand the effect of melanoidins on P removal, N removal, and struvite characteristics in struvite crystallisation. Next to varying melanoidins concentrations, various pH values were also applied. These pH values were chosen based on the literature and the typical pH used in struvite reactors in The Netherlands. Co-precipitation of trace elements with struvite is affected by pH and their availability in solution, which is affected by melanoidins. Therefore, the supernatant and struvite crystals obtained from the experiments were analysed to understand the fate of trace elements released from THP in struvite crystallisation. The influence of pH and relationship between pH-melanoidins on struvite crystallisation was also investigated. Table 3.5 shows the matrix of factorial experimental design for batch struvite crystallisation.

Table 3.5 Matrix of pH and melanoidins concentration for batch struvite crystallisation

Run no.	pH	Melanoidins concentration (g TOC/L)
1	6.50	0
2	6.50	1
3	6.50	2
4	7.25	0
5	7.25	1
6	7.25	2
7	8.00	0
8	8.00	1
9	8.00	2

3.2.2. Determination of induction time

pH and EC were monitored continuously using multi-meter (WTW 3630 IDS, Germany) to determine the induction time. Steady-state implied that the pH and EC values did not change anymore, which indicated that the induction time had been reached and the crystals continued to grow. A straightforward approach to determine the steady-state is to execute a linear regression over a data window and then execute a t-test on the regression slope. If the slope is significantly different from zero, the system is almost absolutely not at steady state (Bethea & Rhinehart, 1991). The obtained data was computed in Python (Version 3.7.6 64-bit for Windows 10) to determine the steady-state. The code was computed to calculate the slope between data points and then counted the moving average of five slope values. Afterwards, the t-test between the moving average of slope and a dataset of zero values was determined. The first time when the p-value of the t-test was higher than 5% significance level after the EC value reached the peak was considered as the induction time because at this point the slope was not significantly different from zero, which meant that the EC values were already constant.

3.2.3. Chemical analysis

TSS

TSS analysis was done to measure the amount of produced struvite crystals. 50 mL of completely stirred sample was filtered through a 1.2 μm filter (Whatman® glass microfiber filters GF/C, diameter 47 mm) using a vacuum filter. The filter was then placed inside a vacuum dryer oven (Lab Companion Jeiotech, Korea), which is equipped by silica beads and vacuum gauge, to dry the struvite sample until the constant weight (at least 48 hours) (Warmadewanthi & Liu, 2009). Struvite should not be dried in an oven because it will destroy the structure of the crystal, as the ammonium and water molecules will also evaporate (Ohlinger et al., 1999). The dried struvite was then weighed in an analytical balance (Mettler Toledo, USA) and TSS value was reported in mg/L.

Struvite elemental analysis

The dried struvite sample was re-dissolved in order to measure the phosphorus, nitrogen, and trace elements concentrations. Approximately 0.1 g of solids were dissolved in 5 mL 1 N nitric acid (HNO_3, Merck, Germany) and then diluted with demineralised water until reaching the volume of 500 mL. The dilution was done in volumetric flasks (Duran Hirschmann, Germany). The solution was then stirred using a magnetic stirrer for an hour (Warmadewanthi & Liu, 2009) and used for analysis.

Orthophosphate and total ammonia nitrogen (TAN)

Phosphorus (in the form of orthophosphate, reported as mg $P-PO_4$/L) and nitrogen (in the form of TAN, reported as mg $N-NH_4$/L) concentrations were analysed in both supernatant and struvite crystals. Phosphorus was analysed using Hach-Lange test kit LCK 350 (Hach, Germany) and nitrogen was analysed using LCK 303 (Hach, Germany). The samples were filtered using a 0.45 μm syringe filter (CHROMAFIL® Xtra PES-45/25 0.45 μm) prior to the analysis.

UV_{254}, colour$_{475}$, TOC, and COD

Due to the heterogenicity of humic substances, several techniques are required to characterise them (Brezinski & Gorczyca, 2019). The most common tools used to characterise humic substances include ultraviolet absorbance at 254 nm (UV_{254}), total organic carbon (TOC), and chemical oxygen demand (COD) (Matilainen et al., 2011). In this study, UV_{254}, colour$_{475}$, TOC, and COD were used to characterised melanoidins. UV_{254} gives the prediction of the aromaticity of the sample, and TOC shows the total concentration of carbon present in the sample (Brezinski & Gorczyca, 2019).

UV_{254} and colour analysis were done using UV-Vis spectrophotometer (Genesys 10S, Thermo Scientific, UK). UV_{254} analysis was done using a quartz cuvette with ultraviolet absorbance at 254 nm, and colour analysis was done using the disposable plastic cuvette with the wavelength of 475 nm (American Public Health Association (APHA) et al., 2017). Demineralised water was used as blank for both techniques. The calibration curve was made using Pt-Co standard solution for colour analysis, and the calibration curve is enclosed in Appendix 2. TOC and COD were done using Hach-Lange test kits LCK 386 and LCK 014, respectively.

Metals and Trace elements

Metal and trace elements in the supernatant and struvite were analysed using ICP-MS (Analytik Jena PlasmaQuant MS, Germany). Several dilutions were necessary to be done to get results within the range of the detection of the machine. Samples were diluted using ultrapure water. The samples were diluted 50 times for analysis of major metals Ca and Mg; meanwhile, for the trace elements the samples were diluted 20 times. The total volume of the sample was 10 mL. The 50 times and 20 times diluted samples were acidified with 0.1 mL and 0.2 mL of 69% HNO_3 (Carl Roth, CAS: 7697-37-2, Germany), respectively. The acid was added in order to solubilise the metals and keep the samples solid-free.

3.2.4. Complexation of Mg-Melanoidins

In order to check the complexation between Mg and melanoidins, approximately 50 mL solution containing a mixture of Mg and melanoidins was filtered using ultrafiltration membrane module (Amicon® Stirred Cell 50 mL, Merck Millipore, Germany). The pH of the solution was adjusted using 2 M HCl and 5 M NaOH. The solution was filtered through 1 kDa membrane (Ultracel® regenerated cellulose, 44.5 mm diameter, Merck Millipore, Germany). The experiment was conducted in 2 bar pressure for approximately 1.5 hours or until 10 mL of permeate was obtained. The influent (feed) solution and the permeate were then tested for Mg concentration (LCK 326, Hach, Germany), colour$_{475}$, and UV_{254}. All experiments were done in triplicates. The set-up for the complexation experiment is shown in Figure 3.3. A similar set of the experiment as shown in Table 3.5 was used in this experiment. The volumes of used Mg stock solution and melanoidins are shown in Appendix 1.
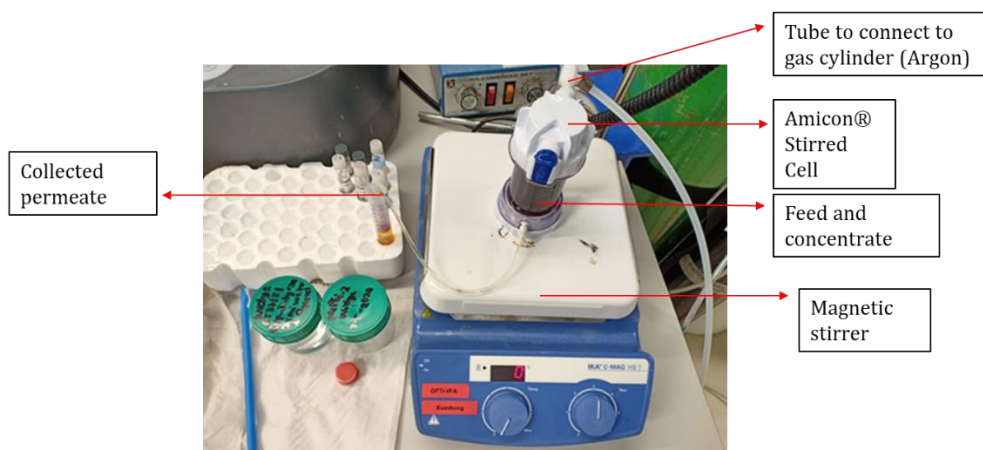
Figure 3.3 Set-up for Mg-melanoidins complexation experiment

3.2.5. Microscopy and particle size analysis

Digital Microscope (Keyence VHX-5000, Belgium) was used to analyse the morphology and diameter of struvite crystals with the magnification of 200 and 1000 times. The diameter of struvite crystals was analysed based on the maximum and minimum diameter. The microscope was used to determine struvite diameter instead of particle size distribution (PSD) analyser, in order to avoid the dissolution of struvite crystals due to the water-carrier in the PSD. All samples for microscopy and particle size analyses were dried according to the procedure mentioned in Section 3.2.3.

3.2.6. Statistical analysis

Statistical analyses (ANOVA and t-test) were done using Ms. Excel Office 365 (Microsoft, USA). Single-factor (one-way) ANOVA was used to determine if there was any significant difference between experiments with varying melanoidins concentrations or pH values. Two factors (two-way) ANOVA with replication was also used to confirm the interaction effects between pH and melanoidins. Two tail one-sample t-test was used to determine if the mass balances and molar ratios were similar to the theoretical values. The significance level (α) was 0.05.

3.2.7. pH-Redox-Equilibrium model (PHREEQC)

PHREEQC is a free software that is often used for geochemical calculations. This software provides menu options that enable researchers and practitioners to solve problems related to geochemical reactions (De Lucia & Kühn, 2013). The main function of this application is to process data of the concentration of chemicals input, carry out the prediction of geochemical reactions, and show the final results of the concentration of compounds formed from these reactions (Parkhurst & Wissmeier, 2015).

Struvite did not exist in the thermodynamics database of PHREEQC (PHREEQC.DAT). However, PHREEQC allows users to create their thermodynamic database. It grants the user the possibility to determine the solubility product constant (Ksp), enthalpy, and stoichiometric coefficient of solid-phase compounds (Warmadewanthi & Liu, 2009). Therefore, struvite and other struvite-like minerals (newberyite, bobbierite, and cattiite) that do not exist in PHREEQC database were defined under the keyword PHASES. The main database used for this study was minteq.v4.dat which covered various metal ions and their complexation. In addition to that, humic and fulvic speciations obtained from Tipping and Hurley database (T_H.DAT) were used to represent melanoidins in this study. T_H.DAT did not include the complexation between humic and fulvic acids with Mg and Ca ions, and these reactions were added to the database by referring to previous studies (Bosire et al., 2018; Bosire & Ngila, 2017).

Keyword SOLUTION was used to define the solution composition in PHREEQC. Solution composition was computed to represent the synthetic reject water used in the lab experiment. Anions which came together with the trace element cations such as SO_4^{2-} and Cl^- were excluded in the input file. All units were presented as mmol/L because the concentration of humic and fulvic acids could not be stated as g TOC/L in PHREEQC.

The concentration of 1 g TOC/L was equal to 0.69 mmol/L HA 9.743 mmol/L FA, meanwhile concentration of 2 g TOC/L was equal to 1.381 mmol/L HA and 19.487 mmol/L FA. The pH was fixed using keyword PHASES Fix_H+, and the values were varied into 6.5, 7.25, and 8. The target mineral, struvite, was written under EQUILIBRIUM_PHASES and the SI was set into 0. The addition of $MgCl_2$ was defined under keyword REACTION. The temperature of the solution was kept constant at 20°C to represent the lab temperature. The PHREEQC code is presented in Appendix 3.

In this study, PHREEQC was used to model the SI of various minerals after struvite crystallisation reaction. The prediction of SI allowed to predict the co-precipitation of struvite-like minerals and other minerals containing heavy metals or trace elements. At the same time, the concentrations of remaining trace elements in the supernatant and the formation of complexes could be examined as well.

3.2.8. Response surface methodology

Response surface methodology (RSM) is a compilation of statistical and mathematical techniques which is helpful for designing, developing, and optimising processes. In RSM, the inputs affecting the processes are called "factors" or "variables", and the resulting measures are termed "responses". The input variables are controlled by the engineer or scientist, partially for testing or experimental purposes (Myers et al., 2016).

In this study, Three-Level Factorial RSM with 2 centre points using DesignExpert software (version 12, Stat-Ease, USA) was used to model the interactions between two factors, namely pH and melanoidins, with six responses related to struvite crystallisation. The six responses were $N-NH_4$ content in the supernatant, $P-PO_4$ content in the supernatant, $N-NH_4$ content in struvite product, $P-PO_4$ content in struvite product, the maximum diameter of struvite crystal, and minimum diameter of struvite crystal. In addition to that, RSM was also used to analyse how pH and melanoidins affected the fate of trace elements (Mn and Ni) in struvite crystallisation. Three-Level Factorial RSM is a unique RSM design which is beneficial for experiments with two factors, as it has good design properties and impervious to outliers and missing data (Stat-Ease, 2014). Miscellaneous statistical parameters are available in DesignExpert software to help the users analysing the significance of RSM model, including analysis of variance (ANOVA), lack of fit test, F-test, and multiple determination coefficients (R^2) tests (Polat & Sayan, 2019).

Models were generated from each response to predict the influence of pH and melanoidins. After the models were finalised, RSM was used to optimise the processes. In this study, the goals were to minimise the contents of N and P in the supernatant, maximise the contents of N and P in struvite, and maximise the maximum and minimum diameters of struvite. First, each response was optimised separately from other responses. Afterwards, all six responses were optimised together. For the integrated optimisation, the importance of the goals was made similar for N and diameters (+++). Meanwhile, for P, the importance was set as the most important (+++++). The software then predicted the optimum pH and melanoidins concentration to reach the goals.

This page intentionally left blank

4. Results and Discussion

4.1. Phosphorus and nitrogen removal

Struvite crystallisation in The Netherlands is basically used to eliminate phosphorus and nitrogen from wastewater (STOWA, 2010). This sub-chapter will elaborate on the results of phosphorus and nitrogen removal obtained from batch-test struvite crystallisation. The results from all experiments without melanoidins, with melanoidins, and with humic acids are interpreted and discussed.

4.1.1. Phosphorus and nitrogen concentrations in the supernatant

The preliminary result of the concentrations of phosphorus and nitrogen in the supernatant after struvite crystallisation is displayed in Figure 4.1. $P-PO_4$ and $N-NH_4$ in the supernatant did not differ considerably with increasing melanoidins concentration. $P-PO_4$ concentration for the experiment without melanoidins (0 g TOC/L) was 12.4 ± 1.2 mg $P-PO_4$/L, and similar values for 0.5, 1, and 1.5 g TOC/L melanoidins were recorded with the average of 13.8 ± 1.1 mg $P-PO_4$/L. A notable increase in phosphorus concentration of 19.8 ± 0.8 mg $P-PO_4$/L was detected for melanoidins concentration of 2 g TOC/L. This could be an indication of the concentration in which melanoidins start to disrupt P removal in struvite crystallisation. On the other hand, $N-NH_4$ concentration tended to increase with increasing melanoidins concentration. This result is in line with early studies which reported that the presence of melanoidins would increase the concentration of nitrogen in the effluent (Barber, 2016). From the preliminary results, up to $97.3\pm0.3\%$ $P-PO_4$ removal and up to $11.1\pm0.8\%$ $N-NH_4$ removal were detected.
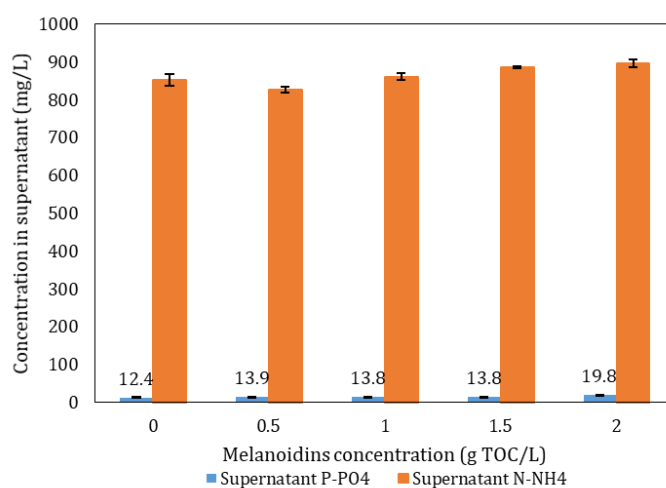
Figure 4.1 Preliminary results of $P-PO_4$ and $N-NH_4$ in the supernatant after struvite crystallisation (using melanoidins)

Contrasting results were obtained from the preliminary experiment using HA. $P-PO_4$ concentration in the supernatant increased substantially, along with increasing HA concentrations (Figure 4.2). With 0.5 g TOC/L HA, $P-PO_4$ concentration in supernatant increased to 48.0 ± 1.1 mg $P-PO_4$/L, approximately four times higher compared to the condition without HA. $P-PO_4$ concentration in supernatant kept increasing with increasing HA concentration. The maximum P removal efficiency with the presence of HA was $89.6\pm0.2\%$. HA seemed to reduce P removal efficiency in struvite crystallisation, as reported by Zhou et al. (2015). $N-NH_4$ concentration in the supernatant, nonetheless, showed a different trend. $N-NH_4$ concentration in the supernatant fluctuated with increasing HA concentration. In the beginning, $N-NH_4$ concentration in the supernatant increased with the presence of 0.5 g TOC/L HA, but then it decreased with higher addition of 1 g TOC/L HA. Finally, it increased again when HA concentration was 1.5 g TOC/L. The peculiar trend made it challenging to draw a conclusion on the effect of HA on N removal. Up to $11.8\pm0.9\%$ $N-NH_4$ removal was detected for the experiment using HA.
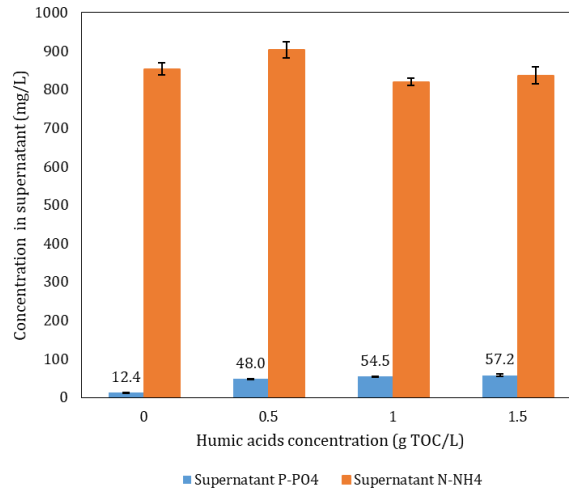
Figure 4.2 Preliminary results of P-PO$_4$ and N-NH$_4$ in the supernatant after struvite crystallisation (using HA)

The different results in P removal were possibly caused by the difference between melanoidins and HA solutions. Even though the concentrations of melanoidins and HA used for the preliminary research were the same, melanoidins solution was fully soluble at pH 8 meanwhile HA solution was not, and some colloidal parts settled after the solution was stored in the fridge. These colloidal fractions might form aggregates during struvite crystallisation process, resulted in the inhibition in the growth of struvite nuclei, and hence disrupting P removal efficiency (Zhou et al., 2015). The presence of insoluble part of HA solution also indicated that HA had higher molecular weight than melanoidins. It was confirmed during the TSS analysis of struvite samples, in which the samples with HA could hardly be filtered. HA has a molecular weight range between 10,000 to 100,000 (Adusei-Gyamfi et al., 2019). Some portion of HA, therefore, might be too big to pass through 1.2 µm filter paper, explaining why it was difficult to filter the samples.

The results obtained from the preliminary research was used as the basis to perform primary research. As there was only notable difference of P-PO$_4$ in the supernatant when melanoidins concentration was 2 g TOC/L, the primary research only used three variations of melanoidins concentrations: 0, 1, and 2 g TOC/L melanoidins. The primary research was also only performed using melanoidins and not HA. The phosphorus concentration in the supernatant after struvite crystallisation in primary research is shown in Figure 4.3. Compared to the preliminary research, the P-PO$_4$ concentrations in the supernatant were lower because of the different technique used for MgCl$_2$ addition. An instant addition of MgCl$_2$ resulted in better performance of struvite crystallisation from reject water of anaerobically digested sludge, even though de Buck (2012) reported gradual MgCl$_2$ was better for struvite crystallisation from the slurry phase of anaerobic digester. With respect to pH, the results showed that with higher pH, the supernatant contained a lower concentration of P-PO$_4$. It is in line with the literature, that higher pH will enhance phosphorus removal (Li, Huang, et al., 2019; Md Mukhlesur Rahman et al., 2014). pH influences the solubility and supersaturation of struvite, and hence affecting the phosphorus removal efficiency (Li, Huang, et al., 2019). The solubility of struvite decreased and its supersaturation increased when pH increased from 6.5 to 8, therefore P removal efficiency increased as well. When the pH was 6.5, the highest P removal was 62.7±0.9% and it increased to 92.9±0.3% when the pH was 7.25. P removal efficiency reached 98.4±0.3% when pH raised into 8. The lowest P-PO$_4$ concentration in the supernatant from the primary research was 7.21 ± 1.59 mg P-PO$_4$/L, which was achieved with pH 8 and melanoidins concentration of 2 g TOC/L.

It was evident that the P-PO$_4$ concentrations in the supernatant of the experiments at pH 7.25 and pH 8 were almost identical for all melanoidins concentrations. At pH 6.5, however, higher melanoidins resulted in lower P-PO$_4$ concentrations in the supernatant. These different results might be caused by the different reactions between melanoidins and struvite reactants in different pH values. It has been reported that complexation mechanisms of melanoidins and NOM were similar (Ćosović et al., 2010), therefore it is likely

that magnesium will also interact with melanoidins to form soluble and solid complexes. The formation of complexes is dependent on pH (Yan et al., 2015); therefore, the trend of P-PO$_4$ concentrations in the supernatant was different with different pH values. An increase in pH will also increase the chance of Mg-HS bonding (Yan et al., 2015). If there had been more Mg complexes with melanoidins, it would have disrupted struvite crystallisation, decreased P removal efficiency, and consequently would have increased the concentration of P-PO$_4$ in the supernatant. However, results at pH 6.5 showed that higher melanoidins concentration gave lower P-PO$_4$ concentrations in the supernatant, which meant the presence of melanoidins enhanced struvite crystallisation. A possible explanation behind this phenomenon is that the solutions with melanoidins had buffering capacity because the melanoidins solution contained bicarbonate. Furthermore, melanoidins also have numerous acid and base adsorption sites (Pertusatti & Prado, 2007). The buffering capacity resulted in the tendency of pH to slightly increase again after reaching 6.5, hence promoting P-PO$_4$ removal and lowering P-PO$_4$ concentration in the supernatant. Another plausible explanation is that due to the buffering capacity, pH did not drop as fast as the condition without melanoidins. This led to the removal of P-PO$_4$ that happened in higher pH condition before the pH was adjusted into 6.5. The changes in pH are further discussed in Section 4.3.1.
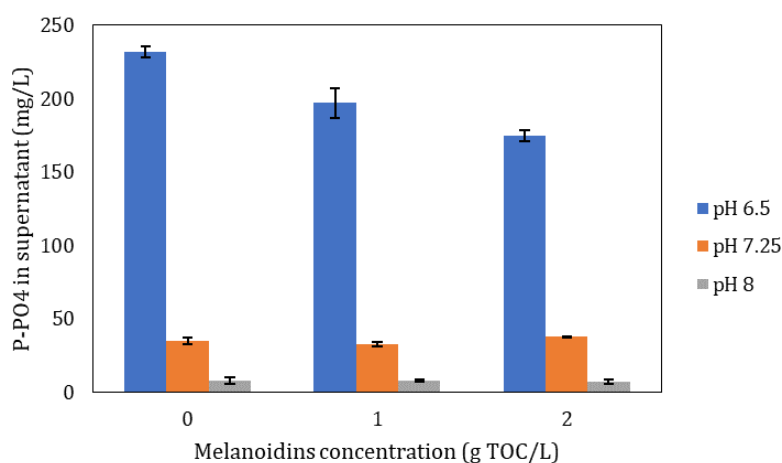
Figure 4.3 P-PO$_4$ in the supernatant after struvite crystallisation

The difference in P-PO$_4$ concentration in the supernatant at pH 6.5 was confirmed by ANOVA, resulting in statistically significant difference with the $p = 0.0001$. At pH 7.25, a statistically significant difference between samples with varying melanoidins concentration was also recorded, even though the p-value was rather close to 0.05 ($p = 0.024$). It was confirmed that at pH 8, there was no statistically significant difference ($p > 0.05$) in P-PO$_4$ concentration in the supernatant with the varying melanoidins concentration. These findings explained that at higher pH, e.g. pH 7.25 and pH 8, the solutions were highly saturated to form struvite; therefore, the effect of melanoidins was less apparent and even diminished at pH 8. Melanoidins affected P-PO$_4$ concentration in the supernatant, but pH could be adjusted to minimise the effect.

Fluctuating trends were obtained for the concentration of N-NH$_4$ in the supernatant. As can be seen in Figure 4.4, in general, higher pH values resulted in a lower concentration of N-NH$_4$ in the supernatant. The results go in line with Md Mukhlesur Rahman et al. (2014), who concluded that higher pH would enhance N removal. The lowest attained N-NH$_4$ concentration in the supernatant was 734±15 mg N-NH$_4$/L, equal to N-NH$_4$ removal of 21.1±1.6%, with the experimental condition of pH 8 and 0 g TOC/L melanoidins. N-NH$_4$ removal was lower than P-PO$_4$ removal because the limiting reagent for struvite crystallisation is phosphorus. As compared with the results of phosphorus removal, nitrogen removal was also better with the instant dosing of MgCl$_2$. Judging only from Figure 4.4, the effect of melanoidins on nitrogen concentration in the supernatant was unclear as the results fluctuated slightly with the increasing melanoidins concentrations. Statistical analysis using ANOVA showed there was a significant difference

between experiments with varying melanoidins concentrations in all pH values ($p < 0.05$). The presence of melanoidins resulted in slightly higher N-NH$_4$ concentration in the supernatant in all pH values, as reported by early studies (Barber, 2016; Driessen et al., 2018; Dandan Zhang et al., 2019).
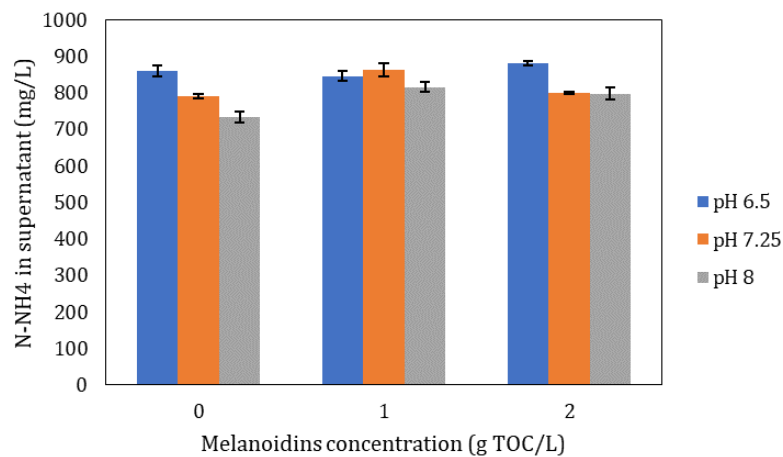
Figure 4.4. N-NH$_4$ concentration in the supernatant after struvite crystallisation

4.1.2. Phosphorus and nitrogen mass balance

In order to identify the contents of phosphorus and nitrogen which ended up in struvite or remained in the supernatant, the mass balance of struvite crystallisation was computed. Figure 4.5 shows the mass balance for phosphorus. It is intelligible that with higher pH, more phosphorus ended up in struvite and less remained in the water. For pH 6.5, half of the phosphorus ended up in struvite and half ended up in the water, meanwhile for pH 7.25 and 8 most phosphorus ended up in struvite and only small fraction remained in the water. It is noteworthy that the mass balances were not completely closed. T-test was conducted to investigate if the obtained mass balances were equal with the theoretical mass balance. It was found that the mass balances were identical to the theoretical mass balance in almost all samples ($p > 0.05$). For phosphorus, all experiments resulted in losses of phosphorus. The possible explanation that caused the losses of phosphorus is the complexation of phosphorus with melanoidins, which resulted in the transformation of soluble orthophosphate into organic phosphorus. Stable organic complexes could be established when HS react with and phosphate (Guardado et al., 2008; He et al., 2006; Wei et al., 2019). As the method used to measure phosphorus was only measuring orthophosphate, organic phosphorus was not considered.
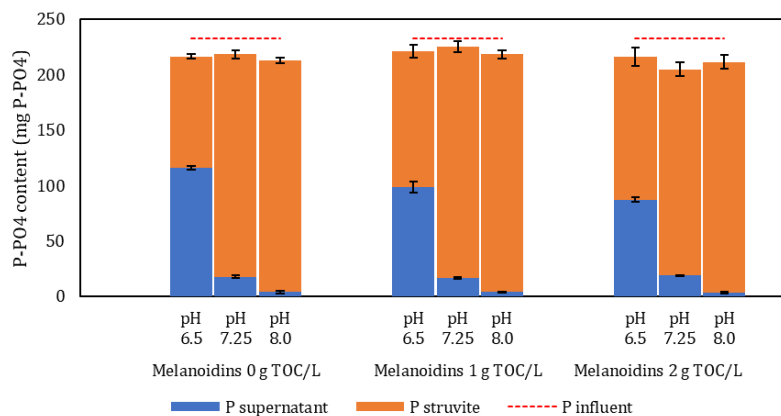
Figure 4.5 Mass balance of phosphorus in various pH values and melanoidins concentrations
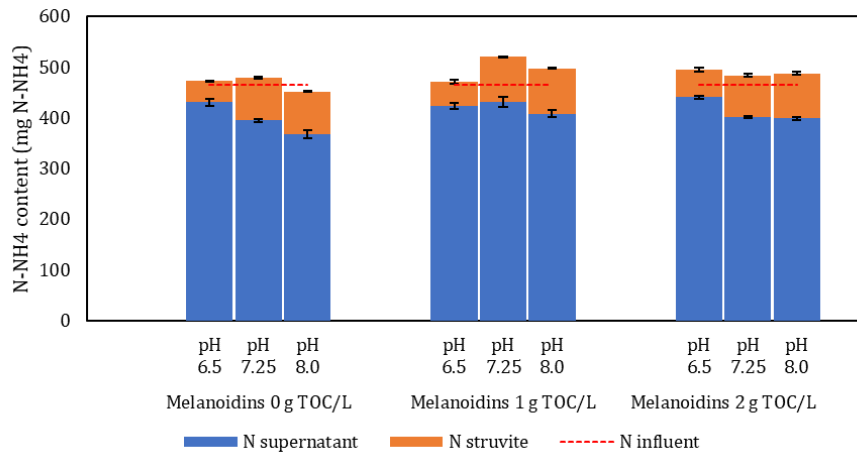
Figure 4.6 Mass balance of nitrogen in various pH values and melanoidins concentrations

Figure 4.6 shows the mass balance for nitrogen. Despite the different pH values, most nitrogen still ended up in the water. Mass balances for nitrogen also were not closed completely. In contrast with phosphorus which mainly lost, results showed that there was nitrogen gained. The possible explanation is that there was a chance of the additional nitrogen from melanoidins that was embodied in struvite crystals and unintentionally included in $N-NH_4$ analysis. Nitrogen in melanoidins is mainly located in the amine ($-NH_2$) functional group, which is also able to coordinate with metal ions (Adusei-Gyamfi et al., 2019).

4.2. Struvite characteristics

This sub-chapter describes the effects of melanoidins and HA on struvite characteristics, including Mg:N-NH_4:P-PO_4 molar ratio, amount of produced struvite, crystal morphology, and crystal diameter.

4.2.1. Mg:N-NH_4:P-PO_4 molar ratio in struvite

Mg:N-NH_4:P-PO_4 molar ratio was calculated to ensure that the produced crystals were struvite. Theoretically, Mg:N-NH_4:P-PO_4 molar ratio of struvite is 1:1:1 as shown by Equation 1 (Shih & Yan, 2016). Struvite is the only mineral that contains N amongst the magnesium and phosphate-based minerals that may co-precipitate during struvite crystallisation (Li, Huang, et al., 2019). These minerals include Newberyite ($MgHPO_4.3H_2O$), Bobierrite ($Mg_3(PO_4)2.8H_2O$), or Cattiite ($Mg_3(PO_4)2.22H_2O$) (Warmadewanthi & Liu, 2009). Therefore, Mg:N-NH_4:P-PO_4 molar ratio in struvite can be used to indicate the purity of struvite (Li, Huang, et al., 2019). The Mg:N-NH_4:P-PO_4 molar ratio was computed to see if there was any difference between experiments.

The result of Mg:N-NH_4:P-PO_4 molar ratio is shown in Figure 4.7. For this calculation, the molar ratio of P is set as the reference (1) (Warmadewanthi & Liu, 2009). Mg molar ratio was found to be higher than 1 and N molar ratio was lower than 1, which might be caused by some impurities that co-precipitated during the crystallisation. Mg presumably was also bound to other constituents that were present in the solution, such as carbonate and sulphate, whereas N in struvite could be replaced by other positive cations competing for PO_4^{3-} ions, such as Na^+ or K^+ (Chauhan & Joshi, 2014; Shih & Yan, 2016). In general, the results came near to the correct Mg:N-NH_4:P-PO_4 molar ratio, which is close to 1:1:1. It was confirmed by using t-test that the molar ratios were not significantly different from the theoretical value ($p > 0.05$).

For the condition without melanoidins (0 g TOC/L), the $N-NH_4$ molar ratio decreased slightly alongside with the increasing pH, which indicated that the purity of struvite decreased with increasing pH. These results can be explained by an early study which reported that pure struvite could be produced at neutral pH, and higher pH will promote the precipitation of phosphate-based minerals containing a lower content of struvite (X. Hao et al., 2013). Nonetheless, the trends were not evident with the presence of melanoidins. The Mg:N-NH_4:P-PO_4 molar ratios on various pH fluctuated slightly with 1 g TOC/L melanoidins, and the similar results applied for the condition with 2 g TOC/L melanoidins. When the Mg:N-NH_4:P-PO_4 molar

ratios at different melanoidins concentrations and the same pH value were compared, e.g. experiments 0; 1; 2 g TOC/L melanoidins at pH 6.5, the Mg:N-NH$_4$:P-PO$_4$ molar ratios also did not show a notable difference. Same results were documented for pH 7.25 and pH 8. These findings indicated that melanoidins did not change the molar ratio of struvite.
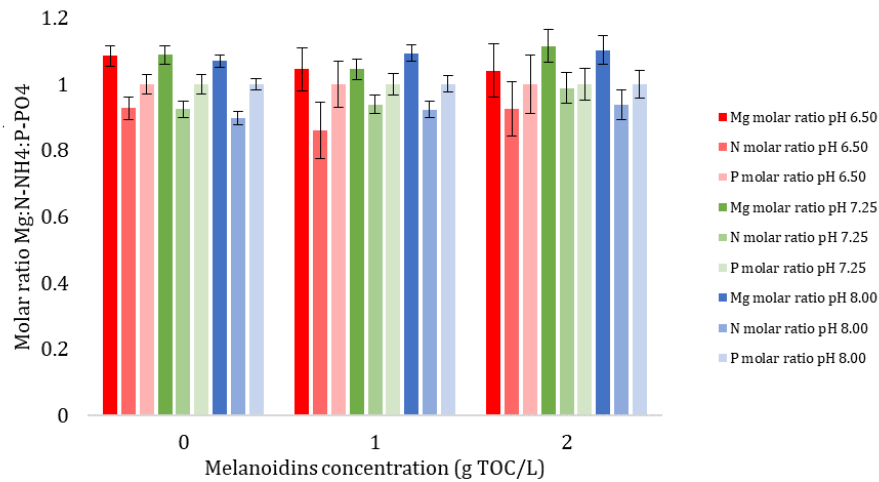
Figure 4.7 Mg:N-NH$_4$:P-PO$_4$ molar ratios in various pH and melanoidins concentrations

4.2.2. Amount of produced struvite

The amount of produced struvite was determined, and the results are shown in Figure 4.8. As can be seen from Figure 4.8, struvite production at pH 6.5 was lower than struvite production at pH 7.25 and pH 8. Struvite production at pH 7.25 was also slightly lower than struvite production at pH 8. pH is one of the most influential factors in struvite crystallisation because it is affecting the supersaturation and solubility of struvite crystals, and hence affecting the phosphorus removal and overall reactions (Li, Huang, et al., 2019). From the obtained results, it was apparent that pH affected struvite production. More struvite was produced at higher pH because of the increasing supersaturation and decreasing solubility of struvite.
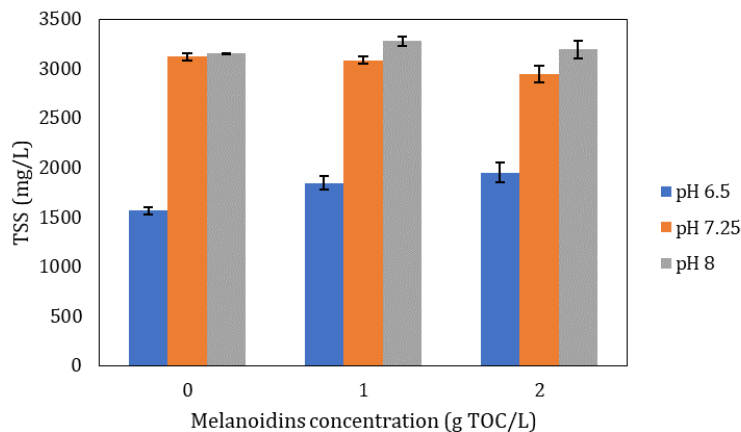
Figure 4.8 Produced struvite reported as TSS (mg/L)

From the results shown in Figure 4.8, the influence of melanoidins on struvite production was also studied. Apparently, the effect of melanoidins on struvite production was not as evident as the effect of pH. The amount of produced struvite fluctuated along with the change in melanoidins concentrations. For pH 6.5, TSS increased with the increasing melanoidins concentrations; meanwhile, the results for pH 7.25 were in the contrary. TSS production at pH 8, on the other hand, fluctuated with increasing melanoidins concentrations. The trend for pH 6.5 could be related to the observed trend of phosphorus concentration in the supernatant shown in Figure 4.3. For pH 6.5, TSS increased and P-PO$_4$ concentration in supernatant

decreased with the increasing melanoidins concentrations, meaning more phosphorus was removed from the water and turned into struvite crystals. ANOVA was conducted to analyse the difference in TSS production. Results showed that there was a significant difference between experiments with and without melanoidins at pH 6.5 (p = 0.001658) and at pH 7.25 (p = 0.0248). At pH 8, there was no significant difference between experiments with and without melanoidins (p = 0.087).

PHREEQC was also used to predict the production of struvite with varying pH values and HS concentrations. The results of modelling using PHREEQC (Figure 4.9) showed that amount of produced struvite changed along with the change in pH and HS concentration. The presence of HA and FA affected the ionic strength of the solution. Higher ionic strength resulted in a lower SI for struvite and hence less struvite production (Desmidt et al., 2013). This effect was more apparent at pH 6.5; however, the result contradicted with the lab result in Figure 4.8. There was a chance that melanoidins might precipitate and erroneously analysed as TSS during the experiment, which led to the difference between lab and PHREEQC results. At pH 7.25 and 8, there was barely any change in the amount of produced struvite, similarly as what was obtained in the lab. This result can be an indication that the effect of ionic strength on struvite production was suppressed by high pH value because pH also influenced SI. In the full-scale WWTPs, pH adjustment, therefore, can be executed to withhold the effect of melanoidins.
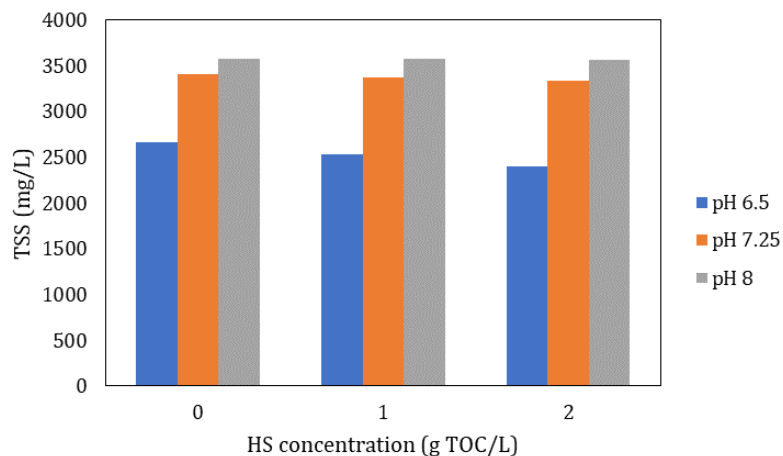
Figure 4.9 Prediction of struvite production using PHREEQC

4.2.3. Crystal morphology (macroscopic observations)

The morphology of produced struvite was analysed both macroscopically and microscopically (Section 4.2.4). In general, struvite in all of the examined samples was sandy-like crystals. On the other hand, the ones produced with HA were agglomerating and stickier like soil. The comparison is shown in Figure 4.10. The difference grain texture of the struvite produced with melanoidins and HA explains that melanoidins and HA had different characteristics, even though the pH and concentrations were the same. HA has been identified to contain hydrophobic colloidal fractions (Matilainen et al., 2011; Pertusatti & Prado, 2007) and this colloidal part of HA might have interfered struvite crystal formation, which subsequently resulted in the agglomerating and sticky texture of struvite crystals.
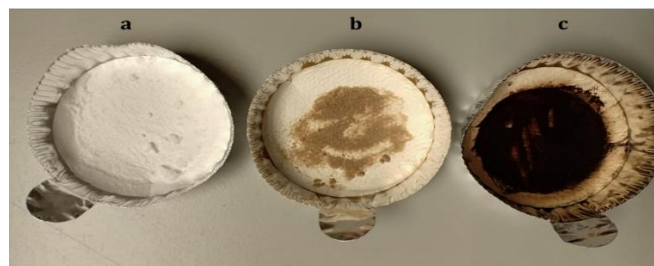
Figure 4.10 Produced struvite crystals. a) without melanoidins and HA, b) with melanoidins, and c) with HA

Struvite crystals without melanoidins and HA were white, but the colour became brownish with the presence of melanoidins. The brown colour got darker with the increasing melanoidins concentrations. The results are shown in Figure 4.11. The change in colour indicated that melanoidins were either attached to the surface of struvite crystals or incorporated inside the crystal structure.

Figure 4.11 The colour of produced struvite crystals. a) 0 g TOC/L melanoidins, b) 0.5 g TOC/L melanoidins, and c) 1 g TOC/L melanoidins

The crystals produced at pH 6.5 were then examined by washing the crystals to eliminate the outer layers of the crystal. The crystals were washed using demineralised water and NaOH. However, after being washed, the colour did not disappear (Figure 4.12 and Figure 4.13). The results ensured that melanoidins were likely to be entrapped inside the crystals structure or were attached firmly. This experiment was only done for the samples of pH 6.5; thus, the results should not be generalised for pH 7.25 and pH 8 as it might have different results. The mechanisms on how melanoidins changed the colour of the crystal are yet to be known, but the presence of impurities could change electron distributions in crystals which resulted in a change in crystal colour. In addition to that, the π-electrons in carbon atoms of melanoidins might move freely inside the crystal structure, resulting in light absorption that gave brownish colour (Nassau, 1978).
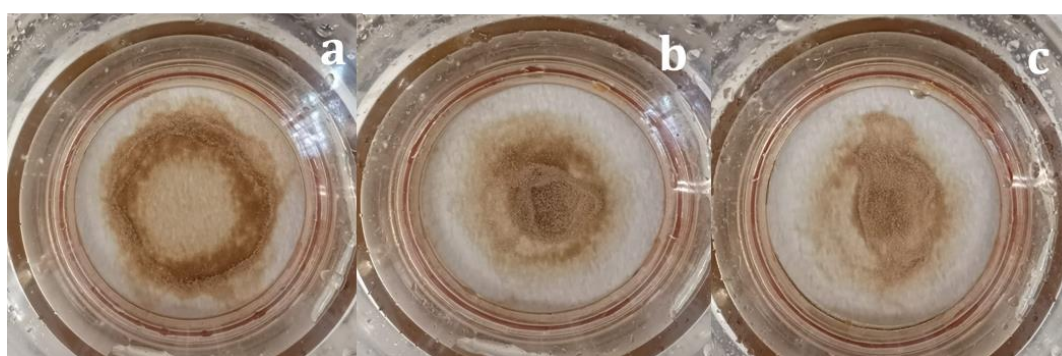
Figure 4.12 Colour of struvite crystals. a) 1 g TOC/L melanoidins, not washed, b) 1 g TOC/L melanoidins, washed with demineralised water, c) 1 g TOC/L melanoidins, washed with demineralised water and 0.1 M NaOH
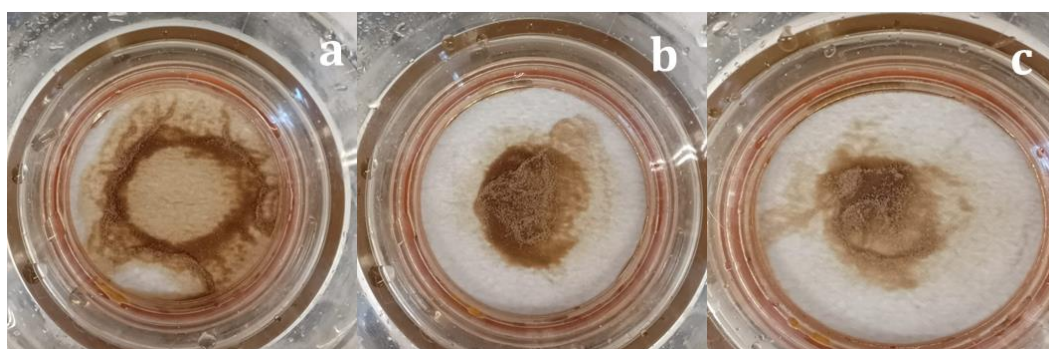
Figure 4.13 Colour of struvite crystals. a) 2 g TOC/L melanoidins, not washed, b) 2 g TOC/L melanoidins, washed with demineralised water, c) 2 g TOC/L melanoidins, washed with demineralised water and 0.5 M NaOH

4.2.4. Crystal morphology (microscopically)

In order to understand the effect of melanoidins on the morphology of struvite crystals, crystal analysis using a digital microscope was performed. The images of struvite crystals under 200x magnification are presented in Figure 4.14. The shape of the crystals without melanoidins was a mixture of X-shaped and rod-like, long, and sharp at the end. This shape was similar to previous studies (Manzoor et al., 2019; Ronteltap et al., 2010; Shaddel et al., 2019). On the contrary, the shape of the crystals with melanoidins transformed into square and pyramid-like. The shift in crystal morphology was also observed by Wei et al. (2019) and Zhou et al. (2015), as shown in Figure 2.10 and Figure 2.11. The addition of HS obstructed the active growing sites of struvite crystals, which resulted in the alteration of growth of particular crystal faces (Zhou et al., 2015). Similar blocking mechanism might have occurred with the presence of melanoidins, and hence changed the morphology of struvite crystals. It is essential to highlight that the numbers of crystals shown in Figure 4.14 do not correspond to the amount of produced struvite. The images were taken just to visualise the shape of struvite crystals.
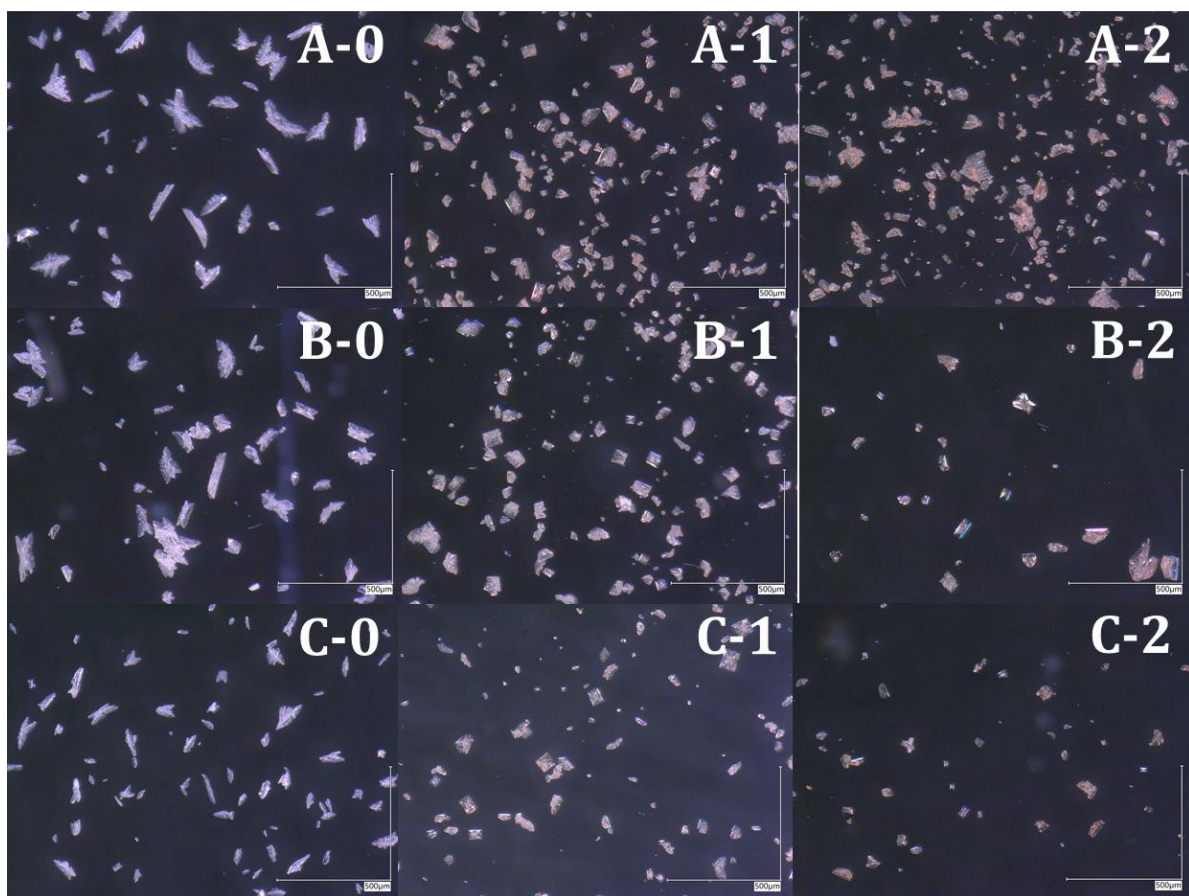
Figure 4.14 Struvite crystals under the microscope with 200 times magnification. a) The crystals obtained at pH 6.5, with 0; 1; 2 g TOC/L melanoidins, b) The crystals obtained at pH 7.25, with 0; 1; 2 g TOC/L melanoidins, c) The crystals obtained at pH 8, with 0; 1; 2 g TOC/L melanoidins.

With respect to pH, struvite crystals appeared to be smaller with the increasing pH. It can be clearly seen by comparing Figure 4.14 A-0, B-0, and C-0. There are visibly bigger particles at pH 6.5 compared to pH 7.25 and pH 8. Increase in pH will promote the formation of more nuclei, which therefore result in the production of smaller crystals (Md Mukhlesur Rahman et al., 2014). It can be concluded that nucleation was more favoured than crystal growth in higher pH values. It was also found that there were more X-shaped crystals in lower pH of 6.5. The present result is supported by the study by Manzoor et al. (2019) who found large X-shaped crystals in lower pH (6-7), and the shape shifted into twinned, elongated, and dendritic crystals at higher pH (8-9). Nonetheless, X-shaped struvite crystal was also found at pH 8.5 (Shaddel et al., 2019) and pH 10 (Ronteltap et al., 2010). A similar reduction in crystal size was also found

for the experiments with melanoidins, even though it is less visible. The decrease in crystal size is discussed further in Section 4.2.5.

Samples were also observed with 1000x magnification. The aim was to clearly see whether melanoidins were only on the surface of struvite or entrapped inside the crystal structure. Diverse crystal morphology was noticed, which indicated the heterogenicity in the shape of produced crystals. Some documented images are provided in Figure 4.15. Figure 4.15 only displays the images of big crystals; thus, the presence of melanoidins in the crystals could be apparent. By evaluating Figure 4.15 A-0, A-1, and A-2, it is visible that there were brownish spots inside struvite crystals, especially in the middle part. The edge of the crystals with melanoidins also appeared smoother with the presence of melanoidins. Similar observations can be seen in Figure 4.15 B-0, B-1, B-2 and C-0, C-1, C-2; however, the crystals seem to be more square with increasing melanoidins concentration. These results could be an indication that melanoidins adsorbed on the active growth site of struvite, hence prevent the crystals from growing into the normal shape (without melanoidins). These results reinforce the presumption that melanoidins were incorporated inside the crystal structure; therefore, affecting the shape of the crystals.
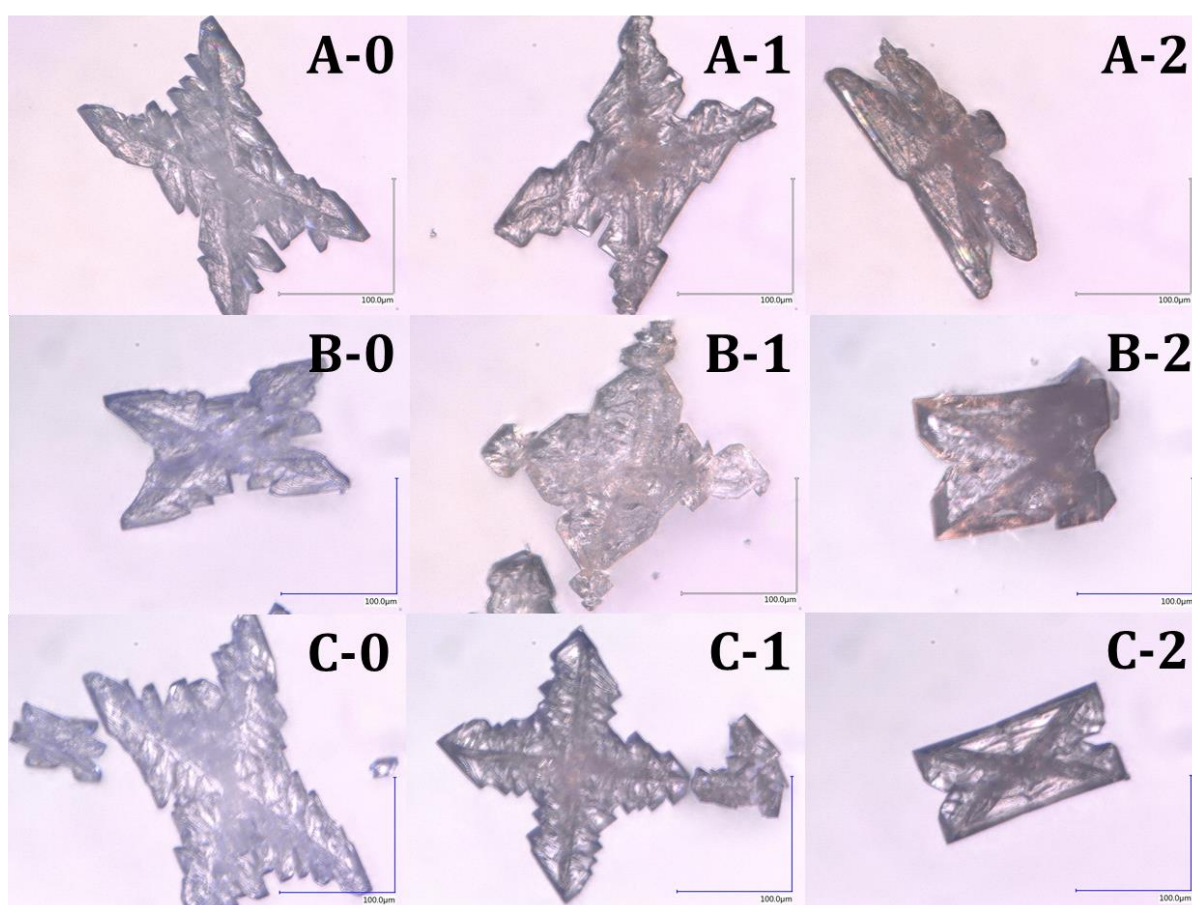
Figure 4.15 Struvite crystals under the microscope with 1000 times magnification. a) The crystals obtained at pH 6.5, with 0; 1; 2 g TOC/L melanoidins, b) The crystals obtained at pH 7.25, with 0; 1; 2 g TOC/L melanoidins, c) The crystals obtained at pH 8, with 0; 1; 2 g TOC/L melanoidins.

As a comparison, struvite crystals produced during preliminary research using HA was also observed using the microscope (Figure 4.16). The shape of the crystals was also different compared to the struvite produced with and without melanoidins. The crystals were square, and some were bigger compared to others. With 1000x magnification, it could be seen that the crystals were more amorphous compared to uncontaminated struvite crystals (0 g TOC/L melanoidins) and struvite with melanoidins. Some crystals were even enormous, as shown in Figure 4.16b. It is well-known that HA can form aggregates in altering environmental condition. The presence of metal ions, such as Mg^{2+}, will increase the chance of aggregation

through metal bridging (Pertusatti & Prado, 2007). The big crystals found in the sample with HA was possibly HA that agglomerated with struvite crystal.
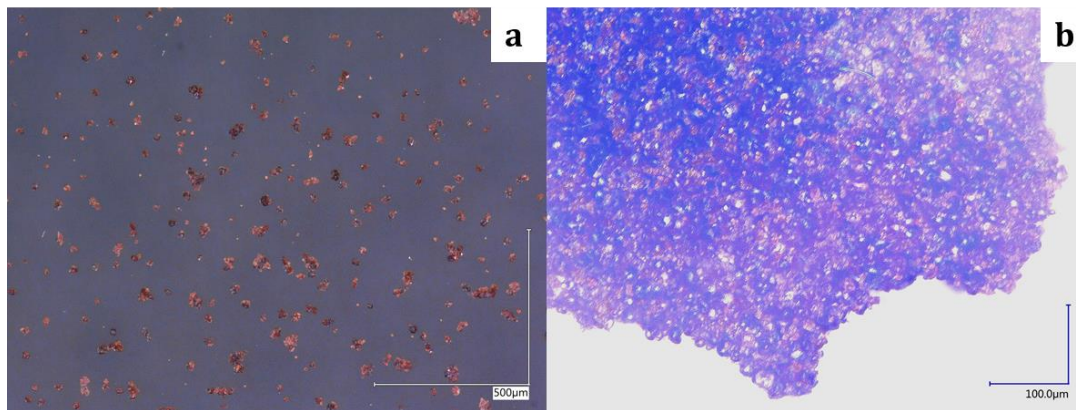
Figure 4.16 Struvite crystals with the presence of 1 g TOC/L HA. (a) with 200x magnification (b) with 1000x magnification

4.2.5. Crystal diameter

Crystal diameter analysis was done simultaneously with crystal morphology observation. Crystal diameter analysis confirmed the visible change of crystal size explained in Section 4.2.4. In general, both maximum and minimum diameters of the crystal became smaller with the presence of melanoidins as presented in Figure 4.17. A similar observation was found by Wei et al. (2019), in which the crystal size of struvite decreased along with the increasing concentration of HA. It is noteworthy that the crystal size varied greatly in all experiments, as shown by the wide error bars. These results indicated that the crystals were heterogeneous and did not have the same size. Even though the diameter became smaller, the smaller error bars were found with the presence of melanoidins. Y. Liu & Qu (2017) who studied struvite crystallisation from anaerobic digester supernatant also revealed that the presence of polymers with high concentration inhibited the growth of struvite crystals, and subsequently affecting the formation of smaller crystals with narrow size distribution.

Crystals were also getting smaller with increasing pH. These results were especially evident for the experiment with 0 and 2 g TOC/L. It has been reported that pH influences the crystal size of struvite, in which higher pH decreases the crystal size of struvite (Li, Huang, et al., 2019; Md Mukhlesur Rahman et al., 2014). This occurrence can be explained by the fact that increase in pH favours the formation of more crystal nuclei rather than growth, hence causing the production of smaller crystals (Md Mukhlesur Rahman et al., 2014).
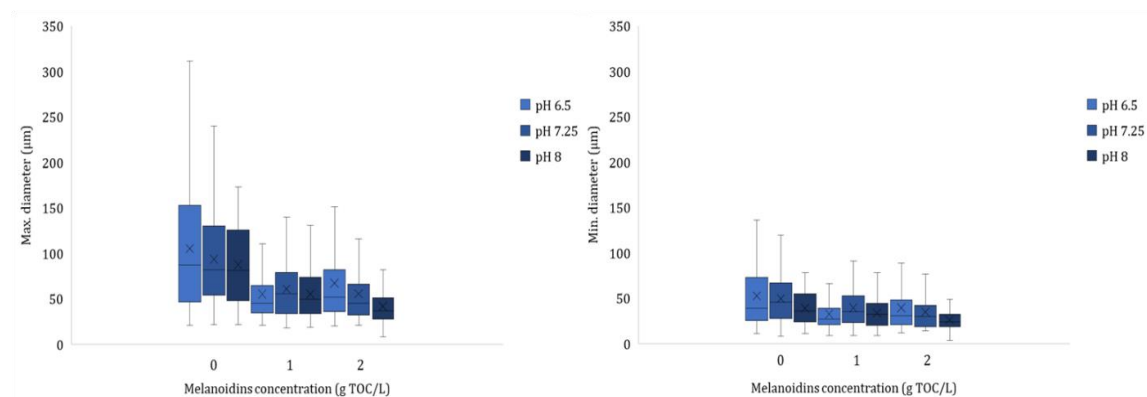
Figure 4.17 Maximum (left) and minimum (right) diameter of struvite crystals in various pH and melanoidins concentrations. The error bars show the minimum and maximum diameter, the middle bar shows the median, the X shows the mean, and the boxes show the first and third quartiles.

Crystal size is an important parameter in struvite crystallisation because it determines the efficiency of the downstream processes in real WWTP, including settling, filtering, and drying (Shaddel et al., 2019). In addition to that, crystal size will also affect the market value of struvite. Fine struvite crystals have low market value as fertilisers (Crutchik et al., 2017). It is because larger crystals are easier to be managed, transported, and applied in the field (Li, Huang, et al., 2019). Therefore, it is vital to understand the overall parameters that affect the crystal size of struvite. According to particle settling theory formulated by Newton and Stokes, a particle with a larger diameter will have bigger settling velocity and therefore will settle faster (Metcalf & Eddy, 2014). On the other hand, the fine particles with low settling velocity tend to be washed out from the reactor (Crutchik et al., 2017; Shaddel et al., 2019). In addition to crystal size, crystal shape and density will also influence the settleability of struvite crystals (Tarragó et al., 2016). Between the different morphologies, biggest settling velocity was observed in the bipyramidal crystals, followed by X-shaped crystals, and the lowest settling velocity was found for the dendritic (needle-shape) crystals (Shaddel et al., 2019). These findings are interesting because the struvite produced without melanoidins were mainly the X-shaped crystals and the ones with melanoidins were pyramid-like crystals. Even though settleability test was not conducted in this study, it is likely that the big X-shaped crystals will settle faster compared to small pyramid crystals. However, small crystals are more favourable for the formation of granules than X-shaped crystals because the X-shaped crystals cannot agglomerate densely despite their large particle sizes (Y. Liu & Qu, 2017). Regardless of the bigger size of X-shaped crystals, its formation should be avoided.

Experiment without melanoidins at pH 6.5 resulted in more X-shaped crystals and low phosphorus removal efficiency, meanwhile experiment at pH 7.25 and 8 showed less X-shaped crystals (more rod-like crystals) and high phosphorus removal efficiency. Based on these results and the information provided by the literature, the operation at pH 7.25 or 8 is, therefore, more beneficial. Although Y. Liu & Qu (2017) stated that small crystals are more favourable for the formation of struvite granules, it remains unclear if smaller crystals resulted from the experiments with melanoidins would have better granulation properties compared to the bigger rod-like crystals without melanoidins, especially when the settleability is also considered.

4.3. Melanoidins disruption mechanisms on struvite crystallisation

Despite the similarities between melanoidins and HS, the preliminary research has proven that they behaved differently and affected struvite crystallisation in different ways. The disruption mechanisms of HS on struvite crystallisation can be explained in two ways: complexation with struvite reactants and adsorption on active growth sites of struvite crystals. First, HS could reduce the solution supersaturation by complexing with magnesium or phosphate ions in the solution. At the same time, HS will increase the ionic strength of the solution, resulting in lower ion activity. Second, HS can retard struvite crystallisation by adsorption on active growth sites of the crystals, hence preventing the growth of crystals and altering crystals shape (Wei et al., 2019). On the contrary, the melanoidins disruption mechanisms on struvite crystallisation are yet to be known. This sub-chapter will elaborate more on this matter.

4.3.1. Nucleation and growth of crystals

As demonstrated by Wei et al. (2019), both complexation of HS with struvite reactants and their adsorption on active growth sites of struvite impeded the induction time and growth of struvite crystals. Prolonged induction time might happen because the complexation of HS with struvite reactants reduces SI of the solution, and SI is one of the factors influencing nucleation (Mehta & Batstone, 2013). It was predicted that the presence of melanoidins would result similarly in the nucleation and growth of struvite crystal.

Figure 4.18 shows the results of pH measurements. A rapid decrease of pH in the first minutes of the reaction can be an indication of nucleation. The drop of pH occurred immediately after the addition of $MgCl_2$ when the reactants started to react to release protons and form struvite crystals (Shih & Yan, 2016). For the experiments at pH 6.5, the pH dropped and remained constant in the experiment without melanoidins; meanwhile, in the experiments with melanoidins, the pH slightly fluctuated. The unsteadiness of pH values for experiments with melanoidins might be due to the buffering capacity of melanoidins. This finding is

supported by the fact that HA could greatly resist pH change, especially in a range between pH 5.5 and 8. The buffering capacity of HA comes from the weak acid and base groups on HA structure. Addition of OH^- or H^+ ions will dislocate proton distributions in HA structure. Afterwards, neutralisation happens due to the interaction between the phenolic and carboxyl groups of HA (Pertusatti & Prado, 2007). These results made the determination of induction time using pH data is not straightforward because acid and base dosing were done repeatedly to keep the desired pH value.
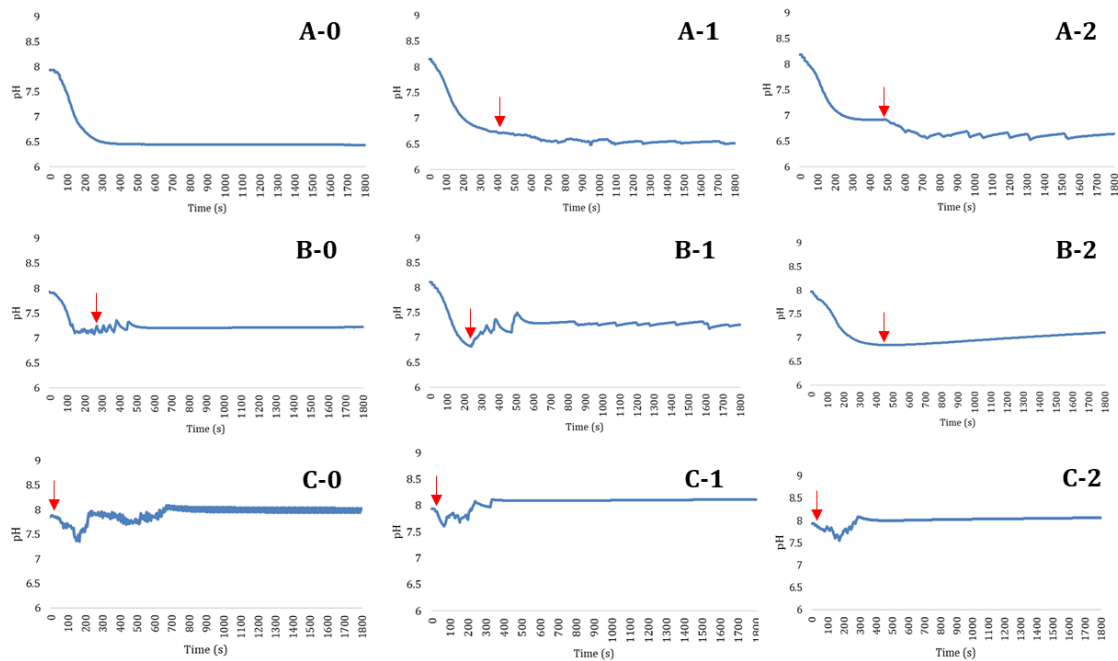
Figure 4.18 pH measurements during struvite crystallisation. The red arrow shows the first pH adjustment. a) The pH measurement obtained at pH 6.5, with 0; 1; 2 g TOC/L melanoidins, b) The pH measurement obtained at pH 7.25, with 0; 1; 2 g TOC/L melanoidins, c) The pH measurement obtained at pH 8, with 0; 1; 2 g TOC/L melanoidins.

To overcome the problem, EC was also used to monitor nucleation and induction time. Ideally, EC values will decrease as ions are removed from the solution, transformed from soluble into solid struvite crystals. However, the release of H^+ during struvite crystallisation could also affect EC values (Kabdaşli et al., 2006). Figure 4.19 shows the EC reading for all experimental conditions in one of the triplicates. Higher melanoidins concentrations resulted in higher EC values, which implied higher ionic strength in the solution. Higher ionic strength will decrease the saturation index of struvite and reduce the thermodynamic force for struvite crystallisation (J. Wang et al., 2006). The reaction lasted for 1 hour, but the data shown here are only until 30 minutes because the EC values were already stagnant. As shown in Figure 4.19, there was initially a rapid increase in EC value, which indicated the time where $MgCl_2$ was injected to the solution. Afterwards, the reactants started to react, ions were removed from the solution, and EC values decreased slowly. The final EC values were higher than initial EC values, which might be caused by the remaining Cl^- (from $MgCl_2$ or HCl) and Na^+ (from NaOH) ions in the solution. The EC stabilised and became constant after some minutes, and this was considered as the induction time. After this point, it was presumed that chemical reaction already stopped; meanwhile, physical crystal growth still occurred. It was estimated that the crystallisation reaction happened so fast in the first minutes, and the remaining time was just for the agglomeration to grow larger crystals. Literature also reported that struvite crystallisation happens reasonably fast. Equilibrium between solid struvite crystals and ions could be reached within the first 10 minutes of struvite crystallisation (Crutchik & Garrido, 2016); meanwhile, the time required to grow the crystals could be days (Mehta & Batstone, 2013).
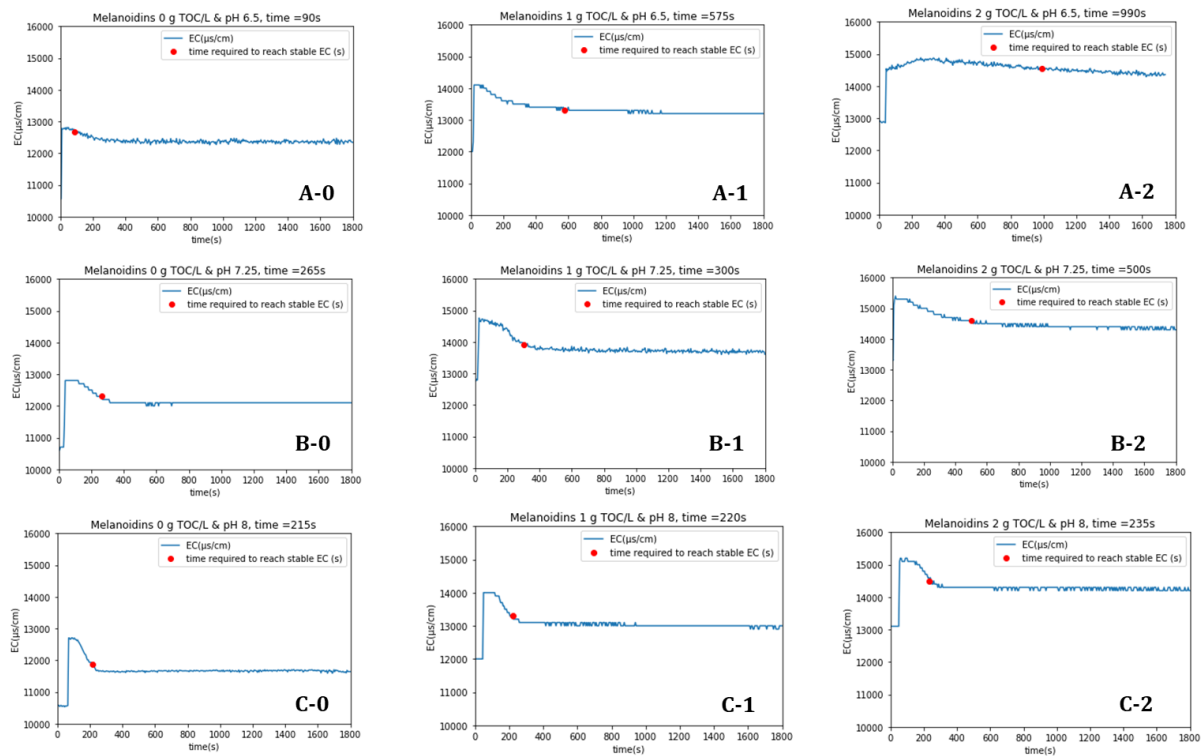
Figure 4.19. EC records during struvite crystallisation in one of the triplicates. a) The EC measurement obtained at pH 6.5, with 0; 1; 2 g TOC/L melanoidins, b) The EC measurement obtained at pH 7.25, with 0; 1; 2 g TOC/L melanoidins, c) The EC measurement obtained at pH 8, with 0; 1; 2 g TOC/L melanoidins.
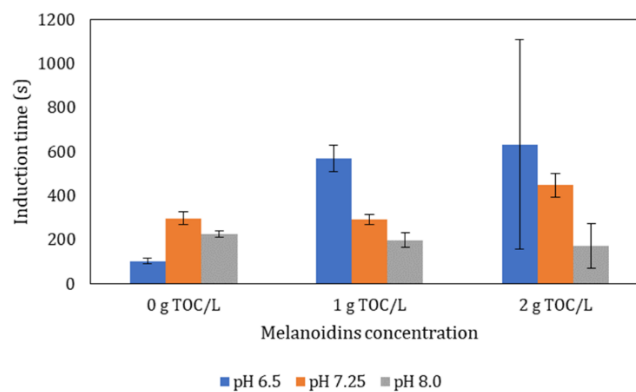
Figure 4.20 Induction time of struvite crystallisation in various pH and melanoidins concentration

Figure 4.20 shows the summarised result of the determination of induction time of struvite crystallisation in various pH and melanoidins concentrations for all the triplicates. The induction time was shorter with the increasing pH except for experiment with 0 g TOC/L melanoidins and pH 6.5. This result indicated that pH has a strong influence in induction time. The solubility of struvite decreases and the ion activity product increases along with a rise in pH, which subsequently result in the increase of supersaturation in the system (Crutchik & Garrido, 2016; Md Mukhlesur Rahman et al., 2014). Therefore, higher pH made the solution became supersaturated and nucleated faster.

The presence of melanoidins also seemed to prolong the induction time, except for the experiments at pH 8. The induction time results at pH 8 can be an indication that pH 8 made the system supersaturated, and hence the effect of melanoidins or ionic strength on nucleation diminished. It should be highlighted that experiments using 2 g TOC/L using pH 6.5 and pH 8 had high standard deviations. Due to the high standard

deviations, ANOVA had proven that there was no significant difference in induction time for the experiments at pH 6.5 and 8 in various melanoidins concentrations ($p > 0.05$). There was no significant difference between experiments using 0 and 1 g TOC/L at pH 7.25, but there was a significant difference when melanoidins concentration was 2 g TOC/L, in which melanoidins led to longer induction time. The previous study obtained appreciably longer induction time in struvite crystallisation as the concentration of HA increased from 0 to 100 mg HA/L (Wei et al., 2019). However, the results of the experiment using HA do not necessarily correspond to the experiment using melanoidins, as results described in Section 4.1 also show different P-removal. Various factors could explain this difference, including the different molecular weight between HA and melanoidins, different experimental conditions (pH, molar ratio Mg:N-NH$_4$:P-PO$_4$, ionic strength, temperature, seeding, etc.), and different technique used to determine the induction time. Furthermore, possible explanations for the peculiar pattern of induction time are disturbance or interference in EC reading and the stochasticity of reaction. Nucleation in crystallisation is a stochastic chemical process (Capasso & Salani, 2000), in which the process will behave randomly and as a result, the results are not reproducible (Lee et al., 2020). The stochastic event of nucleation could be identified with 100-200% deviation in induction time (Jiang & Ter Horst, 2011). It is acknowledged that a well-designed seeding technique would provide better product reproducibility between batches of crystallisation and minimise the stochasticity of nucleation (Roberts et al., 2017). The absence of seeding in this study amplified this random behaviour; therefore, the induction time in all experiments varied greatly.

The stochasticity of nucleation was also confirmed by analysis using focused beam reflectance measurement (FBRM) as shown in Appendix 5. FBRM is a probe-based device that can be used to observe in situ development of particle characterisation including its size and structure; therefore it is widely used for monitoring the crystallisation process (Kumar et al., 2013). FBRM was initially used to identify nucleation and growth; however, the results were inconclusive.

Figure 4.21 shows the visual observation of crystal growth. Even though EC was already constant after the first minutes of reaction, crystals continued to grow up to 30 minutes of observation. If the observation had been continued, the crystals would have continued to grow. It was apparent from time to time observation that crystals became larger. From this observation, it was also evident that crystal shape was different due to the presence of melanoidins. Figure 4.22 shows the change in diameter as a result of crystal growth. Both maximum and minimum diameter became larger over time. Similar result as explained in Section 4.2.5 was obtained, in which melanoidins resulted in smaller crystal diameter. This result supported the theory that melanoidins altered crystal growth (Wei et al., 2019).
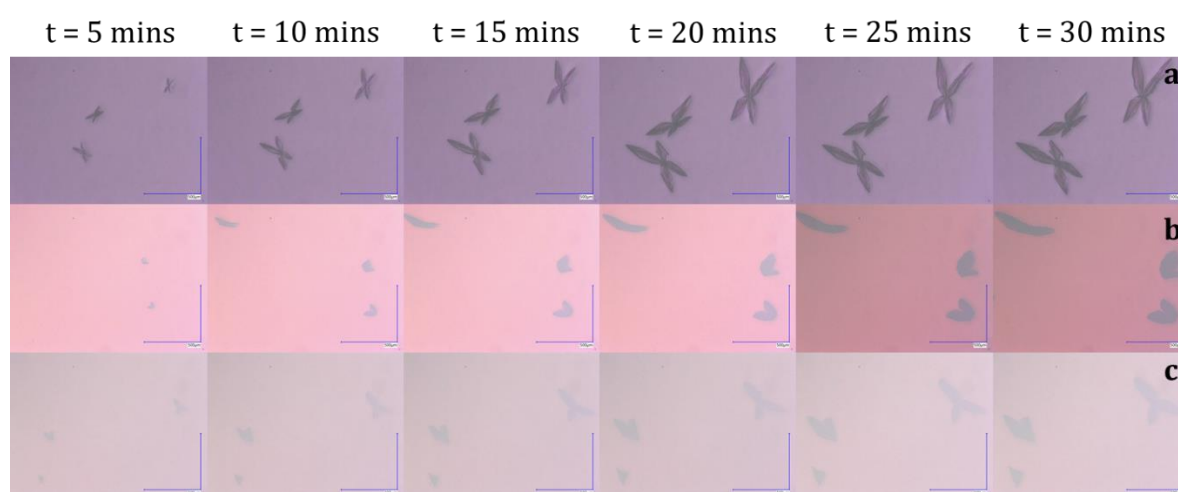
Figure 4.21 Visual observation of crystal growth for the experiment at pH 6.5. a) 0 g TOC/L b) 1 g TOC/L c) 2 g TOC/L. The blue bar is equal to 500 μm.
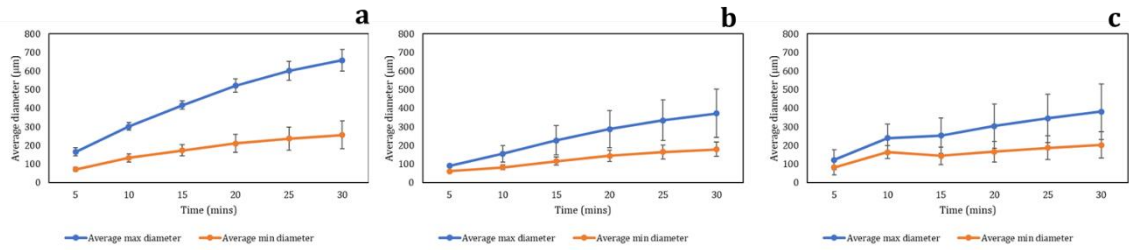
Figure 4.22 Change in diameter as a result of crystal growth for the experiment at pH 6.5. a) 0 g TOC/L b) 1 g TOC/L c) 2 g TOC/L

4.3.2. Complexation between melanoidins and reactants of struvite

In this study, the formation of complexes between melanoidins and reactants of struvite was investigated for only magnesium. In order to understand the complexation between Mg and melanoidins, lab experiment and PHREEQC modelling were done. In the lab experiment, the complexation was studied by using ultrafiltration membrane, in which the concentrations of Mg in influent (feed) and the permeate were measured. If Mg forms complexes with melanoidins during the experiment, the resulting complexes will probably be larger than the membrane pore size (Adusei-Gyamfi et al., 2019). Therefore, the complexes cannot pass through the membrane. As a result, the decrease in Mg concentration in the permeate indicates the formation of complexes between Mg and melanoidins.
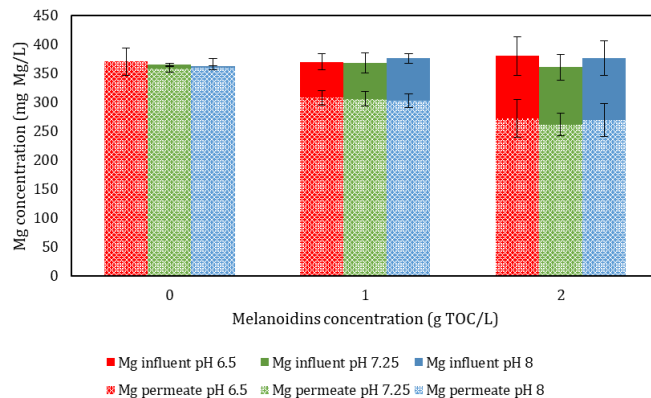
Figure 4.23 Complexation of Mg-melanoidins, showing the different concentration of Mg in the influent and the permeate

Figure 4.23 shows the results of Mg-melanoidins complexation. It can be seen in Figure 4.23 that for the experiment without melanoidins (0 g TOC/L), the concentrations of Mg in influent and permeate were nearly equal. As no compound reacted with Mg ions in this condition, Mg was not retained by the membrane because the ultrafiltration membrane does not retain salt ions (Metcalf & Eddy, 2014). The permeate of ultrafiltration will consequently contain the same ion concentration as the feed (Adusei-Gyamfi et al., 2019). Different observations were found for the experiment with 1 and 2 g TOC/L melanoidins. There was less Mg detected in the permeate than in the influent. This result indicated the formation of Mg-melanoidins complexes. The concentration of Mg in the permeate was even less with the higher melanoidins concentration, explaining that there were more Mg that formed complexes with melanoidins. The average percentage of Mg that complexed with melanoidins was 17.5±1.6% and 27.9±0.7% for 1 and 2 g TOC/L melanoidins initial concentrations, respectively. One of the factors affecting Mg-HS complexation is the binding capacity of carboxylic and phenolic group of HS to Mg ions (Yan et al., 2015). Higher melanoidins concentration provided more binding sites for Mg; therefore, more complexes could be formed, and less Mg was found in the permeate, accordingly. In this experiment, however, the effect of pH on Mg-melanoidins complexation was not visible. There was no notable difference between the experiment in different pH values (p > 0.05). This result contradicts with the study by Yan et al. (2015) who stated that

44

the formation of complexes is pH-dependent, in which there will be more complexes with the increasing pH from 5–11. However, this study used a wide pH step (5, 7, and 11), which probably made the effect of pH more visible.

The results of the complexation experiment verified the results from previous studies that declared the formation of Mg-HS complexes in the various experimental conditions (Adusei-Gyamfi et al., 2019; Wei et al., 2019; Yan et al., 2015). The formation of these complexes leads to a decrease in the supersaturation and thereby suppressing the nucleation and growth of struvite crystals (Wei et al., 2019). Next to complexing with Mg, melanoidins might as well form aggregates due to the association of divalent cations like Mg with the carboxyl groups in melanoidins (Adusei-Gyamfi et al., 2019). There was a possibility that the formed aggregates attached to struvite crystals and inevitably affected the morphology of struvite crystals.
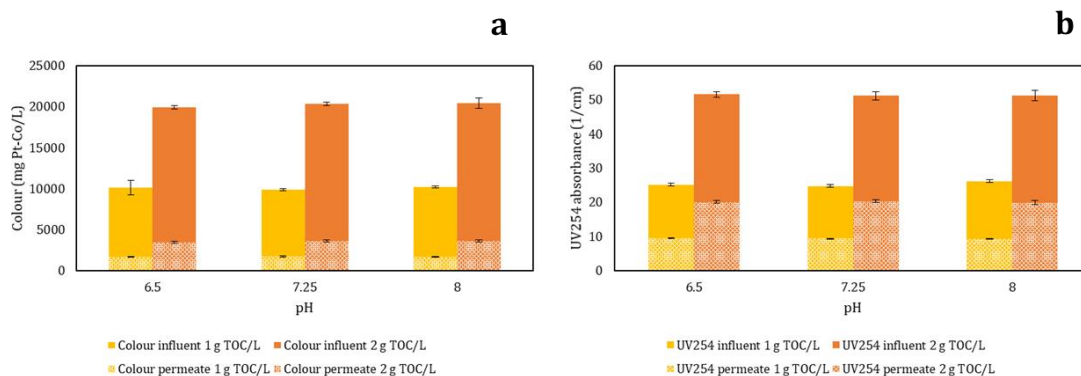
Figure 4.24 Complexation of Mg-melanoidins, showing different colour (a) and UV absorbance (b) in the influent and the permeate

The influent and permeate of complexation experiment were also tested for colour (475 nm) and UV_{254} absorbance. The colours of the influent and permeate were visibly different. The differences could be explained by the results given in Figure 4.24. The colour and UV_{254} in the permeate were lower than those in the influent, which explains that melanoidins were partially rejected by the membrane. In general, HS are mainly eliminated during membrane filtration by size exclusion, charge repulsion, and hydrophobic interactions (Adusei-Gyamfi et al., 2019). For the size exclusion mechanism, these results indicated that some fractions of melanoidins were unable to pass through the 1 kDa membrane because melanoidins consist of both HMW and LMW fractions (Ćosović et al., 2010; H. Y. Wang et al., 2011). Figure 4.24b shows lower UV_{254} in the permeate, indicating that some aromatic groups of melanoidins could not pass through the membrane. As for the charge repulsion mechanism, melanoidins are negatively charged (H. Y. Wang et al., 2011) and the regenerated cellulose membrane could be either neutral or negatively charged, in which negatively charged membrane would have better rejection for negatively charged compounds (Shao et al., 2011). Melanoidins consist of both hydrophilic and hydrophobic fractions (Adusei-Gyamfi et al., 2019) and the used membrane was hydrophilic. Hence, the hydrophilic membrane repulsed the hydrophobic fraction (Galanakis, 2015). Similar to the results of Mg, the effect of pH on colour and UV_{254} was also not evident.

The complexation between melanoidins and magnesium was also computed using PHREEQC. Melanoidins were represented as HA and FA speciations because PHREEQC database does not contain melanoidins in its database. The results of modelling using PHREEQC (Figure 4.25) showed that HA formed more complexes with Mg than FA in all modelled pH values. The concentrations of Mg-FA complexes were lower compared to Mg-HA. The possible explanation behind this result is the chemical composition of HA, which contain substantially higher carboxyl and phenolic groups, leading to its stronger complexing effect than FA (Grassi & Rosa, 2010). It was reported that Mg forms stronger complexes with carboxylic group of HS compared to phenolic group (Adusei-Gyamfi et al., 2019), but little information could be found if Mg tends to bind to HA or FA. PHREEQC input represented the melanoidins used in this study, which contained considerably higher FA than HA. The lower concentration of Mg-FA complexes might indicate that Mg

favoured binding to HA than FA. Regardless, lab result has proven that Mg formed complexes with melanoidins. The concentration of formed complexes decreased with increasing pH, and this trend was detected for both Mg-HA and Mg-FA complexes. It might be caused by the tendency of Mg to bind stronger to the carboxylic group than the phenolic group, and the carboxylic group is more dominant at low pH (Adusei-Gyamfi et al., 2019). The results from PHREEQC also revealed that higher initial concentrations of HA and FA led to the higher concentration of formed complexes. As the increase in HA and FA also increased the number of available binding sites, the concentration of formed complexes also increased. The similar trend was also documented in the lab experiment, as explained previously. The PHREEQC simulation showed that at the end of the batch reaction, most HA and FA remained at their free form in the solution.
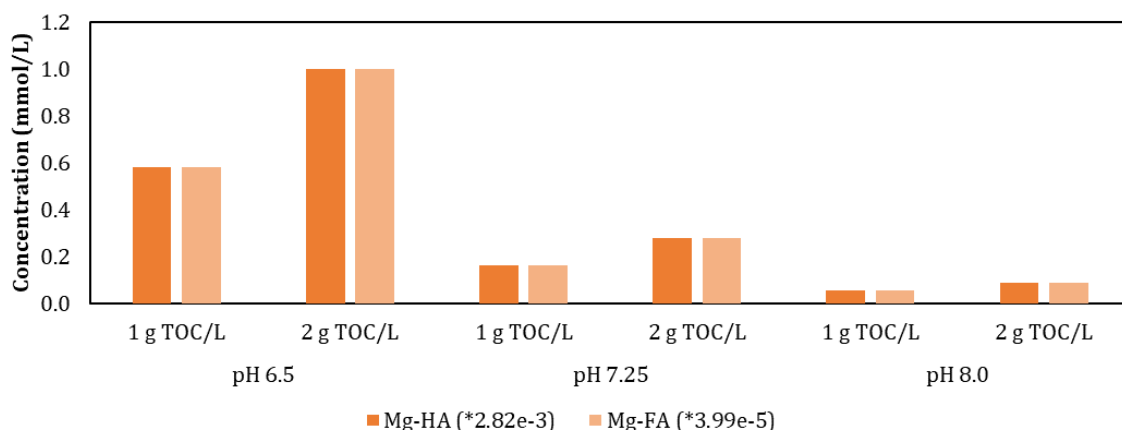
Figure 4.25 Results of PHREEQC modelling for Mg-HA and Mg-FA complexation in different pH values and different initial HA and FA concentrations

Literature also reported the complexation between HS and phosphate in aqueous solution (Guardado et al., 2008; He et al., 2006; Wei et al., 2019). The establishment of the complexes between P and HS will also alter struvite crystallisation. There are different possible ways for the formation of these complexes. Firstly, phosphorus may bind with –OH in HS, and then join with C–OH groups to form orthophosphate monoesters (Wei et al., 2019). Secondly, stable organic complexes might be formed between HS and phosphate with the presence of metal bridges. The formation of complexes in the solution can involve diverse metals, including divalent (Zn, Cu, Mn, Ca, and Mg) and multivalent (Fe and Al) metals. The formation of the complexes is affected by pH, in which different metals form different configurations (monodentate, bidentate, and chelate) with HS and P at different pH values (Guardado et al., 2008; Lawrance, 2010). As the synthetic reject water contained these various metals, there was likely formation of phosphate-metal-humic complexes during struvite crystallisation. Similarities between melanoidins and HS intensify the chance that similar complexes were formed in this study. The formation of these complexes might be responsible for the decrease of supersaturation and affecting P-removal and crystal morphology.

Ammonium could also react with HS. Their interactions are mainly found in soil. It was found that after the application of fertiliser, the ammonia applied to HS-containing soil was not readily available for plants (Thorn & Mikita, 1992). Furthermore, soil minerals coated with HA showed significant adsorption of ammonium (W. Z. Zhang et al., 2013). This phenomenon is caused by the chemical reaction between ammonium and HS. Ammonium could be incorporated with HS by fixation with phenolic groups of HS. With the help of O_2, phenol is converted into quinone, which eventually reacts with ammonia to establish a complex polymer. pH also has a strong influence in the complexation between ammonium and HS, because ammonia fixation is more favoured at pH value higher than 7 (Thorn & Mikita, 1992). In respect to this study, reactions between melanoidins and ammonium in different pH values would affect struvite crystallisation.

4.4.   The fate of trace elements

Due to the high concentration of ammonia nitrogen in reject water of anaerobically digested sludge, it cannot be entirely removed by struvite crystallisation. Following struvite crystallisation unit in full-scale WWTP, several side-stream or reject water treatment are still required to provide final effluent that fulfils the effluent standard. In The Netherlands, many WWTPs employ partial nitritation followed by anaerobic ammonium oxidation (PN/A) reactors to treat the remaining ammonia nitrogen (Lou, 2019). In PN/A process, ammonia nitrogen is partially oxidised into nitrite by ammonium oxidising bacteria (AOB). Afterwards, nitrite is used as an electron acceptor to anaerobically oxidise the remaining ammonia nitrogen into nitrogen gas by anaerobic ammonium oxidisers (AAO) (Sri Shalini & Joseph, 2012). In order to support the growth of microorganisms in these processes, essential trace elements are required. Next to the presence of macroelements (C, N, P), optimal growth for AOB and AAO requires certain trace elements Ca, Fe, Zn, Co, Mn, Cu, Mo, Ni, Se, and B (Sri Shalini & Joseph, 2012; Van De Graaf et al., 1996). Therefore, it is crucial to ensure the bioavailability of these trace elements. In WWTPs that employ THP, the complexation of trace elements with melanoidins has the possibility to decrease the bioavailability of these vital trace elements (Driessen et al., 2020). On the other hand, the trace elements may also co-precipitate with struvite and coincidentally be removed from the water (Tang et al., 2019). In this study, the fate of the trace elements in struvite crystallisation was studied by a lab experiment and PHREEQC modelling.

4.4.1.   Lab experiment

Both supernatant and struvite crystal were analysed by ICP-MS to determine the concentrations of trace elements. Initially, it was planned to investigate the fate of 10 trace elements which are required by AOB and AAO bacteria and 2 additional heavy metals, as explained in Section 3.1.3. However, it was not anticipated that the presence of chloride ions (Cl^-), which came from $MgCl_2$ and HCl would interfere with the ICP-MS analysis. Chloride gives interference by forming isotopically identical polyatomic species with the analytes, such as $^{35}Cl^{16}O^1H^+$, $^{37}Cl^{18}O^1H^+$, $^{12}C^{16}O^{37}Cl^+$ that interfere with the determination of ^{52}Cr, ^{56}Fe, and ^{65}Cu, respectively (May & Wiedmeyer, 1998). The formation of these species will subsequently result in a faulty reading of ICP-MS (Lum & Sze-Yin Leung, 2016; Wilschefski & Baxter, 2019). From a total of 12 elements analysed in ICP-MS, only 3 showed accurate results. The accurate results were obtained for Ca, Mn, and Ni and will be discussed in this section. The other elements (Al, B, Co, Cr, Cu, Fe, Mo, Se, Zn) will only be discussed based on PHREEQC modelling in Section 4.4.2. The full ICP-MS results are enclosed in Appendix 6.
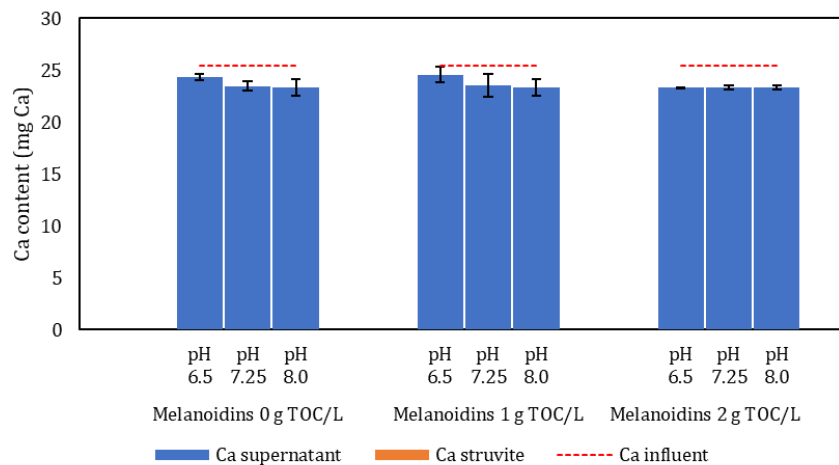
Figure 4.26 Mass balance of calcium

Figure 4.26 shows the mass balance of calcium. The results show that in all pH values and all melanoidins concentrations, most Ca ended up in supernatant. The difference between the experiments was not substantial. The concentrations of Ca in struvite crystals were below the detection limit of ICP-MS. As the mass balances for Ca were not completely closed, it is likely that there was some Ca which ended up in

struvite, but the concentration was too low. Even though Ca is known to hinder struvite crystallisation by competing to react with phosphate ions (Warmadewanthi & Liu, 2009), the concentration of Ca in this study is much lower than that of Mg; therefore the formation of struvite is more favourable than Ca-phosphate. Low Ca concentration in the influent will result in high purity struvite (Li, Huang, et al., 2019). This explains the absence of Ca in struvite product. The majority of Ca which remained in the supernatant, therefore, might be utilised by AOB and AAO bacteria. As Ca was present in the supernatant despite the melanoidins concentrations, it could not be easily concluded if Ca formed complexes with melanoidins. Nonetheless, Ca is known to bind to either carboxylic or phenolic groups of HS at both low pH (4.4) and high pH (9.5) (Adusei-Gyamfi et al., 2019; Cabaniss, 2011).

The result of the mass balance of manganese is given in Figure 4.27. Without the presence of melanoidins, some Mn were found in struvite, indicating the potential of co-precipitation. Mn might co-precipitate with struvite in the form of $Mn(OH)_2$ or Mn_2O_3 (Tang et al., 2019). As seen in Figure 4.27, the concentration of Mn in supernatant for the experiment without melanoidins decreased along with the increasing pH. This was because the precipitation of $Mn(OH)_2$ is affected by pH. The development of $Mn(OH)_2$ requires alkaline environment (Tang et al., 2019). As melanoidins concentrations increased, there were more Mn ended up in supernatant and there were less Mn ended up in struvite. This result indicated that Mn reacted with melanoidins, which made Mn did not co-precipitate easily with struvite in comparison to the condition without melanoidins. It was reported that Mn formed complexes with HS; however, the formed complexes were less stable compared to other metals, for example Cu or Fe (Pandey et al., 2000; Pradhan et al., 2018). The mass balance of Mn was confirmed to be equal to the theoretical value ($p > 0.05$).
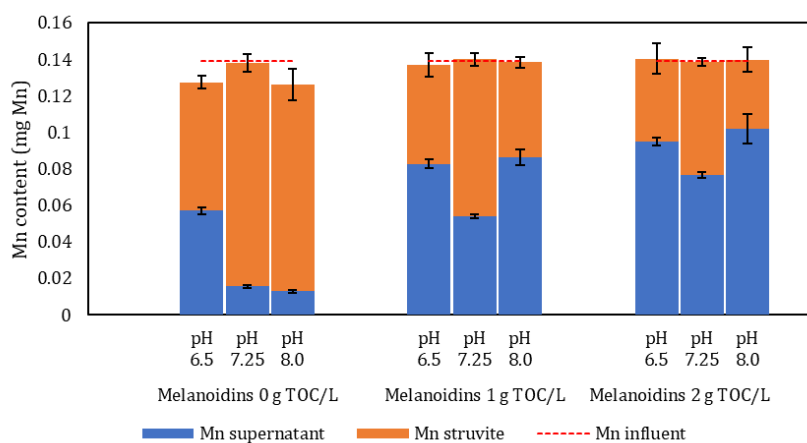
Figure 4.27 Mass balance of manganese

Ni is one of the trace elements regulated in struvite regulatory framework in The Netherlands, but also included in essential trace elements for the growth of AAO and AOB bacteria (Sri Shalini & Joseph, 2012; Van De Graaf et al., 1996). The experimental result which is depicted in Figure 4.28 shows the fate of Ni. Without the presence of melanoidins, the major part of Ni ended up in struvite. Ni could co-precipitate with struvite in the form of $Ni(OH)_2$. Even though the mechanism between Ni deposition in struvite is not clearly established yet, it was suggested that the presence of amino, hydroxyl, and phosphate groups in struvite might facilitate the adsorption of metals by either the formation of coordination or by the adherence of metal hydroxide into struvite through hydrophilic interaction (Tang et al., 2019). In addition to this mechanism, both Ni and Mn might encounter ion exchange during the reaction process, as shown in Equation 2, where M represents trace element cations including Ni and Mn (Tang et al., 2019).

$$M^{2+} + MgNH_4PO_4 .6H_2O \rightarrow MNH_4PO_4.6H_2O + Mg^{2+} \text{ (2)}$$
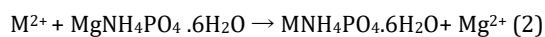
Such contrary results were found with the presence of melanoidins, in which most Ni ended up in supernatant. As expected, Ni also formed complexes with melanoidins. Ni^{2+} tends to bind strongly to the amine-containing groups of HS (Cabaniss, 2011). In comparison to Mn, the stability constant of Ni-HS

complexes is bigger than Mn-HS complexes, meaning that Ni-HS complexes are more stable than Mn-HS complexes. On the one hand, the presence of melanoidins yielded clean struvite with low Ni content, but on the other hand, melanoidins will complex with Ni and reduce the availability of Ni for the AAO and AOB bacteria. The mass balance of Ni was confirmed to be equal to the theoretical value ($p > 0.05$).
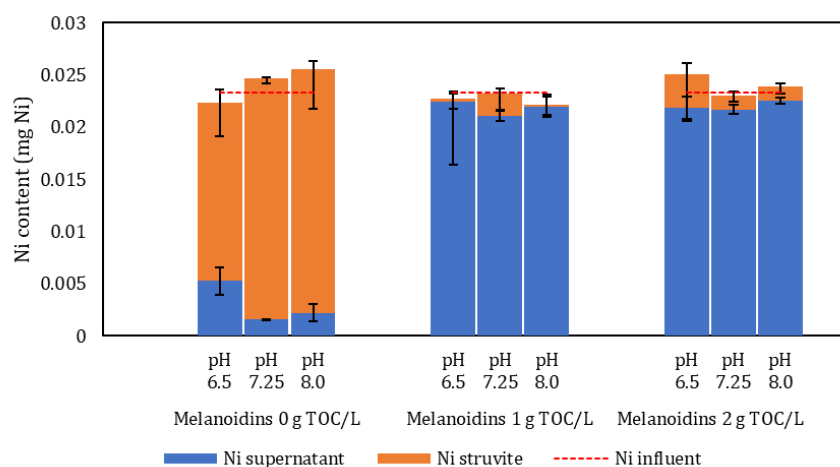
Figure 4.28 Mass balance of nickel

4.4.2. PHREEQC modelling

PHREEQC modelling was used to complement the results obtained from the lab experiment. PHREEQC was used to model the establishment of complexes between HA and FA with Ca, Cu, and Fe(III). The formation of complexes indicated the chance that some trace elements remained in supernatant after struvite crystallisation. The results are given in Figure 4.29. For Ca, the concentration of the formed Ca-HA complex slightly increased along with the increase in pH value. The higher concentration of HA and FA led to a higher concentration of Ca-HA and Ca-FA complex. Similar to Mg-FA complexes (Figure 4.25), a very low concentration of Ca-FA complex was detected. Ca forms stronger complexes with HS compared to Mg, and it is mostly bound to carboxyl groups of HS at low pH or phenolic groups at high pH (Adusei-Gyamfi et al., 2019).

As for Cu, the concentration of Cu-HA and Cu-FA complexes did not differ considerably with increasing pH and increasing initial concentration of HA and FA. Cu is greatly bound to HS, in which it can bind with either the carboxyl, phenolic, and amine groups of HS (Adusei-Gyamfi et al., 2019; Cabaniss, 2011). The comparatively constant concentration of Cu complexes could indicate the stability of Cu-HS complexes, as reported by Pandey et al. (2000). However, the concentration of Cu-FA complexes were higher than Cu-HA complexes.

A similar trend as for Mg-HS complexes was detected for Fe-HS complexes, in which the concentration of formed complex decreased with higher pH and increased with higher HA and FA concentrations. At pH 8, the concentrations of Fe-HA and Fe-FA complexes were very low to be seen in Figure 4.29. The strong effect of pH on Fe-HS complexation is confirmed by Adusei-Gyamfi et al. (2019), who stated that the formation of complexes was profoundly affected by pH. One of the reasons behind this is the fact that Fe has different species in different pH values, thus affecting the way it binds to HS (Marsac et al., 2013). In contrary to Mg and Ca, PHREEQC showed that the concentration of formed complexes between Fe-FA is higher than Fe-HA. Fe binds equally to both carboxyl and phenolic sites of HS (Marsac et al., 2013), but it is can hardly be found if Fe binds stronger to either FA or HA. In general, aside from complexing with Fe(II) and Fe(III), HS also tend to decrease the formation of iron oxides and hydroxides, and also inhibit the aggregation of Fe nanoparticles (Pédrot et al., 2011).
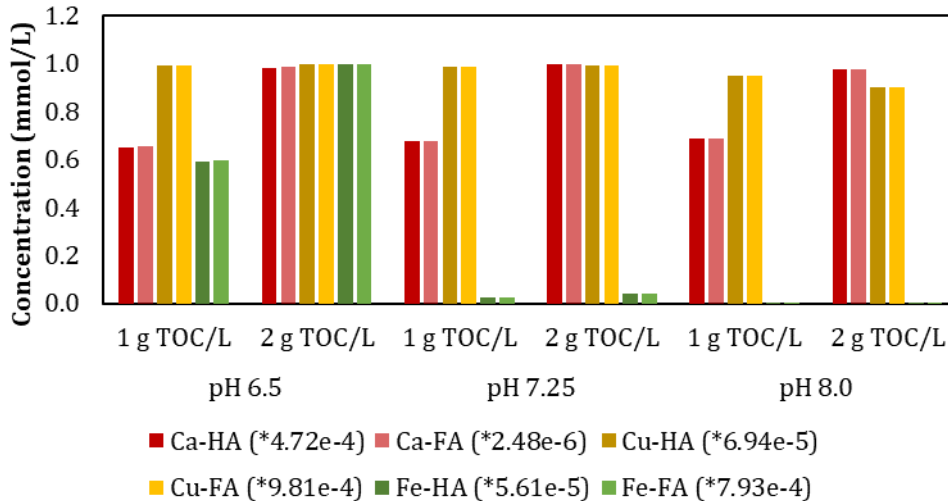
Figure 4.29 Results of PHREEQC modelling for Ca, Cu, and Fe complexation with HA and FA

Due to the limitations in PHREEQC, the complexation between HS with Al, B, Cr, Ni, Mo, Zn could not be predicted. Even though PHREEQC could not predict all complexation reactions between the trace elements and HS, these results gave an idea that some trace elements are forming complexes with HS and similar mechanisms might happen for melanoidins, hence reducing their bioavailability for AAO and AOB bacteria.

Struvite purity is one of the concerns regarding the trade of struvite in the market. It is known that some trace elements and even heavy metals may present in wastewater, leading to the chance of co-precipitation with struvite (Tang et al., 2019). Therefore, next to predicting the complexation between certain trace elements with HS, PHREEQC was also used to predict the co-precipitation of trace elements and heavy metals with struvite. Co-precipitation of trace elements and heavy metals was estimated by analysing SI values. SI values < 0 indicated undersaturation meanwhile SI > 0 indicated supersaturation. Modelling results using PHREEQC showed that in all pH values, there was no B, Ni, Mo, and Zn-containing minerals that reached SI value larger than 0. In addition to that, Se-containing minerals only reached positive SI value when the pH was 8. The result implies that B, Ni, Mo, and Zn remained in the supernatant and did not co-precipitate with struvite. It is a good indication that there would be B, Ni, Mo, and Zn available for AOB and AAO bacteria, and on the other hand, struvite crystal was not contaminated by these trace elements. However, the presence of B, Ni, Mo, and Zn in supernatant did not guarantee their bioavailability for AOB and AAO bacteria. B, Ni, Mo, and Zn might be available for AOB and AAO in the case where melanoidins are not present, but with the presence of melanoidins, this might be different due to the chance of complex formation. Even though PHREEQC did not detect possible precipitation of Ni, Ni was found in the struvite product for the experiment without melanoidins. The difference between PHREEQC and lab was possibly caused by co-precipitation of Ni-containing mineral that was not included in PHREEQC database.

The results of modelling using PHREEQC showed that the SI values changed along with the change of pH and HS concentrations. Changes in SI values for some co-precipitating minerals are shown in Figure 4.30, and the complete results are enclosed in Appendix 4. For most minerals, SI values increased with increasing pH. However, an exception was noticed for Al-minerals, in which the SI values increased with decreasing pH. This indicates that Al-containing minerals favour precipitation in lower pH. In all pH values, only Al, Ca, Co, Cr, Cu, Fe, and Mn minerals had SI > 0. It indicates that these minerals are likely to co-precipitate with struvite and alter struvite purity. There was also co-precipitation of some minerals that contain more than one trace elements, such as $CuFe_2O_4$ and CuSe. Among these minerals, Fe-containing minerals have tremendously higher SI values than other minerals. Even though Fe is not considered as heavy metals or pollutant in struvite fertiliser according to Dutch law (Uitvoeringsbesluit Meststoffenwet BWBR0019031) and the presence of Fe is needed to support the growth of crops (Kobayashi et al., 2019), the presence of Fe in solid-phase instead of in supernatant means the reduced available Fe for AOB and AAO bacteria. Just

as importantly, the fact that Al and Cr also co-precipitated with struvite should be noticed because this indicated the potential contamination of heavy metals in struvite crystals.
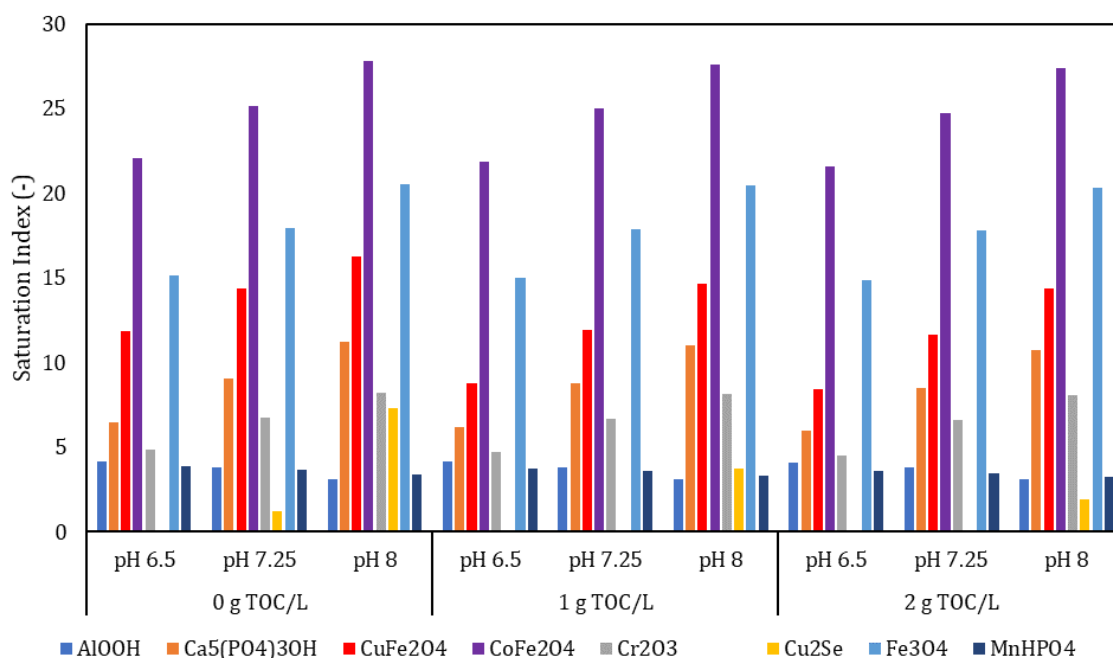
Figure 4.30 Changes in SI values for Al, Ca, Co, Cr, Cu, Fe, Mn, and Se-containing minerals

As previously discussed, melanoidins and HS contributed to the increase of ionic strength of the solution. Based on PHREEQC results, all minerals showed decreasing SI with increasing HA and FA concentrations. Increase in ionic strength will reduce ion activity and the thermodynamic force for crystallisation, hence reduce SI (J. Wang et al., 2006). The decrease of SI implies that there would be less co-precipitation of Al, Ca, Co, Cr, Cu, Fe, Mn, and Se in struvite crystal. Nonetheless, their presence in supernatant will not ensure the bioavailability of the trace elements for AOB and AAO due to the chance of complexation with HS. The model in PHREEQC only included the complexation between Ca, Cu, Fe, Mg with HS; therefore, full experiment to investigate the complexation between all trace elements with melanoidins or HS should be conducted.

4.5. Optimisation using response surface methodology

The experimental data were analysed using RSM to understand the correlation and interactive outcomes of pH and melanoidins on struvite crystallisation. RSM has been used to determine the effects of fundamental variables on struvite crystallisation, including pH, temperature, duration of the reaction, and concentration of additives (Polat & Sayan, 2019; Ye et al., 2010; T. Zhang et al., 2020).

Firstly, the Pearson correlation between the two factors (A-pH and B-melanoidins) and the six responses (N-NH_4 content in the supernatant, P-PO_4 content in the supernatant, N-NH_4 content in struvite product, P-PO_4 content in struvite product, the maximum diameter of struvite crystal, and minimum diameter of struvite crystal) was analysed. Correlation matrix (Figure 4.31) shows that pH was strongly negatively correlated with P concentration in supernatant. The negative correlation of -0.888 explained that with higher pH, the concentration of P in supernatant became lower. On the other hand, melanoidins were strongly negatively correlated with the maximum diameter. The correlation was -0.803, indicating that the maximum diameter decreased with increasing melanoidins concentration. The presence of melanoidins eventually changed the shape of the crystals, from long rod-like into square-like. As a consequence, the maximum diameter decreased markedly.
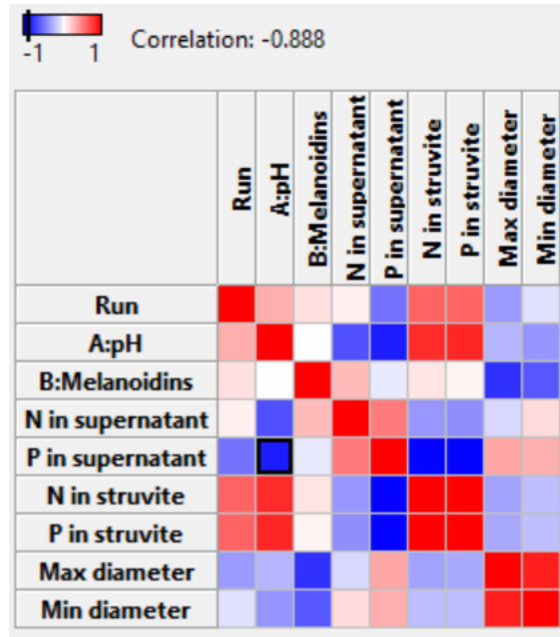
Figure 4.31 Correlation matrix obtained from RSM analysis
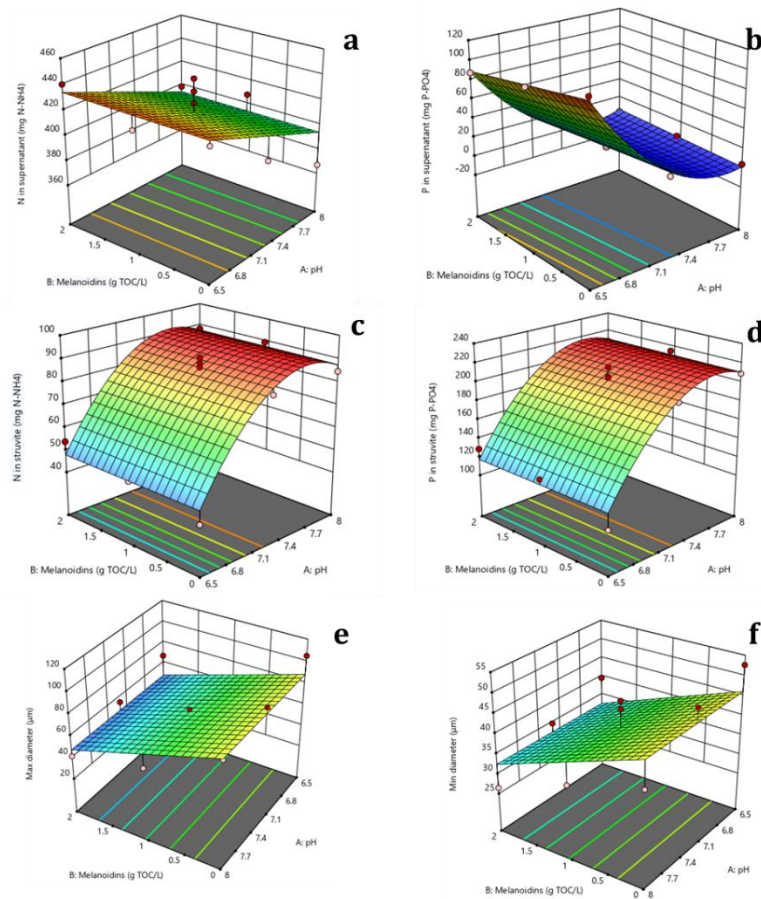
Figure 4.32 Model graphs for six responses obtained from RSM. a) N-NH$_4$ content in the supernatant b) P-PO$_4$ content in the supernatant c) N-NH$_4$ content in struvite d) P-PO$_4$ content in struvite e) Maximum crystal diameter f) Minimum crystal diameter

Each of the six responses had different significant terms for the models. Figure 4.32 shows the model graphs for all the six responses obtained from RSM. The analysis indicated that pH was the only significant term affecting N-NH$_4$ content in the supernatant. A linear model with a relatively low coefficient of determination (R^2, 0.4660) was detected for this response, which was probably caused by the fluctuations in the obtained experimental data. In contrary to N-NH$_4$, a quadratic model with a high R^2 (0.9948) was obtained for P-PO$_4$ content in the supernatant. pH, pH^2, melanoidins, and interaction between pH and melanoidins were significant terms for this response. For both N and P content in struvite, quadratic models with respectively 0.9646 and 0.9478 R^2 values were acquired, with pH and pH^2 being the significant terms. As discerned from the four responses that have been mentioned, most of the responses only included pH as the significant term. However, this was not the case for diameter responses, as both maximum and minimum diameters models comprised melanoidins as the significant term. A linear model with R^2 of 0.6455 was formulated for the maximum diameter and R^2 of 0.4312 for the minimum diameter. It is noteworthy that the R^2 values for the maximum and minimum diameter were also reasonably low. This was most likely due to big standard deviations in the triplicates of each sample. Table 4.1 shows the model equations for these six responses. The detailed ANOVA and fit statistics of the models are enclosed Appendix 7. Overall, RSM showed that both pH and melanoidins concentrations influenced struvite crystallisation. The effect of pH was dominant on ammonium and phosphate removal; meanwhile, melanoidins were more influential on the diameter of struvite crystals. The effect of pH could be either linear or quadratic, depending on the response. On the other hand, the effect of melanoidins was linear. As can be seen from Figure 4.32b for example, P-PO$_4$ content in supernatant decreased quadratically as pH increased, but the changes due to varying melanoidins concentration appeared to be linear. The linear change of N-NH$_4$ content in the supernatant due to change in pH is shown by Figure 4.32a; meanwhile, the linear change of crystal diameter due to the presence of melanoidins is visible at Figure 4.32e and f.

Table 4.1 Model equations for six responses. [*)] For coded equations, A represents pH and B represents melanoidins. A and B should be replaced by levels of each factor, for example -1, 0, or +1 which respectively represent pH values of 6.5, 7.25, 8 and 0, 1, 2 g TOC/L melanoidins. [**)] For actual equation, pH and Mel should be replaced by real values of pH and melanoidins.

Responses	Coded equation[*)]	Actual equation [**)]
N-NH$_4$ in supernatant	414.24 - 20.00A	607.57 - (26.67 x pH)
P-PO$_4$ in supernatant	17.22 - 48.40A - 4.63B + 7.06AB + 35.03A^2	3830.94 - (976.84 x pH) - (72.85 x Mel) + (9.41 x pH x Mel) + (62.27 x pH^2)
N-NH$_4$ in struvite	86.39 + 19.80A - 18.74A^2	-1855.95 + (509.41 x pH) - (33.31 x pH^2)
P-PO$_4$ in struvite	202.50 + 46.61A - 38.61A^2	-3855.68 + (1057.35 x pH) - (68.63 x pH^2)
Max. diameter	68.16 - 20.33B	88.48 - (20.33 x Mel)
Min. diameter	39.37 - 6.80B	46.17 - (6.79 x Mel)

Once the models were finalised, RSM was used to predict the optimum conditions for struvite crystallisation. The prediction was made within the experimental boundaries. First, each response was optimised separately from other responses. By doing the separated optimisation, the suitable pH and melanoidins concentration for each optimised response (minimum concentration of N-NH$_4$ and P-PO$_4$ in the supernatant, maximum N-NH$_4$ and P-PO$_4$ in struvite product, and maximum struvite diameters) could be obtained. The result of separated optimisation is displayed in Table 4.2. Based on the separated optimisation, it could be seen that the presence of melanoidins was still acceptable to achieve low P content in the supernatant and high N and P content in struvite. However, the presence of melanoidins was not admissible to get crystal with a big diameter. Melanoidins were an insignificant term for N-NH$_4$ content in the supernatant; therefore, it was excluded from the optimisation for this response.

Secondly, integrated optimisation for all responses was done. The optimum conditions were found to be pH 7.9 and a very low melanoidins concentration close to 0 g TOC/L melanoidins (Figure 4.33). This result suggested that the presence of melanoidins is not favoured for struvite crystallisation. Nonetheless, both experiment and model results confirmed that the effects of melanoidins could be restricted by adjusting the pH. As melanoidins have a substantial effect on crystal diameter, the use of seed materials in struvite crystallisation would be useful to produce crystal with the desired size while maintaining good N-NH$_4$ and P-PO$_4$ removal efficiencies.

Table 4.2 Result of RSM optimisation. 1: minimise N content in the supernatant, 2: minimise P content in the supernatant, 3: maximise N content in struvite, 4: maximise P content in struvite, 5: maximise the maximum diameter, 6: maximise the minimum diameter. The highlighted values show the achieved goals.

No.	pH	Melanoidins (g TOC/L)	N in supernatant (mg N-NH$_4$)	P in supernatant (mg P-PO$_4$)	N in struvite (mg N-NH$_4$)	P in struvite (mg P-PO$_4$)	Max. diameter (µm)	Min. diameter (µm)
1	8.000	0.000	394.242	1.419	87.452	210.511	88.486	46.172
2	7.815	0.316	399.175	0.167	90.670	215.709	82.057	44.022
3	7.590	0.597	405.165	3.044	91.514	215.708	76.353	42.115
4	7.712	0.747	401.933	0.772	91.477	216.569	73.294	41.092
5	6.500	0.000	434.242	112.330	47.845	117.285	88.486	46.172
6	6.500	0.000	434.242	112.330	47.845	117.285	88.486	46.172
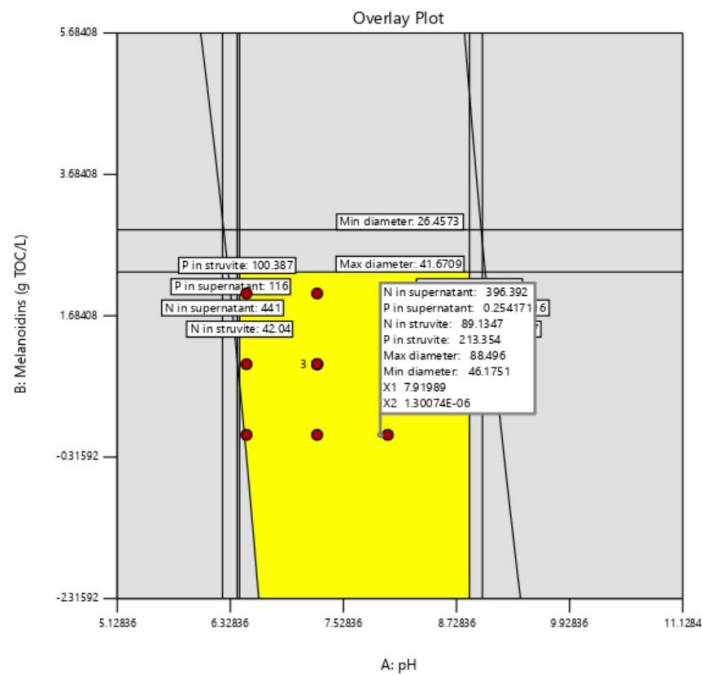
Figure 4.33 Graphical optimisation obtained from RSM analysis

In addition to those six responses explained previously, RSM was also used to confirm how pH and melanoidins determine the fate of trace elements in struvite crystallisation. Mn and Ni contents in both supernatant and struvite were chosen as the responses. Figure 4.34 shows the model graphs for the fate of Mn and Ni in struvite crystallisation. All responses resulted in the quadratic models with high R^2 values. The R^2 values for Mn content in the supernatant, Ni content in the supernatant, Mn content in struvite, and Ni content in struvite were 0.9738, 0.9980, 0.9345, and 0.9614, respectively. Melanoidins were the most significant term in all four models. pH was an insignificant term for all four models, but pH term was required to support model hierarchy. Model equations are shown in Table 4.3. Increase in melanoidins concentration quadratically increased Mn and Ni content in supernatant; on the other hand, increase in melanoidins concentration quadratically decreased Mn and Ni content in struvite. These results imply that even though melanoidins were not favoured for production of big struvite crystals, melanoidins could help in maintaining the purity of struvite. Nonetheless, as explained in Section 4.4, the consequences for PN/A process efficiencies should also be considered.
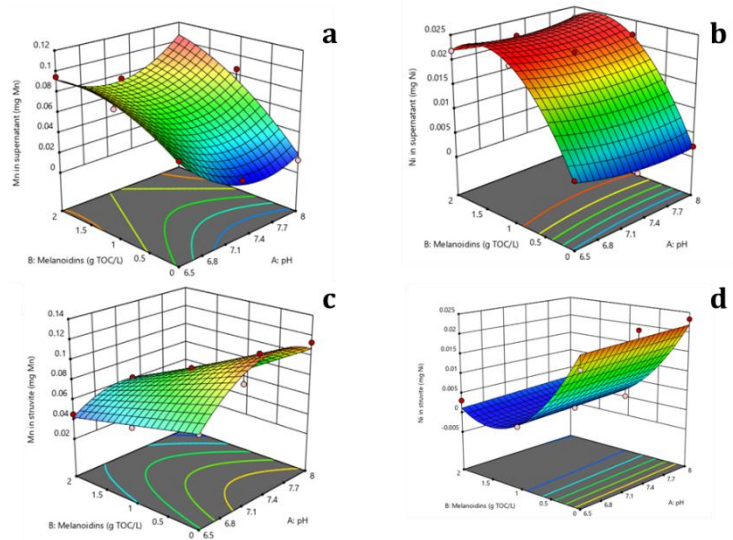
Figure 4.34 Model graphs for the fate of Mn and Ni in struvite crystallisation. a) Mn content in supernatant b) Ni content in supernatant c) Mn content in struvite d) Ni content in struvite

Table 4.3 Model equations for the fate of Mn and Ni in struvite crystallisation. [*] For coded equations, A represents pH and B represents melanoidins. A and B should be replaced by levels of each factor, for example -1, 0, or +1 which respectively represent pH values of 6.5, 7.25, 8 and 0, 1, 2 g TOC/L melanoidins. [**] For actual equation, pH and Mel should be replaced by real values of pH and melanoidins.

Responses	Coded equation[*]	Actual equation[**]
Mn in supernatant	$0.0560 - 0.0056A + 0.0313B + 0.0128AB + 0.0253A^2 - 0.0130B^2$	$2.5519 - (0.06762 \times pH) - (0.0666 \times Mel) + (0.0171 \times pH \times Mel) + (0.0449 \times pH^2) - (0.0130 \times Mel^2)$
Ni in supernatant	$0.0210 - 0.0005A + 0.0095B + 0.0009AB + 0.0012A^2 - 0.0093B^2$	$0.1321 - (0.0339 \times pH) + (0.0191 \times Mel) + (0.0012 \times pH \times Mel) + (0.0022 \times pH^2) - (0.0093 \times Mel^2)$
Mn in struvite	$0.0884 + 0.0055A - 0.0269B - 0.0127AB - 0.0262A^2$	$-2.5116 + (0.7003 \times pH) + (0.0960 \times Mel) - (0.0169 \times pH \times Mel) - (0.0466 \times pH^2)$
Ni in struvite	$0.0014 + 0.0007A - 0.0096B + 0.0102B^2$	$0.0141 + (0.0009 \times pH) - (0.0299 \times Mel) + (0.0101 \times Mel^2)$

This page intentionally left blank

5. Research limitations and recommendations

The hypothesis suggested in this study declared that melanoidins could react with the reactants of struvite (Mg, ammonium, and phosphate), thereby reduce P and N removal efficiencies and alter the characteristics of produced struvite. In addition to that, the formation of complexes between melanoidins and trace elements would affect the fate of the trace elements in struvite crystallisation. This research aimed to verify these hypotheses. Because of some limitations at the period when this study was conducted, some experiments could not be done to answer the research questions fully. This chapter will discuss the steps that still need to be taken further to improve this study and the recommendations for future studies.

This study has given the relevant fundamental understanding of the effects of THP on struvite crystallisation. However, synthetic wastewater used in this study was simpler than the real wastewater matrix, as well as the synthetic melanoidins and HA. Different initial N-NH$_4$:P-PO$_4$ molar ratios in wastewater feed will naturally result in different struvite crystallisation process efficacy. Furthermore, different operating time and temperature of THP installations will also affect the quality of the generated melanoidins. Experiment using real reject water of anaerobically digested sludge from different WWTPs with and without THP installations needs to be performed to clarify the effects of THP on struvite crystallisation in full-scale condition.

As discussed in Section 4.2.5, the market prefers big struvite crystals which favour granulation. Experiments without melanoidins produced bigger crystals, but smaller crystals like the ones produced from experiments with melanoidins might have a better tendency to granulate (Y. Liu & Qu, 2017). On the other hand, bigger crystals have better settleability than smaller crystals (Crutchik et al., 2017). The granulation properties and settleability of struvite crystals produced with and without melanoidins remained obscure. Besides, the hardness of the produced crystals between the experiments also needs to be investigated. Further research is required to get a comprehensive understanding of the characteristics of struvite crystals produced with and without melanoidins.

Because of the buffering capacity of melanoidins, determination of induction time using pH was not feasible in this study. EC was used to determine the induction time, and the results gave a hint that melanoidins prolonged the induction time, but ANOVA had proven that there was no statistically significant difference between experiments at varying melanoidins concentrations. The stochasticity of nucleation led to the uncertainty of this result, considering that the crystallisation was conducted without seeding (Capasso & Salani, 2000; Jiang & Ter Horst, 2011; Lee et al., 2020). It is suggested to do follow-up research by using seed materials; therefore, the stochasticity of nucleation could be minimised, and the effect of melanoidins on the kinetics of struvite crystallisation could be well established. In addition to that, crystal growth observation in this study was done under the microscope without a proper stirring. It is well-known that stirring influences struvite crystallisation, therefore crystal growth observation using a more advanced device that allows simultaneous stirring and image recording is recommended.

Due to the corona crisis, it was not possible to perform advanced crystal analysis using SEM-EDX, FTIR, and XRD. The utilisation of these devices would be beneficial to understand better how melanoidins affected struvite crystallisation. By using SEM-EDX, the images of the crystal surface and the distribution of elements on the crystal surface could be obtained. The crystal surface was expected to be different with and without the presence of melanoidins, as documented by Zhou et al. (2015) that the presence of HS resulted in less porous struvite crystal surface. Therefore, SEM-EDX could certify whether melanoidins blocked the active growing sites of newly established struvite crystals. SEM-EDX could also confirm if there is any difference in the elemental composition of struvite produced with and without melanoidins. As melanoidins contained carbon, the high peak of carbon in samples with melanoidins could indicate the incorporation of melanoidins onto struvite. Furthermore, the existence of trace elements that co-precipitate with struvite could also be detected and compared between experiments. FTIR could be used to determine various functional groups that were present in the crystal product. It was confirmed that FTIR patterns of struvite crystals with and without the presence of HS were different (Wei et al., 2019). As struvite should not contain any carbon, the peak stretch that indicated C-bond could be an indication of

interaction between melanoidins and struvite. It is not only carbon stretch that could indicate the presence of melanoidins because some other stretches of HS are already known (Matilainen et al., 2011). XRD could also be used to investigate whether melanoidins change the structure of struvite crystals, by observing the widening or shifting in XRD patterns of struvite produced with and without melanoidins (Wei et al., 2019; Zhou et al., 2015).

The results of this study have shown that melanoidins formed complexes with magnesium. The formation of these complexes was one of melanoidins disruption mechanisms on struvite crystallisation. In fact, other reactants of struvite (ammonium and phosphate) could also react with melanoidins and impede struvite crystallisation. Unfortunately, neither P-melanoidins nor N-melanoidins complexations experiment could be done in the present study. It is recommended that the complexation between melanoidins and ammonium and phosphate is investigated in future studies. This is essential because an increase in the nutrient release was detected in WWTPs that employ THP. If all complexation experiments are completed, which reagent that complexes the most with melanoidins can be determined. Thus, melanoidins disruption mechanisms on struvite crystallisation could be better explained. Different methods are available to analyse P and N complexations with melanoidins. P-melanoidins complexation could be investigated by performing FTIR or fluorescence spectroscopy (Guardado et al., 2008); meanwhile, N-melanoidins complexation could be analysed using NMR spectroscopy (Thorn & Mikita, 1992).

ICP-MS provides sensitive detection of metals even at trace concentration; therefore, it is a beneficial device. However, spectral interference in ICP-MS leads to disturbance in ICP-MS analysis. In this study, the interference came from chloride ions (Cl^-) that were present in the samples. Cl^- interfered with almost all trace elements analysed in this study due to the formation of polyatomic species which are isotopically identical with the analytes. Future studies need to eliminate the presence of Cl^- in the samples to avoid this problem. Shifting from $MgCl_2$ to other sources of Mg will reduce the concentration of Cl^-; however, this should be done carefully because other chemicals might as well influence struvite crystallisation. pH adjustment using HNO_3 instead of HCl could also be made to reduce Cl^- concentration further. Experiment using real wastewater with low Cl^- concentration is also an option to overcome this problem. The use of real wastewater will also cover other trace heavy metals that were not included in this study but might present in wastewater, such as Pb, Cd, and Hg.

From both lab experiment and PHREEQC modelling, it was confirmed that melanoidins and HS formed complexes with Mg and various trace elements. The fate of these elements was determined, in which some ended up in struvite product, and some other ended up in supernatant. However, PHREEQC modelling of HS was still limited. Geochemical modelling which is done in the future should include HS complexation with Al, B, Co, Cr, Mn, Mo, Ni, Se, and Zn. In addition to that, the future model should incorporate the potential of surface complexation and ion exchange between HS and trace elements. By doing so, the amount of trace elements that complexes with HS and at which HS-sites could be better understood. In addition to that, the bioavailability of the trace elements which ended up in supernatant for AOB and AAO bacteria remained undiscovered. Therefore, it is interesting for future studies to investigate if AOB and AAO bacteria are able to take up the trace elements present in the supernatant with and without the presence of melanoidins.

The result of this study revealed that the colloidal fractions of HA caused more disruption in struvite crystallisation. If in certain circumstances the melanoidins generated from THP also contain colloidal fractions or HMW insoluble fractions, it is suggested to remove them prior to struvite crystallisation. As shown by the results in Section 4.3.2, ultrafiltration could be used to partially remove melanoidins from the feed water, especially the fractions with MW bigger than 1 kDa. However, membrane fouling is the major concern in the ultrafiltration process of HS-containing water and therefore, the application of ultrafiltration for this purpose could be costly (Sutzkover-Gutman et al., 2010). Several other ways are available to degrade melanoidins, including by coagulation, ion exchange, adsorption, and advanced oxidation processes. Coagulation has been considered as one the most suitable technologies for NOM removal and this might work for melanoidins; however, the best coagulant and coagulant dose still needs

to be investigated (Sillanpää, Ncibi, Matilainen, et al., 2018). Ion exchange is claimed to be more efficient than coagulation to remove charged NOM, but its application is currently limited on the water with low NOM concentration (< 10 ppm) in drinking water treatment (Levchuk et al., 2018). Therefore, it is less suitable for the case of melanoidins removal in WWTP. Adsorption using various kinds of adsorbents (activated carbons, iron oxide particles, chitosan/zeolite, etc.) has also been applied, but the presence of other ions in (waste)water might inhibit NOM adsorption (Bhatnagar & Sillanpää, 2017). Advanced oxidation process might as well be used to oxidise melanoidins partially; however, its implementation in WWTP is currently restricted on disinfection of final effluent due to the expensive installation and operation (Sillanpää, Ncibi, & Matilainen, 2018). After all, it should be highlighted that if an additional treatment unit is placed before struvite crystallisation, it will change wastewater composition and presumably affect the processes to some extent. Further research is needed to find the most feasible approach to eliminate melanoidins (especially the colloidal fractions), by evaluating the impacts in overall treatment units, environment, and economic aspects.

Additional recommendation concerning the production of struvite for WWTPs with THP installation is to control the reaction time and temperature of THP to minimise the generation of melanoidins. RSM model suggested that struvite crystallisation is more favoured to produce big crystals when there are no melanoidins, but when THP installation is already present, it could be impractical to eliminate melanoidins prior to struvite crystallisation entirely. Colloidal fractions might be separated by performing techniques mentioned in the previous paragraph; nonetheless, soluble melanoidins might still present in wastewater. pH could be adjusted to minimise the impact of melanoidins up to melanoidins concentration of 2 g TOC/L. Therefore, melanoidins concentration higher than 2 g TOC/L should be avoided as it might have a more adverse impact on struvite crystallisation and pH should not be adjusted too far from 7.5 in order to ensure product purity (X. Hao et al., 2013).

This page intentionally left blank

6. Conclusions

This study aimed to understand the effects of THP on P removal using struvite crystallisation from reject water of anaerobically digested sludge. In order to achieve the research objective, three sub-research questions were formulated. Correspond to the results of the conducted research, the defined sub-research questions can be answered as follows:

1. **What are the effects of humic-like substances (melanoidins and humic acids) on P removal, N removal, and struvite characteristics in struvite crystallisation?**

   Melanoidins affected P removal in struvite crystallisation, especially at pH 6.5 and 7.25. At pH 6.5, melanoidins enhanced P removal, but at pH 7.25, it slightly reduced P removal efficiency. At pH 8, there was no significant effect of melanoidins on P removal. Melanoidins affected $P-PO_4$ concentration in the supernatant, but pH could be adjusted to minimise the effect. In contrary to melanoidins, HA were found to reduce P removal efficiency at pH 8 drastically. Maximum P removal with the presence of melanoidins was 98.4±0.3%, and that of HA was 89.6±0.2%. In terms of N removal, the presence of melanoidins resulted in slightly higher $N-NH_4$ concentration in the supernatant in all pH values, but no apparent effect was detected for HA. The maximum N removal obtained was 21.1±1.6% for the experiment with melanoidins, and that of HA was 11.8±0.9%. The highest N and P removal efficiencies were achieved at pH 8.

   Melanoidins affected the amount of produced struvite at pH 6.5 and 7.25, but not at pH 8. Both melanoidins and HA affected crystal colour and morphology. Struvite crystals without melanoidins and HA were white, but it changed into brownish and black with the presence of melanoidins and HA. Struvite in all examined samples had a sandy-like structure, but the ones produced with HA had a stickier soil-like structure. The crystal shape without melanoidins was a mixture of X-shaped and long rod-like crystals, but in the opposite, the crystals with melanoidins and HA transformed into square-shaped crystals. On top of that, melanoidins affected the diameter of struvite crystals. Both maximum and minimum diameter of the crystal became smaller with the presence of melanoidins. Despite these effects, melanoidins did not change the $Mg:N-NH_4:P-PO_4$ molar ratio of produced struvite crystals.

2. **How do melanoidins affect struvite crystallisation?**

   The result showed that melanoidins did not significantly influence induction time, except at pH 7.25 and 2 g TOC/L melanoidins. Melanoidins increased the ionic strength of the solution; therefore, it reduced the ion activity of the solution and saturation index of struvite. As a result, melanoidins prolonged the induction time. Melanoidins were found to form complexes with magnesium. The formation of Mg-complexes was presumed to alter struvite crystallisation by reducing the supersaturation in the solution. The average percentage of Mg that complexed with melanoidins was 17.5±1.6% for 1 g TOC/L melanoidins and 27.9±0.7% for 2 g TOC/L melanoidins. Nonetheless, there was no significant effect of pH on the formation of Mg-melanoidins complexes. Melanoidins might as well form complexes with phosphate and ammonium in different pH values, which further decreased the supersaturation and affected struvite crystallisation.

3. **What is the fate of trace elements released from THP in struvite crystallisation?**

   Different elements had different fate on struvite crystallisation. Based on the lab experiment, it was found that most Ca ended up in supernatant regardless of pH and presence of melanoidins. Mn and Ni ended up in struvite when there were no melanoidins present in the solution. On the contrary, a high concentration of Mn and Ni in the supernatant was found when melanoidins were present, indicating that melanoidins formed complexes with Mn and Ni. Based on PHREEQC modelling, HS formed complexes with Ca, Cu, and Fe, which might influence their bioavailability for AOB and AAO bacteria. B, Ni, Mo, and Zn were found to remain in the supernatant and did not co-precipitate with struvite. It is a good indication that there would be B, Ni, Mo, and Zn available for AOB and AAO bacteria, and on the other hand, struvite crystal was not contaminated by these

trace elements. However, the presence of B, Ni, Mo, and Zn in supernatant did not guarantee their bioavailability for AOB and AAO bacteria. Certain trace elements (Ca, Co, Cu, Fe, and Mn) and heavy metals (Al and Cr) were found to co-precipitate with struvite in all experimental conditions, with Fe minerals being the ones with highest SI. Se minerals only co-precipitated at pH 8. All minerals showed decreasing SI with increasing HS concentrations. The decrease of SI implied that there would be less co-precipitation of Al, Ca, Co, Cr, Cu, Fe, Mn, and Se in struvite crystal. Nonetheless, their presence in supernatant would not guarantee the bioavailability of the trace elements for AOB and AAO bacteria due to the chance of complexation with HS.

In addition to answering these sub-research question, by using RSM it was found that the optimum conditions to achieve the minimum contents of $N-NH_4$ and $P-PO_4$ in the supernatant, maximum contents of $N-NH_4$ and $P-PO_4$ in struvite product, and maximum struvite diameters were pH 7.9 and 0 g TOC/L melanoidins. This result suggested that the presence of melanoidins generated from THP is not favoured for struvite crystallisation. Nonetheless, both experiment and model results confirmed that the effects of melanoidins could be restricted by adjusting the pH. Although melanoidins were not favoured for production of big struvite crystals, melanoidins could assist the production of struvite with low trace elements content.

Finally, it could be concluded that THP affected struvite crystallisation in different ways. The hypotheses could be accepted partially, that melanoidins decreased P removal efficiency at pH 7.25, decreased N removal efficiency at all tested pH values, decreased amount of produced struvite at pH 7.25, and prolonged induction time at pH 7.25. The presence of melanoidins altered morphology and decreased the diameter of struvite crystal. Melanoidins also led to higher trace elements concentrations in supernatant due to the formation of complexes. Further research is still required to ensure the production of good quality struvite crystals in WWTPs with THP installation.

References

Abma, W. R., Driessen, W., Haarhuis, R., & Van Loosdrecht, M. C. M. (2010). Upgrading of sewage treatment plant by sustainable and cost-effective separate treatment of industrial wastewater. *Water Science and Technology*, *61*(7), 1715–1722. https://doi.org/10.2166/wst.2010.977

Adusei-Gyamfi, J., Ouddane, B., Rietveld, L., Cornard, J. P., & Criquet, J. (2019). Natural organic matter-cations complexation and its impact on water treatment: A critical review. *Water Research*, *160*, 130–147. https://doi.org/10.1016/j.watres.2019.05.064

Alfaro, N., Cano, R., & Fdz-Polanco, F. (2014). Effect of thermal hydrolysis and ultrasounds pretreatments on foaming in anaerobic digesters. *Bioresource Technology*, *170*, 477–482. https://doi.org/10.1016/j.biortech.2014.08.013

Ali, M. I., & Schneider, P. A. (2005). Crystallization of struvite from metastable region with different types of seed crystal. *Journal of Non-Equilibrium Thermodynamics*, *30*(2), 95–111. https://doi.org/10.1515/JNETDY.2005.007

American Public Health Association (APHA), American Water Works Association (AWWA), & Water Environment Federation (WEF). (2017). *Standard Methods for the Examination of Water and Wastewater 23rd Edition* (R. B. Baird, A. D. Eaton, E. W. Rice, & L. L. Bridgewater (eds.); 23rd ed.). American Public Health Association. https://doi.org/10.1017/CBO9781107415324.004

Appels, L., Degrève, J., Van der Bruggen, B., Van Impe, J., & Dewil, R. (2010). Influence of low temperature thermal pre-treatment on sludge solubilisation, heavy metal release and anaerobic digestion. *Bioresource Technology*, *101*(15), 5743–5748. https://doi.org/10.1016/j.biortech.2010.02.068

Barber, W. P. F. (2016). Thermal hydrolysis for sewage treatment: A critical review. *Water Research*, *104*, 53–71. https://doi.org/10.1016/j.watres.2016.07.069

Bethea, R. M., & Rhinehart, R. R. (1991). *Applied Engineering Statistics*. Marcel Dekker.

Bhatnagar, A., & Sillanpää, M. (2017). Removal of natural organic matter (NOM) and its constituents from water by adsorption – A review. *Chemosphere*, *166*, 497–510. https://doi.org/10.1016/j.chemosphere.2016.09.098

Bhuiyan, M. I. H., Mavinic, D. S., & Beckie, R. D. (2007). A solubility and thermodynamic study of struvite. *Environmental Technology*, *28*(9), 1015–1026. https://doi.org/10.1080/09593332808618857

Borcan, A. C. (2019). *Enhancing nutrient recovery by Non- Photochemical Nucleation Enhancing nutrient recovery by Nucleation*. TU Delft.

Bosire, G. O., & Ngila, J. C. (2017). *Effect of Natural Organic Matter on Scale reduction in Cooling Water Circuits : A Comprehensive assessment based on Empirical Characterization and Theoretical PHREEQCI Model computations*. *1*(1).

Bosire, G. O., Ngila, J. C., & Nkambule, T. T. I. (2018). Geochemical scaling potential simulations of natural organic matter complexation with metal ions in cooling water at eskom power generation plants in South Africa. *Water SA*, *44*(4), 707–718. https://doi.org/10.4314/wsa.v44i4.19

Bougrier, C., Albasi, C., Delgenès, J. P., & Carrère, H. (2006). Effect of ultrasonic, thermal and ozone pre-treatments on waste activated sludge solubilisation and anaerobic biodegradability. *Chemical Engineering and Processing: Process Intensification*, *45*(8), 711–718. https://doi.org/10.1016/j.cep.2006.02.005

Brezinski, K., & Gorczyca, B. (2019). An overview of the uses of high performance size exclusion chromatography (HPSEC) in the characterization of natural organic matter (NOM) in potable water, and ion-exchange applications. *Chemosphere*, *217*, 122–139. https://doi.org/10.1016/j.chemosphere.2018.10.028

Cabaniss, S. E. (2011). Forward modeling of metal complexation by NOM: II. Prediction of binding site properties. *Environmental Science and Technology*, *45*(8), 3202–3209. https://doi.org/10.1021/es102408w

Capasso, V., & Salani, C. (2000). Stochastic birth-and-growth processes modelling crystallization of polymers with spatially heterogeneous parameters. *Nonlinear Analysis: Real World Applications*, *1*(4), 485–498. https://doi.org/10.1016/S0362-546X(99)00289-8

Capdevielle, A., Sýkorová, E., Béline, F., & Daumer, M. L. (2014). Kinetics of struvite precipitation in synthetic biologically treated swine wastewaters. *Environmental Technology (United Kingdom)*, *35*(10), 1250–1262. https://doi.org/10.1080/09593330.2013.865790

Capdevielle, A., Sýkorová, E., Béline, F., & Daumer, M. L. (2016). Effects of organic matter on crystallization of struvite in biologically treated swine wastewater. *Environmental Technology (United Kingdom)*, *37*(7), 880–892. https://doi.org/10.1080/09593330.2015.1088580

Chauhan, C. K., & Joshi, M. J. (2014). Growth and characterization of struvite-Na crystals. *Journal of Crystal Growth*, *401*, 221–226. https://doi.org/10.1016/j.jcrysgro.2014.01.052

Chimenos, J. M., Fernández, A. I., Hernández, A., Haurie, L., Espiell, F., & Ayora, C. (2006). Optimization of phosphate removal in anodizing aluminium wastewater. *Water Research*, *40*(1), 137–143. https://doi.org/10.1016/j.watres.2005.10.033

Cordell, D., & Neset, T. S. S. (2014). Phosphorus vulnerability: A qualitative framework for assessing the vulnerability of national and regional food systems to the multi-dimensional stressors of phosphorus scarcity. *Global Environmental Change*, *24*(1), 108–122. https://doi.org/10.1016/j.gloenvcha.2013.11.005

Ćosović, B., Vojvodić, V., Bošković, N., Plavšić, M., & Lee, C. (2010). Characterization of natural and synthetic humic substances (melanoidins) by chemical composition and adsorption measurements. *Organic Geochemistry*, *41*(2), 200–205. https://doi.org/10.1016/j.orggeochem.2009.10.002

Crutchik, D., & Garrido, J. M. (2016). Kinetics of the reversible reaction of struvite crystallisation. *Chemosphere*, *154*, 567–572. https://doi.org/10.1016/j.chemosphere.2016.03.134

Crutchik, D., Morales, N., Vázquez-Padín, J. R., & Garrido, J. M. (2017). Enhancement of struvite pellets crystallization in a full-scale plant using an industrial grade magnesium product. *Water Science and Technology*, *75*(3), 609–618. https://doi.org/10.2166/wst.2016.527

Cusick, R. D., & Logan, B. E. (2012). Phosphate recovery as struvite within a single chamber microbial electrolysis cell. *Bioresource Technology*, *107*, 110–115. https://doi.org/10.1016/j.biortech.2011.12.038

de Boer, M. A., Romeo-Hall, A. G., Rooimans, T. M., & Slootweg, J. C. (2018). An assessment of the drivers and barriers for the deployment of urban phosphorus recovery technologies: A case study of the Netherlands. *Sustainability (Switzerland)*, *10*(6), 1–19. https://doi.org/10.3390/su10061790

de Buck, W. (2012). *Struvite crystallization and separation in digested sludge*. TU Delft.

De Lucia, M., & Kühn, M. (2013). Coupling R and PHREEQC: Efficient programming of geochemical models. *Energy Procedia*, *40*, 464–471. https://doi.org/10.1016/j.egypro.2013.08.053

de Vries, S., Postma, R., Scholl, L., Blom-Zandstra, G., Verhagen, J., & Harms, I. (2017). *Economic feasibility and climate benefits of using struvite from the Netherlands as a phosphate (P) fertilizer in West Africa*. 22–24. https://doi.org/10.18174/417821

Decrey, L., Udert, K. M., Tilley, E., Pecson, B. M., & Kohn, T. (2011). Fate of the pathogen indicators phage ΦX174 and Ascaris suum

eggs during the production of struvite fertilizer from source-separated urine. *Water Research*, *45*(16), 4960–4972. https://doi.org/10.1016/j.watres.2011.06.042

Desmidt, E., Ghyselbrecht, K., Monballiu, A., Rabaey, K., Verstraete, W., & Meesschaert, B. D. (2013). Factors influencing urease driven struvite precipitation. *Separation and Purification Technology*, *110*, 150–157. https://doi.org/10.1016/j.seppur.2013.03.010

Dewil, R., Baeyens, J., & Appels, L. (2007). Enhancing the use of waste activated sludge as bio-fuel through selectively reducing its heavy metal content. *Journal of Hazardous Materials*, *144*(3), 703–707. https://doi.org/10.1016/j.jhazmat.2007.01.100

Dodds, W. K., Bouska, W. W., Eitzmann, J. L., Pilger, T. J., Pitts, K. L., Riley, A. J., Schloesser, J. T., & Thornbrugh, D. J. (2009). Eutrophication of U. S. freshwaters: Analysis of potential economic damages. *Environmental Science and Technology*, *43*(1), 12–19. https://doi.org/10.1021/es801217q

Donatello, S., & Cheeseman, C. R. (2013). Recycling and recovery routes for incinerated sewage sludge ash (ISSA): A review. *Waste Management*, *33*(11), 2328–2340. https://doi.org/10.1016/j.wasman.2013.05.024

Driessen, W., Van Veldhoven, J. T. A., Hendrickx, T., & Van Loosdrecht, M. C. M. (2018). Successful treatment of sidestream dewatering liquors from thermally hydrolized and mesophilic anaerobically digested (THP-MAD) biosolids. *IWA Nutrient Removal and Recovery Conference*, *1*, 2–5.

Driessen, W., Van Veldhoven, J. T. A., Janssen, M. P. M., & Van Loosdrecht, M. C. M. (2020). Treatment of sidestream dewatering liquors from thermally hydrolised and anaerobically digested biosolids. *Water Practice and Technology*. https://doi.org/10.2166/wpt.2020.007

Dwyer, J., Starrenburg, D., Tait, S., Barr, K., Batstone, D. J., & Lant, P. (2008). Decreasing activated sludge thermal hydrolysis temperature reduces product colour, without decreasing degradability. *Water Research*, *42*(18), 4699–4709. https://doi.org/10.1016/j.watres.2008.08.019

Ebbers, B., Ottosen, L. M., & Jensen, P. E. (2015). Electrodialytic treatment of municipal wastewater and sludge for the removal of heavy metals and recovery of phosphorus. *Electrochimica Acta*, *181*, 90–99. https://doi.org/10.1016/j.electacta.2015.04.097

Egle, L., Rechberger, H., Krampe, J., & Zessner, M. (2016). Phosphorus recovery from municipal wastewater: An integrated comparative technological, environmental and economic assessment of P recovery technologies. *Science of the Total Environment*, *571*, 522–542. https://doi.org/10.1016/j.scitotenv.2016.07.019

Eliquo Water & Energy. (2015). *Innovative energy and nutrient factory at Amersfoort waste water treatment plant*.

Galanakis, C. M. (2015). Separation of functional macromolecules and micromolecules: From ultrafiltration to the border of nanofiltration. *Trends in Food Science and Technology*, *42*(1), 44–63. https://doi.org/10.1016/j.tifs.2014.11.005

Geraats, B., Manager, T., & Water, E. (2014). LYSOTHERM ® SLUDGE HYDROLYSIS Key words. *19th European Biosolids & Organic Resources Conference & Exhibition*.

Grassi, M., & Rosa, M. (2010). Humic acids of different origin as modifiers of cadmium-ion chemistry: A spectroscopic approach to structural properties and reactivity. *Inorganica Chimica Acta*, *363*(3), 495–503. https://doi.org/10.1016/j.ica.2009.07.033

Guardado, I., Urrutia, O., & Garcia-Mina, J. M. (2008). Some structural and electronic features of the interaction of phosphate with metal-humic complexes. *Journal of Agricultural and Food Chemistry*, *56*(3), 1035–1042. https://doi.org/10.1021/jf072641k

Hanhoun, M., Montastruc, L., Azzaro-Pantel, C., Biscans, B., Frèche, M., & Pibouleau, L. (2011). Temperature impact assessment on struvite solubility product: A thermodynamic modeling approach. *Chemical Engineering Journal*, *167*(1), 50–58. https://doi.org/10.1016/j.cej.2010.12.001

Hao, X. D., Wang, C. C., & van Loosdrecht, M. C. M. (2008). Struvite formation, analytical methods and effects of pH and Ca2+. *Water Science and Technology*, *58*(8), 1687–1692. https://doi.org/https://doi.org/10.2166/wst.2008.557

Hao, X., Wang, C., Van Loosdrecht, M. C. M., & Hu, Y. (2013). Looking beyond struvite for P-recovery. *Environmental Science and Technology*, *47*(10), 4965–4966. https://doi.org/10.1021/es401340s

He, Z., Ohno, T., Cade-Menun, B. J., Erich, M. S., & Honeycutt, C. W. (2006). Spectral and Chemical Characterization of Phosphates Associated with Humic Substances. *Soil Science Society of America Journal*, *70*(5), 1741–1751. https://doi.org/10.2136/sssaj2006.0030

Huang, H., Li, B., Li, J., Zhang, P., Yu, W., Zhao, N., Guo, G., & Young, B. (2019). Influence of process parameters on the heavy metal (Zn2+, Cu2+ and Cr3+) content of struvite obtained from synthetic swine wastewater. *Environmental Pollution*, *245*, 658–665. https://doi.org/10.1016/j.envpol.2018.11.046

Huang, H., Xiao, D., Zhang, Q., & Ding, L. (2014). Removal of ammonia from landfill leachate by struvite precipitation with the use of low-cost phosphate and magnesium sources. *Journal of Environmental Management*, *145*, 191–198. https://doi.org/10.1016/j.jenvman.2014.06.021

Huang, H., Zhang, P., Zhang, Z., Liu, J., Xiao, J., & Gao, F. (2016). Simultaneous removal of ammonia nitrogen and recovery of phosphate from swine wastewater by struvite electrochemical precipitation and recycling technology. *Journal of Cleaner Production*, *127*, 302–310. https://doi.org/10.1016/j.jclepro.2016.04.002

Huang, P., Wang, M., & Wang, M. (2005). MINERAL – ORGANIC – MICROBIAL INTERACTIONS. *Encyclopedia of Soils in the Environment*, 486–499. https://doi.org/10.1016/B0-12-348530-4/00220-4

Hutnik, N., Kozik, A., Mazienczuk, A., Piotrowski, K., Wierzbowska, B., & Matynia, A. (2013). Phosphates (V) recovery from phosphorus mineral fertilizers industry wastewater by continuous struvite reaction crystallization process. *Water Research*, *47*(11), 3635–3643. https://doi.org/10.1016/j.watres.2013.04.026

Jiang, S., & Ter Horst, J. H. (2011). Crystal nucleation rates from probability distributions of induction times. *Crystal Growth and Design*, *11*(1), 256–261. https://doi.org/10.1021/cg101213q

Jones, A. G. (2002). *Crystallization Process System* (First ed). Butterworth-Heinemann.

Kabdaşli, I., Parsons, S. A., & Tünay, O. (2006). Effect of major ions on induction time of struvite precipitation. *Croatica Chemica Acta*, *79*(2), 243–251.

Kataki, S., West, H., Clarke, M., & Baruah, D. C. (2016). Phosphorus recovery as struvite: Recent concerns for use of seed, alternative Mg source, nitrogen conservation and fertilizer potential. *Resources, Conservation and Recycling*, *107*, 142–156. https://doi.org/10.1016/j.resconrec.2015.12.009

Kim, D., Kim, J., Ryu, H. D., & Lee, S. I. (2009). Effect of mixing on spontaneous struvite precipitation from semiconductor wastewater. *Bioresource Technology*, *100*(1), 74–78. https://doi.org/10.1016/j.biortech.2008.05.024

Kobayashi, T., Nozoye, T., & Nishizawa, N. K. (2019). Iron transport and its regulation in plants. *Free Radical Biology and Medicine*, *133*(October 2018), 11–20. https://doi.org/10.1016/j.freeradbiomed.2018.10.439

Kumar, V., Taylor, M. K., Mehrotra, A., & Stagner, W. C. (2013). Real-time particle size analysis using focused beam reflectance measurement as a process analytical technology tool for a continuous granulation-drying- milling process. *AAPS PharmSciTech*, *14*(2), 523–530. https://doi.org/10.1208/s12249-013-9934-4

Laurent, J., Casellas, M., Carrère, H., & Dagot, C. (2011). Effects of thermal hydrolysis on activated sludge solubilization, surface

properties and heavy metals biosorption. *Chemical Engineering Journal*, *166*(3), 841–849. https://doi.org/10.1016/j.cej.2010.11.054

Lawrance, G. A. (2010). *Introduction to Coordination Chemistry* (2nd editio). John Wiley & Sons, Incorporated.

Lee, E. C., Parrilla-Gutierrez, J. M., Henson, A., Brechin, E. K., & Cronin, L. (2020). A Crystallization Robot for Generating True Random Numbers Based on Stochastic Chemical Processes. *Matter*, *2*(3), 649–657. https://doi.org/10.1016/j.matt.2020.01.024

Levchuk, I., Rueda Márquez, J. J., & Sillanpää, M. (2018). Removal of natural organic matter (NOM) from water by ion exchange – A review. *Chemosphere*, *192*, 90–104. https://doi.org/10.1016/j.chemosphere.2017.10.101

Li, B., Boiarkina, I., Yu, W., Huang, H. M., Munir, T., Wang, G. Q., & Young, B. R. (2019). Phosphorous recovery through struvite crystallization: Challenges for future design. *Science of the Total Environment*, *648*, 1244–1256. https://doi.org/10.1016/j.scitotenv.2018.07.166

Li, B., Huang, H. M., Boiarkina, I., Yu, W., Huang, Y. F., Wang, G. Q., & Young, B. R. (2019). Phosphorus recovery through struvite crystallisation: Recent developments in the understanding of operational factors. *Journal of Environmental Management*, *248*(January), 109254. https://doi.org/10.1016/j.jenvman.2019.07.025

Liao, X., Li, H., Zhang, Y., Liu, C., & Chen, Q. (2016). Accelerated high-solids anaerobic digestion of sewage sludge using low-temperature thermal pretreatment. *International Biodeterioration and Biodegradation*, *106*, 141–149. https://doi.org/10.1016/j.ibiod.2015.10.023

Lipczynska-Kochany, E., & Kochany, J. (2008). Effect of humic substances on the Fenton treatment of wastewater at acidic and neutral pH. *Chemosphere*, *73*(5), 745–750. https://doi.org/10.1016/j.chemosphere.2008.06.028

Liu, X., Wang, W., Gao, X., Zhou, Y., & Shen, R. (2012). Effect of thermal pretreatment on the physical and chemical properties of municipal biomass waste. *Waste Management*, *32*(2), 249–255. https://doi.org/10.1016/j.wasman.2011.09.027

Liu, Y. H., Kwag, J. H., Kim, J. H., & Ra, C. S. (2011). Recovery of nitrogen and phosphorus by struvite crystallization from swine wastewater. *Desalination*, *277*(1–3), 364–369. https://doi.org/10.1016/j.desal.2011.04.056

Liu, Y., & Qu, H. (2017). Interplay of digester supernatant composition and operating pH on impacting the struvite particulate properties. *Journal of Environmental Chemical Engineering*, *5*(4), 3949–3955. https://doi.org/10.1016/j.jece.2017.07.065

Lou, J. (2019). *Evaluation of compounds generated in the thermal hydrolysis process on microbial activities in partial nitritation / anammox process By* [TU Delft]. https://repository.tudelft.nl/islandora/object/uuid:e6fc202f-9e51-4471-8e4a-bcf766d30abe

Lum, T. S., & Sze-Yin Leung, K. (2016). Strategies to overcome spectral interference in ICP-MS detection. *Journal of Analytical Atomic Spectrometry*, *31*(5), 1078–1088. https://doi.org/10.1039/c5ja00497g

Manceau, A., & Matynia, A. (2010). The nature of Cu bonding to natural organic matter. *Geochimica et Cosmochimica Acta*, *74*(9), 2556–2580. https://doi.org/10.1016/j.gca.2010.01.027

Manzoor, M. A. P., Mujeeburahiman, M., Duwal, S. R., & Rekha, P. D. (2019). Investigation on growth and morphology of in vitro generated struvite crystals. *Biocatalysis and Agricultural Biotechnology*, *17*(January), 566–570. https://doi.org/10.1016/j.bcab.2019.01.023

Marcovecchio, J., Blanca, C. C. B., & Freije, H. (2007). *Heavy metals, major metals, trace elements. May 2017*.

Marsac, R., Davranche, M., Gruau, G., Dia, A., Pédrot, M., Le Coz-Bouhnik, M., & Briant, N. (2013). Effects of Fe competition on REE binding to humic acid: Origin of REE pattern variability in organic waters. *Chemical Geology*, *342*, 119–127. https://doi.org/10.1016/j.chemgeo.2013.01.020

Martins, S. I. F. S., Jongen, W. M. F., & Boekel, M. A. J. S. Van. (2008). The damnation of Faust. *Opera News*, *73*(6), 36. https://doi.org/10.2307/3717028

Matilainen, A., Gjessing, E. T., Lahtinen, T., Hed, L., Bhatnagar, A., & Sillanpää, M. (2011). An overview of the methods used in the characterisation of natural organic matter (NOM) in relation to drinking water treatment. *Chemosphere*, *83*(11), 1431–1442. https://doi.org/10.1016/j.chemosphere.2011.01.018

May, T. W., & Wiedmeyer, R. H. (1998). A Table of Polyatomic Interferences in ICP-MS. *Atomic Spectroscopy*, *19*(5), 150–155.

Mehta, C. M., & Batstone, D. J. (2013). Nucleation and growth kinetics of struvite crystallization. *Water Research*, *47*(8), 2890–2900. https://doi.org/10.1016/j.watres.2013.03.007

Metcalf, & Eddy. (2014). *Wastewater Engineering* (G. Tchobanoglous, H. D. Stensel, R. Tsuchihashi, & F. Burton (eds.); Fifth edit). McGraw-Hill Education.

Muhmood, A., Wu, S., Lu, J., Ajmal, Z., Luo, H., & Dong, R. (2018). Nutrient recovery from anaerobically digested chicken slurry via struvite: Performance optimization and interactions with heavy metals and pathogens. *Science of the Total Environment*, *635*, 1–9. https://doi.org/10.1016/j.scitotenv.2018.04.129

Mullin, J. W. (2001). *Crystallization* (4th Editio). Elsevier Science & Technology.

Myers, R. H., Montgomery, D. C., & Anderson-Cook, C. M. (2016). *Response Surface Methodology: Process and Product Optimization Using Designed Experiments*. John Wiley & Sons.

Nassau, K. (1978). *American Mineralogist, Volume 63, pages 219-229, 1978. 63*, 219–229.

Nelson, N. O., Mikkelsen, R. L., & Hesterberg, D. L. (2003). Struvite precipitation in anaerobic swine lagoon liquid: Effect of pH and Mg:P ratio and determination of rate constant. *Bioresource Technology*, *89*(3), 229–236. https://doi.org/10.1016/S0960-8524(03)00076-2

Nursten, H. E. (2005). *The Maillard Reaction: Chemistry, Biochemistry, and Implications*. Royal Society of Chemistry. https://doi.org/https://doi.org/10.1039/9781847552570

Ødeby, T., Netteland, T., & Solheim, O. E. (1996). Thermal Hydrolysis as a Profitable Way of Handling Sludge. In *Chemical Water and Wastewater Treatment IV* (Hahn H.H.,). Springer, Berlin, Heidelberg. https://doi.org/https://doi.org/10.1007/978-3-642-61196-4_38

Ohlinger, B. K. N., Member, S., Young, T. M., Member, A., & Schroeder, E. D. (1999). *K INETICS E FFECTS ON P REFERENTIAL S TRUVITE. 125*(August), 730–737.

Oosterhuis, M., Ringoot, D., Hendriks, A., & Roeleveld, P. (2014). Thermal hydrolysis of waste activated sludge at Hengelo Wastewater Treatment Plant, the Netherlands. *Water Science and Technology*, *70*(1), 1–7. https://doi.org/10.2166/wst.2014.107

Pandey, A. K., Pandey, S. D., & Misra, V. (2000). Stability constants of metal-humic acid complexes and its role in environmental detoxification. *Ecotoxicology and Environmental Safety*, *47*(2), 195–200. https://doi.org/10.1006/eesa.2000.1947

Parkhurst, D. L., & Wissmeier, L. (2015). PhreeqcRM: A reaction module for transport simulators based on the geochemical model PHREEQC. *Advances in Water Resources*, *83*, 176–189. https://doi.org/10.1016/j.advwatres.2015.06.001

Pasek, M. (2019). A role for phosphorus redox in emerging and modern biochemistry. *Current Opinion in Chemical Biology*, *49*, 53–58. https://doi.org/10.1016/j.cbpa.2018.09.018

Pédrot, M., Boudec, A. Le, Davranche, M., Dia, A., & Henin, O. (2011). How does organic matter constrain the nature, size and availability of Fe nanoparticles for biological reduction? *Journal of Colloid and Interface Science*, *359*(1), 75–85. https://doi.org/10.1016/j.jcis.2011.03.067

Pereboom, J., Luning, L., Hol, A., van Dijk, L., & de Man, A. W. A. (2014). Full scale experiences with TurboTec ® continuous thermal hydrolysis at WWTP Venlo (NL) and Apeldoorn (NL). *19th European Biosolids & Organic Resources Conference & Exhibition*.

Pertusatti, J., & Prado, A. G. S. (2007). Buffer capacity of humic acid: Thermodynamic approach. *Journal of Colloid and Interface Science*, *314*(2), 484–489. https://doi.org/10.1016/j.jcis.2007.06.006

Phothilangka, P., Schoen, M. A., & Wett, B. (2008). Benefits and drawbacks of thermal pre-hydrolysis for operational performance of wastewater treatment plants. *Water Science and Technology*, *58*(8), 1547–1553. https://doi.org/10.2166/wst.2008.500

Polat, S., & Sayan, P. (2019). Application of response surface methodology with a Box–Behnken design for struvite precipitation. *Advanced Powder Technology*, *30*(10), 2396–2407. https://doi.org/10.1016/j.apt.2019.07.022

Pradhan, S., Hedberg, J., Rosenqvist, J., Jonsson, C. M., Wold, S., Blomberg, E., & Wallinder, I. O. (2018). Influence of humic acid and dihydroxy benzoic acid on the agglomeration, adsorption, sedimentation and dissolution of copper, manganese, aluminum and silica nanoparticles-A tentative exposure scenario. *PLoS ONE*, *13*(2), 1–24. https://doi.org/10.1371/journal.pone.0192553

Prywer, J., & Olszynski, M. (2013). Influence of disodium EDTA on the nucleation and growth of struvite and carbonate apatite. *Journal of Crystal Growth*, *375*, 108–114. https://doi.org/10.1016/j.jcrysgro.2013.04.027

Rahman, Md M., Liu, Y. H., Kwag, J. H., & Ra, C. S. (2011). Recovery of struvite from animal wastewater and its nutrient leaching loss in soil. *Journal of Hazardous Materials*, *186*(2–3), 2026–2030. https://doi.org/10.1016/j.jhazmat.2010.12.103

Rahman, Md Mukhlesur, Salleh, M. A. M., Rashid, U., Ahsan, A., Hossain, M. M., & Ra, C. S. (2014). Production of slow release crystal fertilizer from wastewaters through struvite crystallization - A review. *Arabian Journal of Chemistry*, *7*(1), 139–155. https://doi.org/10.1016/j.arabjc.2013.10.007

Reijnders, L. (2014). Phosphorus resources, their depletion and conservation, a review. *Resources, Conservation and Recycling*, *93*, 32–49. https://doi.org/10.1016/j.resconrec.2014.09.006

Roberts, K. J., Docherty, R., & Tamura, R. (2017). *Engineering Crystallography: From Molecule to Crystal to Functional Form* (Vol. PartF1). Springer. https://doi.org/10.1007/978-94-024-1117-1_10

Ronteltap, M., Maurer, M., Hausherr, R., & Gujer, W. (2010). Struvite precipitation from urine - Influencing factors on particle size. *Water Research*, *44*(6), 2038–2046. https://doi.org/10.1016/j.watres.2009.12.015

Roy, E. D. (2017). Phosphorus recovery and recycling with ecological engineering: A review. *Ecological Engineering*, *98*, 213–227. https://doi.org/10.1016/j.ecoleng.2016.10.076

Shaddel, S., Ucar, S., Andreassen, J. P., & Sterhus, S. W. (2019). Engineering of struvite crystals by regulating supersaturation - Correlation with phosphorus recovery, crystal morphology and process efficiency. *Journal of Environmental Chemical Engineering*, *7*(1), 102918. https://doi.org/10.1016/j.jece.2019.102918

Shao, J., Hou, J., & Song, H. (2011). Comparison of humic acid rejection and flux decline during filtration with negatively charged and uncharged ultrafiltration membranes. *Water Research*, *45*(2), 473–482. https://doi.org/10.1016/j.watres.2010.09.006

Shepherd, J. G., Sohi, S. P., & Heal, K. V. (2016). Optimising the recovery and re-use of phosphorus from wastewater effluent for sustainable fertiliser development. *Water Research*, *94*, 155–165. https://doi.org/10.1016/j.watres.2016.02.038

Shih, K., & Yan, H. (2016). The Crystallization of Struvite and Its Analog (K-Struvite) From Waste Streams for Nutrient Recycling. *Environmental Materials and Waste: Resource Recovery and Pollution Prevention*, 665–686. https://doi.org/10.1016/B978-0-12-803837-6.00026-3

Sillanpää, M., Ncibi, M. C., & Matilainen, A. (2018). Advanced oxidation processes for the removal of natural organic matter from drinking water sources: A comprehensive review. *Journal of Environmental Management*, *208*, 56–76. https://doi.org/10.1016/j.jenvman.2017.12.009

Sillanpää, M., Ncibi, M. C., Matilainen, A., & Vepsäläinen, M. (2018). Removal of natural organic matter in drinking water treatment by coagulation: A comprehensive review. *Chemosphere*, *190*, 54–71. https://doi.org/10.1016/j.chemosphere.2017.09.113

Song, Y., Dai, Y., Hu, Q., Yu, X., & Qian, F. (2014). Effects of three kinds of organic acids on phosphorus recovery by magnesium ammonium phosphate (MAP) crystallization from synthetic swine wastewater. *Chemosphere*, *101*, 41–48. https://doi.org/10.1016/j.chemosphere.2013.11.019

Sri Shalini, S., & Joseph, K. (2012). Nitrogen management in landfill leachate: Application of SHARON, ANAMMOX and combined SHARON-ANAMMOX process. *Waste Management*, *32*(12), 2385–2400. https://doi.org/10.1016/j.wasman.2012.06.006

STOWA. (2010). *NEWS: THE DUTCH ROADMAP FOR THE WWTP OF 2030*.

STOWA. (2016). *Struviet en struviethoudende producten in communaal afvalwater - marktverkenning en gewasonderzoek* (Issue 2016.12).

Sustec. (2014). *World First Continuous THP*. 2014. https://sustec.nl/2014/12/29/world-first-continuous-thp/

Sutzkover-Gutman, I., Hasson, D., & Semiat, R. (2010). Humic substances fouling in ultrafiltration processes. *Desalination*, *261*(3), 218–231. https://doi.org/10.1016/j.desal.2010.05.008

Tang, C., Liu, Z., Peng, C., Chai, L. Y., Kuroda, K., Okido, M., & Song, Y. X. (2019). New insights into the interaction between heavy metals and struvite: Struvite as platform for heterogeneous nucleation of heavy metal hydroxide. *Chemical Engineering Journal*, *365*(December 2018), 60–69. https://doi.org/10.1016/j.cej.2019.02.034

Tarragó, E., Puig, S., Ruscalleda, M., Balaguer, M. D., & Colprim, J. (2016). Controlling struvite particles' size using the up-flow velocity. *Chemical Engineering Journal*, *302*, 819–827. https://doi.org/10.1016/j.cej.2016.06.036

Thorn, K. A., & Mikita, M. A. (1992). Ammonia fixation by humic substances: a nitrogen-15 and carbon-13 NMR study. *Science of the Total Environment, The*, *113*(1–2), 67–87. https://doi.org/10.1016/0048-9697(92)90017-M

Van De Graaf, A. A., De Bruijn, P., Robertson, L. A., Jetten, M. S. M., & Kuenen, J. G. (1996). Autotrophic growth of anaerobic ammonium-oxidizing micro-organisms in a fluidized bed reactor. *Microbiology*, *142*(8), 2187–2196. https://doi.org/10.1099/13500872-142-8-2187

Vasenko, L., & Qu, H. (2019). Enhancing the recovery of calcium phosphates from wastewater treatment systems through hybrid process of oxidation and crystallization. *Journal of Environmental Chemical Engineering*, *7*(1), 102828. https://doi.org/10.1016/j.jece.2018.102828

Veeken, A. H. M., & Hamelers, H. V. M. (1999). Removal of heavy metals from sewage sludge by extraction with organic acids. *Water Science and Technology*, *40*(1), 129–136. https://doi.org/https://doi-org.tudelft.idm.oclc.org/10.2166/wst.1999.0029

Verdonk, P. (2017). *Optimalisatie Struviet Winning op RWZI Echten*. Hogeschool Van Hall-Larenstein.

Verhults, R. (2017). Phosphorus recycling in the Dutch communal wastewater chain: Barriers to growth. In *Master Thesis*. TU Delft. https://repository.tudelft.nl/islandora/object/uuid%3A89f61b9d-74b2-4da0-8fe9-b47201d71c60

Villamiel, M., del Castillo, M. D., & Corzo, N. (2007). Food Biochemistry and Food Processing. In *Food Biochemistry and Food Processing*. https://doi.org/10.1002/9780470277577

Wang, C. C., Hao, X. D., Guo, G. S., & van Loosdrecht, M. C. M. (2010). Formation of pure struvite at neutral pH by electrochemical deposition. *Chemical Engineering Journal*, *159*(1–3), 280–283. https://doi.org/10.1016/j.cej.2010.02.026

Wang, H. Y., Qian, H., & Yao, W. R. (2011). Melanoidins produced by the Maillard reaction: Structure and biological activity. *Food Chemistry*, *128*(3), 573–584. https://doi.org/10.1016/j.foodchem.2011.03.075

Wang, J., Song, Y., Yuan, P., Peng, J., & Fan, M. (2006). Modeling the crystallization of magnesium ammonium phosphate for phosphorus recovery. *Chemosphere*, *65*(7), 1182–1187. https://doi.org/10.1016/j.chemosphere.2006.03.062

Warmadewanthi, & Liu, J. C. (2009). Recovery of phosphate and ammonium as struvite from semiconductor wastewater. *Separation and Purification Technology*, *64*(3), 368–373. https://doi.org/10.1016/j.seppur.2008.10.040

Wei, L., Hong, T., Cui, K., Chen, T., Zhou, Y., Zhao, Y., Yin, Y., Wang, J., & Zhang, Q. (2019). Probing the effect of humic acid on the nucleation and growth kinetics of struvite by constant composition technique. *Chemical Engineering Journal*, *378*(April), 122130. https://doi.org/10.1016/j.cej.2019.122130

Whittaker, E. J. W. (1981). Isomorphism. In *Mineralogy. Encyclopedia of Earth Science.* Springer.

Williams, T. O., & Burrowes, P. (2016). THERMAL HYDROLYSIS OFFERINGS AND PERFORMANCE. *European Biosolids and Organic Resources Conference*.

Wilschefski, S. C., & Baxter, M. R. (2019). Inductively Coupled Plasma Mass Spectrometry: Introduction to Analytical Aspects. *Clinical Biochemist Reviews*, *40*(3), 115–133. https://doi.org/10.33176/aacb-19-00024

Wilson, C. A., & Novak, J. T. (2009). Hydrolysis of macromolecular components of primary and secondary wastewater sludge by thermal hydrolytic pretreatment. *Water Research*, *43*(18), 4489–4498. https://doi.org/10.1016/j.watres.2009.07.022

Xue, Y., Liu, H., Chen, S., Dichtl, N., Dai, X., & Li, N. (2015). Effects of thermal hydrolysis on organic matter solubilization and anaerobic digestion of high solid sludge. *Chemical Engineering Journal*, *264*, 174–180. https://doi.org/10.1016/j.cej.2014.11.005

Yan, M., Lu, Y., Gao, Y., Benedetti, M. F., & Korshin, G. V. (2015). In-Situ Investigation of Interactions between Magnesium Ion and Natural Organic Matter. *Environmental Science and Technology*, *49*(14), 8323–8329. https://doi.org/10.1021/acs.est.5b00003

Ye, Z. L., Chen, S. H., Wang, S. M., Lin, L. F., Yan, Y. J., Zhang, Z. J., & Chen, J. S. (2010). Phosphorus recovery from synthetic swine wastewater by chemical precipitation using response surface methodology. *Journal of Hazardous Materials*, *176*(1–3), 1083–1088. https://doi.org/10.1016/j.jhazmat.2009.10.129

Zahmatkesh, M., Spanjers, H., & van Lier, J. B. (2018). A novel approach for application of white rot fungi in wastewater treatment under non-sterile conditions: immobilization of fungi on sorghum. *Environmental Technology (United Kingdom)*, *39*(16), 2030–2040. https://doi.org/10.1080/09593330.2017.1347718

Zhang, Dandan, Jiang, H., Chang, J., Sun, J., Tu, W., & Wang, H. (2019). Effect of thermal hydrolysis pretreatment on volatile fatty acids production in sludge acidification and subsequent polyhydroxyalkanoates production. *Bioresource Technology*, *279*(November 2018), 92–100. https://doi.org/10.1016/j.biortech.2019.01.077

Zhang, Dian, Feng, Y., Huang, H., Khunjar, W., & Wang, Z. W. (2020). Recalcitrant dissolved organic nitrogen formation in thermal hydrolysis pretreatment of municipal sludge. *Environment International*, *138*(December 2019), 105629. https://doi.org/10.1016/j.envint.2020.105629

Zhang, T., He, X., Deng, Y., Tsang, D. C. W., Jiang, R., Becker, G. C., & Kruse, A. (2020). Phosphorus recovered from digestate by hydrothermal processes with struvite crystallization and its potential as a fertilizer. *Science of the Total Environment*, *698*, 134240. https://doi.org/10.1016/j.scitotenv.2019.134240

Zhang, W. Z., Chen, X. Q., Zhou, J. M., Liu, D. H., Wang, H. Y., & Du, C. W. (2013). Influence of Humic Acid on Interaction of Ammonium and Potassium Ions on Clay Minerals. *Pedosphere*, *23*(4), 493–502. https://doi.org/10.1016/S1002-0160(13)60042-9

Zhou, Z., Hu, D., Ren, W., Zhao, Y., Jiang, L. M., & Wang, L. (2015). Effect of humic substances on phosphorus removal by struvite precipitation. *Chemosphere*, *141*, 94–99. https://doi.org/10.1016/j.chemosphere.2015.06.089

Zohar, I., Ippolito, J. A., Massey, M. S., & Litaor, I. M. (2017). Innovative approach for recycling phosphorous from agro-wastewaters using water treatment residuals (WTR). *Chemosphere*, *168*, 234–243. https://doi.org/10.1016/j.chemosphere.2016.10.041

Zoroddu, M. A., Aaseth, J., Crisponi, G., Medici, S., Peana, M., & Nurchi, V. M. (2019). The essential metals for humans: a brief overview. *Journal of Inorganic Biochemistry*, *195*(February), 120–129. https://doi.org/10.1016/j.jinorgbio.2019.03.013

This page intentionally left blank

Appendices

Appendix 1

Reactant volumes for batch struvite crystallisation

Table 1. Reactant volumes for batch struvite crystallisation (primary research)

Items	Concentration in the stocks	Concentration in the reactor	Volume in the reactor (mL)	Explanation
Melanoidins (gTOC/L)	23.96	0 / 1 / 2	0 / 20.87 / 41.74	
$MgCl_2$ (mM Mg/L)	1000	15	7.5	
P-PO_4 synthetic wastewater (mM P-PO_4/L)	33.85	15	221.57	
$CaCl_2*2H_2O$ (g/L)	18	180	5	Solution no. 1
$FeSO_4$ (g/L)	5	5	0.5	Solution no. 2
$ZnCl_2$ (g/L)	0.0199	0.199		
$CoCl_2*6H_2O$ (g/L)	0.0247	0.247		
$MnCl2*4H_2O$ (g/L)	0.0994	0.994		
$CuSO_4$	0.0164	0.164	5	Solution no. 3, added all at once
$Na_2MoO_4*2H_2O$ (g/L)	0.0221	0.221		
$NiCl_2*6H_2O$ (g/L)	0.0196	0.196		
Na_2O_3Se (g/L)	0.0105	0.105		
H_3BO_3 (g/L)	0.0014	0.014		
Al (mg Al/L)	8	0.4	25	Solution no. 4, added all at once
Cr (mg Cr/L)	18	0.9		
Demineralised water (mL)			235.43 / 214.57 / 193.70	
Total volume (mL)			500	

Table 2. Reactant volumes for batch struvite crystallisation (preliminary research using melanoidins)

Items	Concentration in the stocks	Concentration in the reactor	Volume in the reactor (mL)
Melanoidins (gTOC/L)	23.96	0 / 0.5 / 1 /1.5 / 2	0 / 11.04 / 22.1 / 33.1 / 44.2
$MgCl_2$ (mM Mg/L)	1000	15	7.5
P-PO_4 synthetic wastewater (mM P-PO_4/L)	33.85	15	250
Demineralised water (mL)			242.5 / 231.5 / 220 / 209 / 198
Total volume (mL)			500

Table 3. Reactant volumes for batch struvite crystallisation (preliminary research using humic acids)

Items	Concentration in the stocks	Concentration in the reactor	Volume in the reactor (mL)
Humic acids (gTOC/L)	3.69	0 / 0.5 / 1 /1.5	0 / 67.63 / 135.3 / 202.9
$MgCl_2$ (mM Mg/L)	1000	15	7.5
P-PO_4 synthetic wastewater (mM P-PO_4/L)	33.85	15	245.5
Demineralised water (mL)			247 / 179.4 / 111.7 / 44.12
Total volume (mL)			500

Table 4. Reactant volumes for Mg-melanoidins complexation

Items	Concentration in the stocks	Concentration in the reactor	Volume in the reactor (mL)
Melanoidins (gTOC/L)	23.96	0 / 1 / 2	0 / 4.17 / 8.35
MgCl$_2$ (mM Mg/L)	1000	15	1.5
Demineralised water (mL)			98.5 / 94.3 / 90.15
Total volume (mL)			100

Table 1. Calibration of colour standard solution

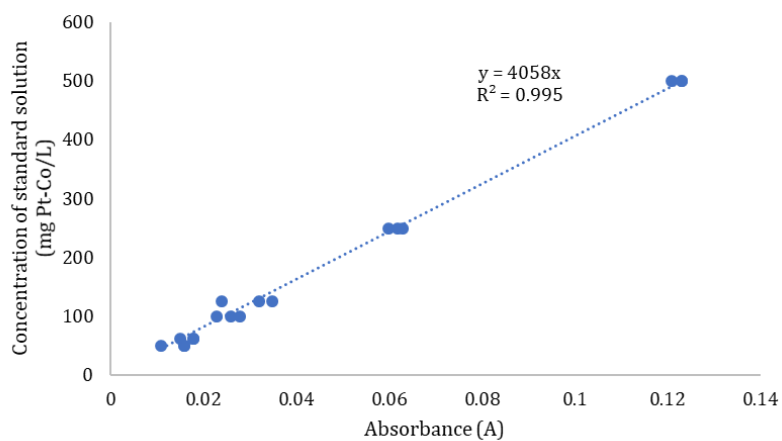| Concentration of standards (mg Pt-Co/L)	Instrument readings (A)
500	0.121
500	0.123
500	0.123
250	0.06
250	0.062
250	0.063
125	0.024
125	0.035
125	0.032
100	0.023
100	0.026
100	0.028
62.5	0.015
62.5	0.018
62.5	0.018
50	0.011
50	0.016
50	0.016

Figure 1. Calibration curve of colour standard solution

```
Acetate         Acetate-        1.0     59.045  59.045
Tartarate       Tartarate-2     0.0     148.072 148.072
Glycine         Glycine-        1.0     74.059  74.059
Salicylate      Salicylate-2    1.0     136.107 136.107
Glutamate       Glutamate-2     1.0     145.115 145.115
Phthalate       Phthalate-2     1.0     164.117 164.117
Fulvate         Fulvate-2       0.0     650.    650.
Humate          Humate-2        0.0     2000.   2000.
```

Figure 1. Addition of fulvic and humic acids speciation from T_H.dat into minteq.v4.dat SOLUTION_MASTER_SPECIES

```
#MgHumate
        Mg+2 + Humate-2 = MgHumate
        log_k   = 0.60
#MgFulvate
        Mg+2 + Fulvate-2 = MgFulvate
        log_k           = -2.4
#CaFulvate
        Ca+2 + Fulvate-2 = CaFulvate
        log_k           = -3
#CaHumate
        Ca+2 + Humate-2 = CaHumate
        log_k           = 0.43
```

Figure 2. Addition of Mg and Ca complexes into the modified minteq.v4.dat SOLUTION_SPECIES

```
PHASES
Struvite
MgNH4PO4:6H2O = Mg+2 + PO4-3 + NH4+ + 6H2O
        log_k   -13.15
        delta_h 23.62 kcal
Newberyite
        MgHPO4:3H2O = Mg+2 + HPO4-2 + 3H2O
        log_k -5.80
        delta_h 0.00
Bobbierite
        Mg3(PO4)2:8H2O = 3Mg+2 + 2PO4-3 + 8H2O
        log_k -25.20
        delta_h 0.00
Cattiite
        Mg3(PO4)2:22H2O = 3Mg+2 + 2PO4-3 + 22H2O
        log_k -23.10
        delta_h 0.00
END
```

Figure 3. Description of struvite and other minerals that are not included in PHREEQC database

```
SOLUTION 1
-units mmol/L
-temp 20
pH                8
P                 15 as PO4 #P-PO4
N(-3)             66.42 #as N-NH4
Ca                1.22437
Fe                0.01794
Zn                0.0007
Co                0.0019
Mn                0.00502
Cu                0.00103
Mo                0.00091
Ni                0.00082
Se(4)             0.00061
B                 0.00023
Al                0.01481
Cr(3)             0.01731
Humate            0.69
Fulvate           9.743
Na                20.86
Alkalinity        20.86 #as HCO3
END
```

Figure 4. Description of the solution. The depicted figure is code for 1 g TOC/L HS. For 2 g TOC/L HS, Humate = 1.381, Fulvate = 19.487, Na and alkalinity = 41.72. For 0 g TOC/L, Humate, Fulvate, Na, and Alkalinity were set into 0.

```
PHASES
        Fix_H+
        H+ = H+
        log_k   0.0
END

USE solution 1
EQUILIBRIUM_PHASES
Fix_H+   -8      NaOH            5.0
Struvite                        0 0
REACTION
MgCl2
15e-3 moles in 1 steps
END
```

Figure 5.   Command to control pH and precipitate struvite by reacting with $MgCl_2$. Fix_H+ was varied to 6.5, 7.25, and 8.

Table 1. Concentrations of HA and FA complexes

pH	HS concentration (g TOC/L)	Mg-HA (mmol/L)	Ca-HA (mmol/L)	Cu-HA (mmol/L)	Fe-HA (mmol/L)	Mg-FA (mmol/L)	Ca-FA (mmol/L)	Cu-FA (mmol/L)	Fe-FA (mmol/L)
6.50	1	1.64E-03	3.08E-04	6.87E-05	3.33E-05	2.32E-05	1.62E-06	9.72E-04	4.71E-04
	2	2.82E-03	4.64E-04	6.94E-05	5.61E-05	3.99E-05	2.44E-06	9.81E-04	7.93E-04
7.25	1	4.57E-04	3.19E-04	6.84E-05	1.30E-06	6.46E-06	1.68E-06	9.66E-04	1.83E-05
	2	7.81E-04	4.72E-04	6.88E-05	2.32E-06	1.10E-05	2.48E-06	9.71E-04	3.28E-05
8.00	1	1.56E-04	3.26E-04	6.58E-05	3.07E-08	2.21E-06	1.71E-06	9.29E-04	4.33E-07
	2	2.53E-04	4.62E-04	6.27E-05	5.64E-08	3.57E-06	2.42E-06	8.85E-04	7.96E-07

Table 2. SI values of possible co-precipitating minerals

Trace elements contained	Minerals name	Minerals formula	SI values 0 g TOC/L pH 6.5	pH 7.25	pH 8	1 g TOC/L pH 6.5	pH 7.25	pH 8	2 g TOC/L pH 6.5	pH 7.25	pH 8
Al	Al(OH)$_3$	Al(OH)$_3$(am)	0.18	-0.16	-0.85	0.17	-0.17	-0.86	0.16	-0.17	-0.87
Al	Al$_2$O$_3$	Al$_2$O$_3$	2.2	1.53	0.14	2.18	1.51	0.12	2.16	1.49	0.1
Al	Boehmite	AlOOH	2.38	2.05	1.35	2.37	2.04	1.34	2.36	2.03	1.33
Al	Diaspore	AlOOH	4.13	3.8	3.10	4.12	3.79	3.09	4.11	3.78	3.08
Al	Gibbsite	Al(OH)$_3$	2.73	2.4	1.71	2.72	2.39	1.69	2.71	2.38	1.68
Al, Fe	Hercynite	FeAl$_2$O$_4$	5.7	6.23	6.16	5.63	6.16	6.09	5.56	6.09	5.92
Ca	Ca$_3$(PO$_4$)$_2$(beta)	Ca$_3$(PO$_4$)$_2$	0.59	1.8	2.74	0.46	1.67	2.66	0.3	1.49	2.48
Ca	Ca$_4$H(PO$_4$)$_3$:3H$_2$O	Ca$_4$H(PO$_4$)3:3H$_2$O	-0.51	0.55	1.2	-0.68	0.38	1.11	-0.88	0.16	0.89
Ca	CaHPO$_4$	CaHPO$_4$	0.27	0.12	-0.17	0.24	0.09	-0.17	0.2	0.04	-0.21
Ca	Hydroxylapatite	Ca$_5$(PO$_4$)$_3$OH	6.45	9.02	11.18	6.21	8.79	11.02	5.94	8.48	10.7
Ca	Aragonite	CaCO$_3$	-	-	-	-1.61	-0.68	0.1	-0.95	-0.04	0.73
Ca	Calcite	CaCO$_3$	-	-	-	-1.41	-0.49	0.3	-0.76	0.15	0.92
Co, Fe	CoFe$_2$O$_4$	CoFe$_2$O$_4$	22.06	25.16	27.8	21.83	24.98	27.61	21.55	24.74	27.37
Cr	Cr(OH)$_3$	Cr(OH)$_3$	-0.1	0.86	1.57	-0.19	0.81	1.54	-0.28	0.77	1.52

| Trace elements contained	Minerals name	Minerals formula	SI values								
			0 g TOC/L			1 g TOC/L			2 g TOC/L		
			pH 6.5	pH 7.25	pH 8	pH 6.5	pH 7.25	pH 8	pH 6.5	pH 7.25	pH 8
Cr	$Cr(OH)_3(am)$	$Cr(OH)_3$	2.07	3.03	3.74	1.99	2.99	3.72	1.89	2.94	3.69
Cr	Cr_2O_3	Cr_2O_3	4.85	6.77	8.19	4.68	6.69	8.14	4.5	6.6	8.09
Cr, Fe	$FeCr_2O_4$	$FeCr_2O_4$	1.94	5.05	7.79	1.71	4.91	7.7	1.47	4.78	7.5
Cr, Fe	$MgCr_2O_4$	$MgCr_2O_4$	-3.88	-1.02	1.47	-4.07	-1.12	1.37	-4.27	-1.23	1.27
Cu, Fe	Cupricferrite	$CuFe_2O_4$	11.86	14.37	16.28	8.77	11.94	14.66	8.44	11.66	14.38
Cu, Fe	Cuprousferrite	$CuFeO_2$	11.5	13.59	15.58	8.45	11.14	13.95	8.15	10.84	13.52
Cu, Se	$Cu_2Se(alpha)$	Cu_2Se	-2.83	1.23	7.27	-8.95	-3.88	3.74	-9.56	-4.66	1.93
Cu, Se	CuSe	CuSe	-2.59	-0.2	3.76	-5.69	-2.84	1.89	-6.04	-3.31	0.64
Fe	$Fe(OH)_{2.7}Cl_{.3}$	$Fe(OH)_{2.7}Cl_{.3}$	6.7	7.32	7.71	6.67	7.3	7.7	6.66	7.28	7.69
Fe	$Fe_3(OH)_8$	$Fe_3(OH)_8$	-1.06	1.76	4.32	-1.2	1.68	4.25	-1.34	1.59	4.09
Fe	Ferrihydrite	$Fe(OH)_3$	2.72	3.53	4.15	2.68	3.51	4.13	2.63	3.5	4.13
Fe	Goethite	FeOOH	5.46	6.27	6.89	5.41	6.25	6.87	5.37	6.23	6.87
Fe	Hematite	Fe_2O_3	13.29	14.91	16.15	13.21	14.88	16.13	13.12	14.85	16.12
Fe	Lepidocrocite	FeOOH	4.76	5.57	6.19	4.72	5.55	6.17	4.67	5.54	6.17
Fe	Maghemite	Fe_2O_3	5.87	7.5	8.73	5.79	7.46	8.71	5.7	7.43	8.7
Fe	Magnesioferrite	Fe_2MgO_4	4.78	7.34	9.64	4.67	7.29	9.56	4.57	7.23	9.51
Fe	Magnetite	Fe_3O_4	15.14	17.96	20.52	15	17.88	20.45	14.87	17.8	20.29
Fe	Strengite	$FePO_4:2H_2O$	3.7	2.85	1.66	3.69	2.87	1.72	3.68	2.89	1.78
Mn	MnHPO4	$MnHPO_4$	3.84	3.66	3.37	3.73	3.56	3.3	3.61	3.45	3.21
	Newberyite	$MgHPO_4:3H_2O$	-0.37	-1.09	-1.83	-0.36	-1.08	-1.81	-0.34	-1.06	-1.8
	Bobbierite	$Mg_3(PO4)_2:8H_2O$	-1.78	-2.28	-2.68	-1.76	-2.26	-2.7	-1.75	-2.26	-2.71
	Cattiite	$Mg_3(PO4)_2:22H_2O$	-3.89	-4.39	-4.79	-3.88	-4.38	-4.81	-3.87	-4.38	-4.83
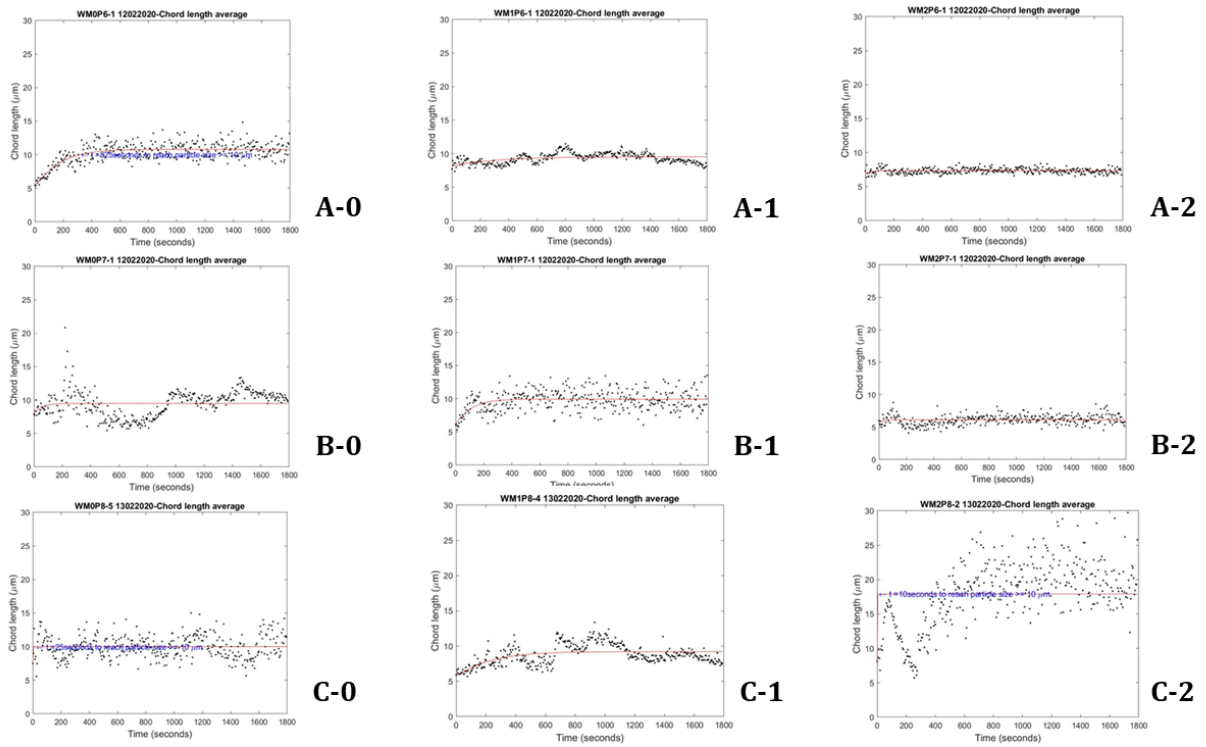
Figure 1. FBRM results. a) at pH 6.5, with 0; 1; 2 g TOC/L melanoidins, b) at pH 7.25, with 0; 1; 2 g TOC/L melanoidins, c) at pH 8, with 0; 1; 2 g TOC/L melanoidins.
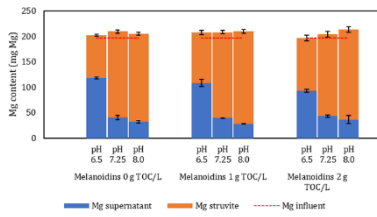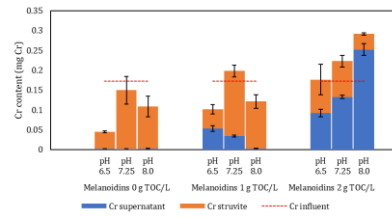
Figure 1. Mass balance of magnesium

Figure 2. Mass balance of aluminium

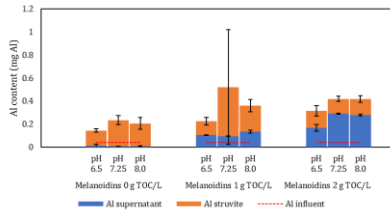Figure 3. Mass balance of boron

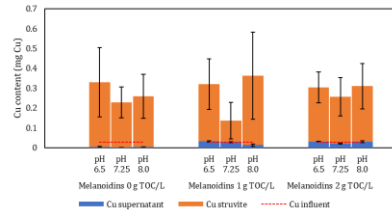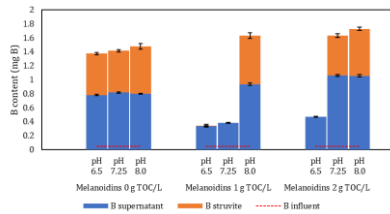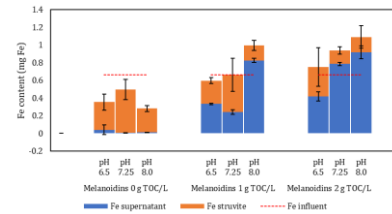Figure 4. Mass balance of cobalt

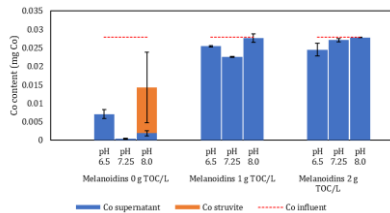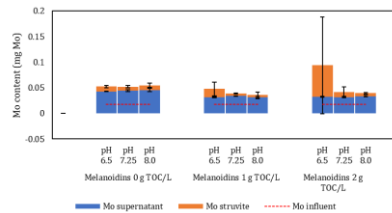Figure 5. Mass balance of chromium

Figure 6. Mass balance of copper

Figure 7. Mass balance of iron

Figure 8. Mass balance of molybdate
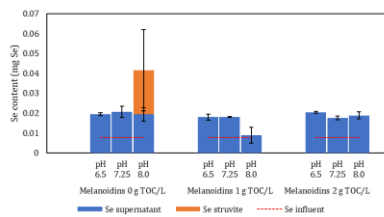
Figure 9. Mass balance of selenium
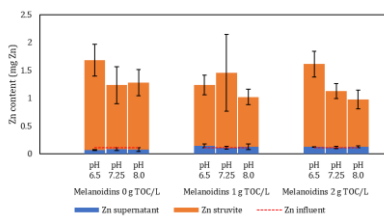
Figure 10. Mass balance of zinc

ANOVA for Reduced Linear model

Response 1: N in supernatant

Source	Sum of Squares	df	Mean Square	F-value	p-value	
Model	2400.00	1	2400.00	7.85	0.0206	significant
A-pH	2400.00	1	2400.00	7.85	0.0206	
Residual	2750.46	9	305.61			
Lack of Fit	2569.80	7	367.11	4.06	0.2116	not significant
Pure Error	180.67	2	90.33			
Cor Total	5150.46	10				

Fit Statistics

Std. Dev.	17.48		R^2	0.4660
Mean	414.24		**Adjusted R^2**	0.4066
C.V. %	4.22		**Predicted R^2**	0.2213
			Adeq Precision	5.3661

ANOVA for Reduced Quadratic model

Response 2: P in supernatant

Source	Sum of Squares	df	Mean Square	F-value	p-value	
Model	17727.94	4	4431.99	284.53	< 0.0001	significant
A-pH	14054.23	1	14054.23	902.27	< 0.0001	
B-Melanoidins	128.53	1	128.53	8.25	0.0283	
AB	199.23	1	199.23	12.79	0.0117	
A^2	3345.95	1	3345.95	214.81	< 0.0001	
Residual	93.46	6	15.58			
Lack of Fit	92.60	4	23.15	53.84	0.0183	significant
Pure Error	0.8600	2	0.4300			
Cor Total	17821.40	10				

Fit Statistics

Std. Dev.	3.95		R^2	0.9948
Mean	36.33		**Adjusted R^2**	0.9913
C.V. %	10.86		**Predicted R^2**	0.9647
			Adeq Precision	41.6823

ANOVA for Reduced Quadratic model

Response 3: N in struvite

Source	Sum of Squares	df	Mean Square	F-value	p-value	
Model	3310.57	2	1655.28	109.03	< 0.0001	significant
A-pH	2353.06	1	2353.06	154.99	< 0.0001	
A^2	957.51	1	957.51	63.07	< 0.0001	
Residual	121.45	8	15.18			
Lack of Fit	112.72	6	18.79	4.30	0.2005	not significant
Pure Error	8.73	2	4.36			
Cor Total	3432.02	10				

Fit Statistics

Std. Dev.	3.90		R^2	0.9646
Mean	76.17		**Adjusted R^2**	0.9558
C.V. %	5.12		**Predicted R^2**	0.9284
			Adeq Precision	19.4648

ANOVA for Reduced Quadratic model

Response 4: P in struvite

Source	Sum of Squares	df	Mean Square	F-value	p-value	
Model	17101.63	2	8550.82	72.59	< 0.0001	significant
A-pH	13036.66	1	13036.66	110.67	< 0.0001	
A^2	4064.98	1	4064.98	34.51	0.0004	
Residual	942.34	8	117.79			
Lack of Fit	871.34	6	145.22	4.09	0.2094	not significant
Pure Error	71.00	2	35.50			
Cor Total	18043.98	10				

Fit Statistics

Std. Dev.	10.85		R^2	0.9478
Mean	181.45		**Adjusted R^2**	0.9347
C.V. %	5.98		**Predicted R^2**	0.9004
			Adeq Precision	16.4480

ANOVA for Reduced Linear model

Response 5: Max diameter

Source	Sum of Squares	df	Mean Square	F-value	p-value	
Model	2478.96	1	2478.96	16.39	0.0029	significant
B-Melanoidins	2478.96	1	2478.96	16.39	0.0029	
Residual	1361.25	9	151.25			
Lack of Fit	1208.58	7	172.65	2.26	0.3405	not significant
Pure Error	152.67	2	76.33			
Cor Total	3840.21	10				

Fit Statistics

Std. Dev.	12.30		R^2	0.6455
Mean	68.16		Adjusted R^2	0.6061
C.V. %	18.04		Predicted R^2	0.4471
			Adeq Precision	7.7522

ANOVA for Reduced Linear model

Response 6: Min diameter

Source	Sum of Squares	df	Mean Square	F-value	p-value	
Model	277.19	1	277.19	6.82	0.0282	significant
B-Melanoidins	277.19	1	277.19	6.82	0.0282	
Residual	365.69	9	40.63			
Lack of Fit	283.03	7	40.43	0.9782	0.5922	not significant
Pure Error	82.67	2	41.33			
Cor Total	642.88	10				

Fit Statistics

Std. Dev.	6.37		R^2	0.4312
Mean	39.37		Adjusted R^2	0.3680
C.V. %	16.19		Predicted R^2	0.1284
			Adeq Precision	5.0013

ANOVA for Quadratic model

Response 1: Mn in supernatant

Source	Sum of Squares	df	Mean Square	F-value	p-value	
Model	0.0085	5	0.0017	37.14	0.0006	significant
A-pH	0.0002	1	0.0002	4.06	0.0999	
B-Melanoidins	0.0059	1	0.0059	129.38	< 0.0001	
AB	0.0007	1	0.0007	14.44	0.0126	
A^2	0.0016	1	0.0016	35.46	0.0019	
B^2	0.0004	1	0.0004	9.43	0.0277	
Residual	0.0002	5	0.0000			
Lack of Fit	0.0002	3	0.0001	96.88	0.0102	significant
Pure Error	1.560E-06	2	7.802E-07			
Cor Total	0.0087	10				

Fit Statistics

Std. Dev.	0.0068		R^2	0.9738
Mean	0.0628		Adjusted R^2	0.9476
C.V. %	10.77		Predicted R^2	0.7517
			Adeq Precision	19.0992

ANOVA for Quadratic model

Response 2: Ni in supernatant

Source	Sum of Squares	df	Mean Square	F-value	p-value	
Model	0.0008	5	0.0002	496.41	< 0.0001	significant
A-pH	1.400E-06	1	1.400E-06	4.50	0.0875	
B-Melanoidins	0.0005	1	0.0005	1744.23	< 0.0001	
AB	3.475E-06	1	3.475E-06	11.16	0.0206	
A^2	3.924E-06	1	3.924E-06	12.60	0.0164	
B^2	0.0002	1	0.0002	708.59	< 0.0001	
Residual	1.558E-06	5	3.115E-07			
Lack of Fit	1.114E-06	3	3.713E-07	1.67	0.3952	not significant
Pure Error	4.437E-07	2	2.218E-07			
Cor Total	0.0008	10				

Fit Statistics

Std. Dev.	0.0006		R^2	0.9980
Mean	0.0166		Adjusted R^2	0.9960
C.V. %	3.36		Predicted R^2	0.9838
			Adeq Precision	50.6942

ANOVA for Reduced Quadratic model

Response 3: Mn in struvite

Source	Sum of Squares	df	Mean Square	F-value	p-value	
Model	0.0070	4	0.0018	21.40	0.0011	significant
A-pH	0.0002	1	0.0002	2.19	0.1893	
B-Melanoidins	0.0043	1	0.0043	52.70	0.0003	
AB	0.0006	1	0.0006	7.87	0.0309	
A²	0.0019	1	0.0019	22.83	0.0031	
Residual	0.0005	6	0.0001			
Lack of Fit	0.0005	4	0.0001	5.77	0.1531	not significant
Pure Error	0.0000	2	0.0000			
Cor Total	0.0075	10				

Fit Statistics

Std. Dev.	0.0091		**R²**	0.9345
Mean	0.0741		**Adjusted R²**	0.8908
C.V. %	12.23		**Predicted R²**	0.6064
			Adeq Precision	14.2684

ANOVA for Reduced Quadratic model

Response 4: Ni in struvite

Source	Sum of Squares	df	Mean Square	F-value	p-value	
Model	0.0008	3	0.0003	58.15	< 0.0001	significant
A-pH	3.178E-06	1	3.178E-06	0.6588	0.4437	
B-Melanoidins	0.0006	1	0.0006	115.17	< 0.0001	
B²	0.0003	1	0.0003	58.63	0.0001	
Residual	0.0000	7	4.825E-06			
Lack of Fit	0.0000	5	5.801E-06	2.43	0.3166	not significant
Pure Error	4.770E-06	2	2.385E-06			
Cor Total	0.0009	10				

Fit Statistics

Std. Dev.	0.0022		**R²**	0.9614
Mean	0.0069		**Adjusted R²**	0.9449
C.V. %	31.72		**Predicted R²**	0.8791
			Adeq Precision	16.0531

```python
1    # -*- coding: utf-8 -*-
2    """
3    Created on Wed Apr 22 13:51:53 2020
4
5    @author: Widya Iswarani
6    """
7
8
9    import numpy as np
10   import matplotlib.pyplot as plt
11   import pandas as pd
12   from scipy import stats
13
14   #EC_test = pd.read_csv('WM0P6_EC_python_new.csv') #ok when n = 5
15   #EC_test = pd.read_csv('WM1P6_EC_python.csv') #ok when n = 5
16   #EC_test = pd.read_csv('WM2P6_EC_python_new.csv') #ok when n = 5
17   #EC_test = pd.read_csv('WM0P7_EC_python.csv') #ok when n = 5
18   #EC_test = pd.read_csv('WM1P7_EC_python_new.csv') #ok when n = 5
19   #EC_test = pd.read_csv('WM2P7_EC_python.csv')  #ok when n = 5
20   #EC_test = pd.read_csv('WM0P8_EC_python.csv') #ok when n = 5
21   #EC_test = pd.read_csv('WM1P8_EC_python.csv') #ok when n = 5
22   EC_test = pd.read_csv('WM2P8_EC_python.csv') #ok when n = 5
23
24   def moving_avg(a, n):
25       Avg = np.cumsum(a)
26       Avg[n : ] = Avg[n : ] - Avg[ : -n]
27       return Avg[n-1 :] / n
28
29   ECgrad = np.gradient(EC_test['average'])
30   n = 5
31   ECgrad_Avg = moving_avg(ECgrad, n)
32   zero_slope_array = np.zeros(len(ECgrad_Avg))
33   nt_bool = 0
34   nt = 0
35   ttest_pval = np.zeros(len(ECgrad_Avg))
```

```python
36
37   for i in range(len(ECgrad_Avg)):
38       ttest_pval[i] = stats.ttest_ind(ECgrad_Avg[i:], zero_slope_array[i:], equal_var=True,
39       if  ttest_pval[i] > 0.05 and i > EC_test.average.idxmax() and nt_bool==0:
40           nt = i
41           nt_bool = 1
42
43   plt.plot(EC_test['t'], EC_test['average'])
44   if nt != 0:
45       plt.plot(EC_test['t'].iloc[nt], EC_test['average'].iloc[nt], 'ro')
46       plt.legend(['EC(µs/cm)', 'time required to reach stable EC (s)'], loc= 'best')
47   if nt == 0:
48       plt.legend(['EC(µs/cm)'], loc= 'best')
49       print('time required to reach stable EC is not found')
50   plt.ylim(10000, 16000)
51   plt.xlim(0, 1800)
52   plt.xlabel('time(s)')
53   plt.ylabel('EC(µs/cm)')
54   #plt.title('Melanoidins 0 g TOC/L & pH 6.5, time =' + str(nt * 5) + 's')
55   #plt.title('Melanoidins 1 g TOC/L & pH 6.5, time =' + str(nt * 5) + 's')
56   #plt.title('Melanoidins 2 g TOC/L & pH 6.5, time =' + str(nt * 5) + 's')
57   #plt.title('Melanoidins 0 g TOC/L & pH 7.25, time =' + str(nt * 5) + 's')
58   #plt.title('Melanoidins 1 g TOC/L & pH 7.25, time =' + str(nt * 5) + 's')
59   #plt.title('Melanoidins 2 g TOC/L & pH 7.25, time =' + str(nt * 5) + 's')
60   #plt.title('Melanoidins 0 g TOC/L & pH 8, time =' + str(nt * 5) + 's')
61   #plt.title('Melanoidins 1 g TOC/L & pH 8, time =' + str(nt * 5) + 's')
62   plt.title('Melanoidins 2 g TOC/L & pH 8, time =' + str(nt * 5) + 's')
63   print('the induction time is', nt * 5, 's')
64   print('the p-value is', ttest_pval[nt])
```